
Exploring Strong Correlations and Strong Disorder in Fermionic Systems:
Independent Investigations

vorgelegt von

SAURABH KUMAR

geboren am 21.08.1997 in Saharsa, Bihar, India



INAUGURAL-DISSERTATION

zur

Erlangung des Doktorgrades
der Mathematisch-Naturwissenschaftlichen Fakultät
der Universität zu Köln

JAHR DER VERÖFFENTLICHUNG: 2025

Berichterstatter: Prof. Dr. Martin Zirnbauer
(Gutachter)

Prof. Dr. Sebastian Diehl

Tag der mündlichen Prüfung: 19.12.2024

Abstract

Despite significant advancements in condensed matter physics, analyzing strongly interacting and disordered systems presents notable challenges that this thesis aims to address. Divided into two distinct projects, this work investigates strongly interacting fermion systems and strongly disordered fermion systems independently. However, both projects share a commonality in the analytical tool employed: the superbosonization formula introduced in [1, 2].

The first project addresses the lack of methods available for analyzing strongly interacting systems. We develop a general analytical framework based on the bosonization formula [1, 2] within the functional integral approach. As a specific application, we examine the one-dimensional strongly interacting Hubbard model at half-filling. However, we encounter challenges in properly defining the continuum limit in time. Consequently, we incorporate the concept of renormalization, exploring how it can be integrated into the bosonization scheme. We acknowledge that the complete execution of these ideas remains a work in progress, reserved for future research.

The second project centers on investigating strongly disordered fermion systems within symmetry class D, as outlined by the Altland-Zirnbauer classification of non-interacting fermions [3]. This research is motivated by the proposal of a novel spontaneous symmetry breaking (SSB) phenomenon in class A [4, 5, 6], and aims to uncover similar phenomena in class D systems. We begin with a general formulation of supersymmetric field theory applied to disordered class D systems, focusing on the strong disorder limit and its implications. To explore the potential for novel spontaneous symmetry breaking in class D, we analyze a specific system: monitored free fermions that exhibit measurement-induced phase transitions. We propose a reformulation of the theory that provides a new perspective on investigating this system. Nevertheless, a complete investigation of the possibility of novel SSB phenomena in class D remains an open question for future exploration.

Acknowledgements

I would like to express my heartfelt gratitude to my advisor, Prof. Martin Zirnbauer, for his invaluable guidance and support throughout my PhD. I am also thankful to my PhD committee members for graciously agreeing to serve on my committee.

I sincerely appreciate the valuable and insightful discussions I had with Charles, Julian, Lorenz, Nick, Rochus, Shao-Yu, and Vivek. My deepest and most heartfelt thanks go to my family and friends, with a special mention of Carsten and Shao-Yu.

Erklärung

„Hiermit versichere ich an Eides statt, dass ich die vorliegende Dissertation selbstständig und ohne die Benutzung anderer als der angegebenen Hilfsmittel und Literatur angefertigt habe. Alle Stellen, die wörtlich oder sinngemäß aus veröffentlichten und nicht veröffentlichten Werken dem Wortlaut oder dem Sinn nach entnommen wurden, sind als solche kenntlich gemacht. Ich versichere an Eides statt, dass diese Dissertation noch keiner anderen Fakultät oder Universität zur Prüfung vorgelegen hat; dass sie - abgesehen von unten angegebenen Teilpublikationen und eingebundenen Artikeln und Manuskripten - noch nicht veröffentlicht worden ist sowie, dass ich eine Veröffentlichung der Dissertation vor Abschluss der Promotion nicht ohne Genehmigung des Promotionsausschusses vornehmen werde. Die Bestimmungen dieser Ordnung sind mir bekannt. Darüber hinaus erkläre ich hiermit, dass ich die Ordnung zur Sicherung guter wissenschaftlicher Praxis und zum Umgang mit wissenschaftlichem Fehlverhalten der Universität zu Köln gelesen und sie bei der Durchführung der Dissertation zugrundeliegenden Arbeiten und der schriftlich verfassten Dissertation beachtet habe und verpflichte mich hiermit, die dort genannten Vorgaben bei allen wissenschaftlichen Tätigkeiten zu beachten und umzusetzen. Ich versichere, dass die eingereichte elektronische Fassung der eingereichten Druckfassung vollständig entspricht.“
Köln, February 26, 2025

UNTERSCHRIFT: DATUM:

Contents

Project 1: Investigation into Strong Interactions in Fermionic Systems	1
1 Introduction to the First Project	2
1.1 Motivation	2
1.2 Bosonization Formula	4
1.3 Outline of the First Project	6
2 A Bosonization Framework Using Functional Integral Language	7
2.1 Steps Involved in the Formalism	7
2.2 Summary	16
3 Application: Functional Integral Bosonization Approach to the Strongly Interacting One-Dimensional Hubbard Model at Half-Filling	17
3.1 The Hubbard Model	17
3.2 Attempt I: Reformulation of the Partition Function Using the $Q(x, t_k) \in U(4)$ Field	19
3.3 Attempt II: Reformulation of the Partition Function Using the $Q(x) \in U(2M)$ Field	28
3.4 Attempt III: Reformulation of the Partition Function Using a $U(1)$ field $e^{i\phi(x, t_k)}$	37
3.4.1 Motivation	37
3.4.2 Implementation of the Reformulation Strategy	39
3.5 Concluding Remarks	41
4 Applying Renormalization to Properly Define the Continuum Limit in Time	42
4.1 Kadanoff Block Spin Transformation	43
4.2 Integrating Renormalization Concepts into the Bosonization Approach	44
5 Conclusion from the First Project	47
Appendices	49
A Linked-cluster expansion	50
B Equations of Motion from Haar Measure Invariance	51
C Derivation of the Equations of Motion for the Matrix Components of the Field $Q(x, t_k)$ in Section 3.2	52
D Derivation of the Equations of Motion for the Matrix Components of the Field $Q(x)$ in Section 3.3	54
E Detailed Calculations for Attempt-III from Section 3.4	56

Project 2: Investigation into Strong Disorder in Fermionic Systems	59
6 Introduction to the Second Project	60
6.1 Motivation	60
6.2 Superbosonization Formula	62
6.3 Outline of the Second Project	64
7 Supersymmetric Field Theory Approach to Strongly Disordered Class D Systems	66
7.1 Symmetry Class D	66
7.2 Supersymmetric Field Theory	67
7.2.1 Model: Hamiltonian	71
7.2.2 Disorder Averaging	72
7.2.3 Superbosonization	73
7.3 Understanding the Strong Disorder Limit	76
8 Application: Measurement-Induced Phase Transitions in Free Fermions of Class D	80
8.1 Introduction	80
8.2 Model: Hamiltonian	81
8.3 Supersymmetry-Based Analysis of the Model	85
8.3.1 Prelude	87
8.3.2 Supersymmetry Approach to the Second Rényi Entropy	93
8.3.3 Averaging Over Random Measurement Outcomes	97
8.4 Summary	102
9 Conclusion from the Second Project	104
References	107

List of Figures

1	Closed-time contour with $+$ denoting the forward channel and $-$ indicating the backward channel.	8
2	Discretization of time T into M discrete intervals.	8
3	The purple block $t_{k-1} \rightarrow t_k$, whose contribution to the partition function is examined below.	9
4	The fields within the purple block are used to define the field $Q(t_k)$, as demonstrated below.	12
5	Local $U(R)$ -transformations applied to the fields, as illustrated below for those within the purple block.	13
6	Flowchart illustrating the outcomes of the formalism.	16
7	Flowchart summarizing the results of the Hubbard model relevant to our analysis below.	19
8	The purple block $(x, t_{k-1}) \rightarrow (x, t_k)$, whose contribution to the partition function is examined below.	20
9	The fields within the purple block are used to define the field $Q(x, t_k)$, as demonstrated below.	22
10	Local $U(1)$ phase rotations applied to the fields, as illustrated below for those within the purple block.	23
11	Flowchart summarizing the analysis conducted thus far.	26
12	Flow diagram depicting the transition from the action to the equations of motion to facilitate the continuum limit in time.	27
13	The contribution of the purple block to the partition function is analyzed below.	29
14	The fields within the purple block are used to define the field $Q(x)$, as demonstrated below.	31
15	Local $U(1)$ phase rotations applied to the fields, as illustrated below for those within the purple block.	32
16	Bipartite lattice illustrating the unit cell.	35
17	Flowchart illustrating the rationale for bosonizing the Hubbard model with a $U(1)$ field.	37
18	Flowchart outlining the steps involved in the bosonization of the 1D Hubbard model. Detailed calculations can be found in Appendix E.	40
19	Two-dimensional lattice. To demonstrate Kadanoff's concept, consider the block labeled b . All four fields linked to the lattice sites within this block (with one site designated as i) are grouped together.	43
20	Cauchy's idea: the value of the contour integral remains unchanged when the contour is rescaled, provided that the rescaling occurs in a region where the function is holomorphic.	77
21	The solution space of the bosonic sector is parametrized by three parameters: r , $\text{Im}(b)$, and $\text{Re}(b)$, with the constraint $r \geq b $. The "light-cone", defined by the surface $r = b $, is highlighted in green.	78
22	Division of $2N$ Majorana fermions into two sets.	83

PROJECT 1

INVESTIGATION INTO STRONG INTERACTIONS IN
FERMIONIC SYSTEMS

1 Introduction to the First Project

1.1 Motivation

For almost a century, the field of condensed matter physics has witnessed significant advances in both the theoretical and experimental domains, driving rapid growth and development. Its capacity to explain a wide range of fascinating physical phenomena continues to draw considerable interest. We were drawn to this field to investigate a specific facet in the first half of the thesis, particularly focusing on strongly correlated electron systems. We begin by outlining some core concepts in this field, followed by a discussion of the motivation for studying strongly correlated systems.

Condensed matter physics deals with understanding the macroscopic behavior of a large collection of simple constituents. The interactions among these constituents can give rise to complex, emergent phenomena. Most of the time, the degrees of freedom describing the low-energy physics of the system are not the microscopic ones. As P.W. Anderson insightfully remarked in his article “More is Different” [7]:

“The ability to reduce everything to simple fundamental laws does not imply the ability to start from those laws and reconstruct the universe.”

“Instead, at each level of complexity entirely new properties appear, and understanding the new behaviors requires research which I think is as fundamental in its nature as any other.”

“...the whole becomes not only more than but very different from the sum of its parts.”

In some instances, the mean-field approximation can provide valuable qualitative insights into physical behavior. For example, the Bardeen-Cooper-Schrieffer (BCS) theory [8] employs a mean-field approximation to describe low-temperature superconductivity. A common technique in quantum field theory for studying fluctuations around the mean-field solution in such scenarios is the Hubbard-Stratonovich (HS) transformation. The core idea of the Hubbard-Stratonovich transformation [9] is to decouple the four-fermion fields interaction term (the two-body interaction term) by coupling it to a collective bosonic field. A schematic representation of the HS transformation is shown below:

$$e^{i\frac{1}{2}\lambda(\bar{\xi}_{\sigma_1}\bar{\tau}_{\sigma_1\sigma_2}\xi_{\sigma_2})^2} \sim \int d\vec{\phi} e^{-i(\frac{1}{2}\vec{\phi}^2 + \sqrt{\lambda}\vec{\phi}\cdot\bar{\xi}_{\sigma_1}\bar{\tau}_{\sigma_1\sigma_2}\xi_{\sigma_2})}. \quad (1)$$

Here $\frac{1}{2}\lambda(\bar{\xi}_{\sigma_1}\bar{\tau}_{\sigma_1\sigma_2}\xi_{\sigma_2})^2$ represents the two-body fermion interaction term, where λ is the strength of the interaction, and $\vec{\phi}$ denotes the bosonic field. It is crucial to note a significant limitation of this approach. This technique is effective for studying fluctuations in the collective bosonic field only when $\lambda \ll 1$ (assuming λ is dimensionless), which corresponds to the weak interaction limit.

However, some of the more challenging and intriguing problems in condensed matter physics over the past few decades cannot be addressed with perturbative methods. This is particularly true for systems with strong correlations. By definition, strongly correlated systems cannot be described straightforwardly as a sum of weakly interacting parts [10].

Notable examples include high-temperature superconductivity, metal-insulator transitions, the fractional quantum Hall effect, and frustrated quantum magnetism, among others.

Currently, effective methods for investigating strongly interacting fermionic systems are scarce. Exact solutions do exist, but only for certain models with strong interactions, such as those solvable by the Bethe Ansatz [11, 12]. This technique is employed to solve one-dimensional interacting quantum systems, like the one-dimensional spin- $\frac{1}{2}$ Heisenberg antiferromagnet chain, providing exact results for ground states and excitation spectra. However, most models cannot be solved exactly.

An alternative strategy is to reformulate complex interacting models to make them weakly interacting [10]. This idea of bosonization was pioneered by Jordan and Wigner [13] in 1928, who illustrated the equivalence between a spin- $\frac{1}{2}$ anisotropic Heisenberg chain and a model of interacting fermions.

Bosonization has become a pivotal non-perturbative technique in quantum field theory, relying on the principle of mapping a system of interacting fermions to an equivalent system of bosons. This review will briefly outline the historical development of this technique and its evolution into an essential tool in the field.¹²

In 1950, Tomonaga [15] posited that the low-energy excitations of an interacting one-dimensional electron gas could be described in terms of collective bosonic modes. Luttinger [16] advanced this concept in 1963 by creating a model based on Tomonaga's theory. However, this model had flaws, including an unbounded Hamiltonian that lacked a ground state. This issue was later resolved by Mattis and Lieb [17] in 1965, marking a key advancement in the development of the bosonization technique.

In 1975, the bosonization method was conceived independently by particle physicists Sidney Coleman [18] and Sidney Mandelstam [19], as well as condensed matter physicists Daniel Mattis [20] and Alan Luther [21]. Their analyses focused on the properties of Dirac fermions in $(1 + 1)$ space-time dimensions.

Using the bosonization method, Haldane [22] provided a low-energy description for a wide range of one-dimensional quantum many-body systems in 1981.³ Another significant advancement in the field occurred in the 1980s when Witten solved the non-Abelian version of bosonization in 1984 [23]. Around the same period, it was also discovered by Polyakov and Wiegmann [24] in 1983, and Knizhnik and Zamolodchikov [25] in 1984. Subsequently, in 1985, Affleck applied the method of non-Abelian bosonization to the problem of spin chains [26].

While we could continue, we will now conclude our exploration of the historical development

¹This is not a complete list but rather highlights key historical milestones in the development of this field.

²We have consulted [10, 14, 9] to explore the history of bosonization and provide a brief summary here.

³In this paper, Haldane coined the term “Luttinger liquid”, which is sometimes referred to as the “Tomonaga-Luttinger liquid”.

of the bosonization technique. To reiterate, this discussion is by no means exhaustive; the aim was to provide a glimpse into how the technique evolved and influenced various applications in condensed matter physics.

There have been several recent developments in this field, both in expanding the method and in applying it to various systems. One example is the work by Huang and Lee [27] in 2021, in which they proposed an extension of Witten’s non-abelian bosonization to two and three spatial dimensions. They applied this extended framework to various systems, including the $SU(2)$ gauge theory of the π -flux phase, and twisted bilayer graphene. Many additional works by different researchers have explored and applied the concept of bosonization; however, these are not detailed here.

In this thesis, we also utilize bosonization to analyze strongly correlated electron systems. Our approach is based on the bosonization formula introduced in [1, 2]. The following section will provide an overview and a brief discussion of this formula.

1.2 Bosonization Formula

The first part of this thesis primarily relies on the bosonization formula introduced in [1, 2]. Using this formula, we develop a method for studying strongly interacting fermionic systems. In this section, we introduce the bosonization formula following [1]. However, we do not provide a derivation here; for a more comprehensive explanation, we recommend consulting [1].

Consider two sets of anti-commuting variables: $\xi_{r,\sigma}$ and $\bar{\xi}_\sigma^r$, with index range $r = 1, \dots, R$ and $\sigma = 1, \dots, n$. Here, r represents the “color” degrees of freedom, while σ indicates the “flavor” degrees of freedom. The anti-commuting variables $\xi_{r,\sigma}$ can be organized into an $R \times n$ rectangular matrix, denoted as ξ , where each matrix element corresponds to $\xi_{r,\sigma}$. Similarly, the variables $\bar{\xi}_\sigma^r$ can be structured into a $n \times R$ rectangular matrix, denoted as $\bar{\xi}$, with elements $\bar{\xi}_\sigma^r$.

Suppose we want to integrate a function $f(\xi, \bar{\xi})$:

$$\int_{\xi} f = \int D\xi f(\xi, \bar{\xi}), \quad (2)$$

where the integration measure is given by:

$$\int D\xi := \prod_{r,\sigma} \frac{\partial^2}{\partial \bar{\xi}_\sigma^r \partial \xi_{r,\sigma}}. \quad (3)$$

Let f in the integral (2) be an analytic and $U(R)$ -invariant function of the variables $\xi, \bar{\xi}$:

$$f(\xi, \bar{\xi}) = f(g\xi, \bar{\xi}g^{-1}), \quad g \in U(R). \quad (4)$$

It is further assumed that f extends to a holomorphic function invariant under $GL(R, \mathbb{C})$. The symmetry relation (4) for this extended function remains valid for all $g \in GL(R, \mathbb{C})$, the

complexified version of $U(R)$.

The bosonization formula enables us to derive a reduction formula for the integral $\int f$ of functions that meet the specified conditions. To present the bosonization formula, the following components are required:

1. First, we use a result from classical invariant theory [28]. The algebra of $GL(R, \mathbb{C})$ -invariant polynomial functions in $\xi, \bar{\xi}$ is generated by invariants that arise at the quadratic level. We now proceed to construct all quadratic invariants under the $U(R)$ symmetry group, using the variables ξ and $\bar{\xi}$:

$$(\bar{\xi} \cdot \xi)_{\sigma\sigma'} = \bar{\xi}_\sigma^r \xi_{r,\sigma'}. \quad (5)$$

The quadratic invariant in equation (5) can be interpreted as an $n \times n$ square matrix represented by $\bar{\xi} \cdot \xi$. We have used the Einstein summation convention over the ‘‘color’’ degrees of freedom in equation (5).

2. Next, consider an $n \times n$ square matrix Q whose matrix elements are represented by $Q_{\sigma\sigma'}$. Impose the following condition on Q :

$$Q = (Q^{-1})^\dagger, \quad (6)$$

which implies that Q is a unitary matrix.

We are now prepared to state the bosonization formula. This formula provides a method for rewriting the integral in equation (2) as an integral over the matrix Q , which has been defined previously. Specifically, the integral can be expressed as follows:

$$\int_\xi f = \int_{U(n)} dQ \text{Det}^{-R}(Q) F(Q). \quad (7)$$

Here, dQ denotes the $U(n)$ Haar measure. $F(Q)$ denotes a function of the unitary matrix Q . Under the substitution $Q \rightarrow \bar{\xi} \cdot \xi$, the function $F(Q)$ becomes equal to the given function $f(\xi, \bar{\xi})$. It is important to note that the choice of the function F is not unique.

The bosonization formula (7) transforms the integration over the Grassmann variables to an integration over the unitary group $U(n)$ defined over the ‘‘flavor’’ space $\mathbb{C}_{\text{flavor}}^n$. To gain a better understanding of the bosonization formula, let us examine the simplest scenario where $R = 1$, and $n = 1$. In this case, the bosonization formula simplifies to:

$$\begin{aligned} \int_\xi f &= \frac{\partial^2}{\partial \bar{\xi} \partial \xi} f(\xi, \bar{\xi}) = \int_0^{2\pi} \frac{d\phi}{2\pi} e^{-i\phi} F(e^{i\phi}) \\ &= \oint \frac{dz}{2\pi iz} \frac{1}{z} F(z), \end{aligned} \quad (8)$$

where we have made the substitution $z = e^{i\phi}$ in the last equality. By examining this simple case, we can interpret the bosonization formula as follows:

Instead of taking partial derivatives with respect to the Grassmann fields, one computes the residue at the poles of the complex contour integral using the residue theorem.

This concludes our review of the bosonization formula. For a comprehensive explanation and proof of the formula, we recommend referring to [1].

1.3 Outline of the First Project

We are now set to explore the realm of strongly interacting systems. The following outline provides a brief roadmap for the first half of this thesis.

In Chapter 2, we describe the functional integral bosonization formalism based on the bosonization formula discussed above to study strongly interacting fermionic systems. We illustrate this formalism using a general model, discuss the obstacles encountered, and outline the strategies employed to overcome them.

In Chapter 3, we apply the formalism to the one-dimensional strongly interacting Hubbard model at half-filling to confirm the validity of our approach and to reproduce established results related to this model. We discuss three different attempts at bosonizing the model; however, we face the persistent challenge of defining a continuum limit in time.

Finally, in Chapter 4, we discuss the concept of renormalization and explore how these ideas can be incorporated into the bosonization scheme to resolve the issue of establishing a well-defined continuum limit. It is important to note that while we discuss the theoretical framework for resolving this issue, the practical execution of these ideas is still a work in progress.

2 A Bosonization Framework Using Functional Integral Language

In this chapter, we introduce our proposed method of functional integral bosonization for investigating strongly correlated electron systems. We begin with the standard steps of constructing a coherent state path integral for fermions. Traditionally, this process involves employing a Hubbard-Stratonovich transformation to decouple the fermion interaction term. However, in this chapter, we will take a different approach by utilizing the bosonization formula (7).

2.1 Steps Involved in the Formalism

Initially, to illustrate the formalism, we will focus on a quantum system described by a 0 + 1 dimensional quantum field theory (QFT) for simplicity. Later, we will extend our analysis to a D+1 dimensional QFT, where D denotes the spatial dimensions and the remaining dimension denotes time.

The single-particle Hilbert space for the system is given by $V = \mathbb{C}^R \otimes \mathbb{C}^n$, where R represents the total number of “color” degrees of freedom, and n describes the total number of “flavor” degrees of freedom. We assume that the Hamiltonian of the system has the following form:

$$H \sim \sum_{\sigma, \sigma'} c_{\sigma}^{\dagger r} c_{r, \sigma'} + \sum_{\sigma, \sigma', \sigma'', \sigma'''} c_{\sigma}^{\dagger r'} c_{\sigma'}^{\dagger r} c_{r, \sigma''} c_{r', \sigma'''}, \quad (9)$$

where r denotes the “color” degrees of freedom, and σ denotes the “flavor” degrees of freedom. We use the Einstein summation convention for the “color” degrees of freedom. The Hamiltonian consists of two terms: a one-body term and a two-body term. Here, $c_{\sigma}^{\dagger r}$ denotes the creation operator for an electron with “color” degree of freedom r and “flavor” degree of freedom σ .

The object of illustration for the formalism is the partition function⁴:

$$\begin{aligned} Z &= \text{Tr} (\rho(T)) \\ &= \text{Tr} \left(e^{-\frac{iHT}{\hbar}} \rho(0) e^{\frac{iHT}{\hbar}} \right), \end{aligned} \quad (10)$$

where $\rho(t)$ denotes the density matrix defined at time t , and Tr denotes the trace over the fermionic Fock space. Diagrammatically, the time evolution of the density matrix can be represented on the closed-time contour⁵ (the Schwinger-Keldysh contour) [29, 30, 31] as follows:

⁴To compute correlation functions, one approach is to introduce source terms into the partition function [29, 30]. However, to illustrate our method, we focus on Z as defined in (10).

⁵The rationale for utilizing the closed-time contour instead of a single time channel will be discussed later in this chapter.

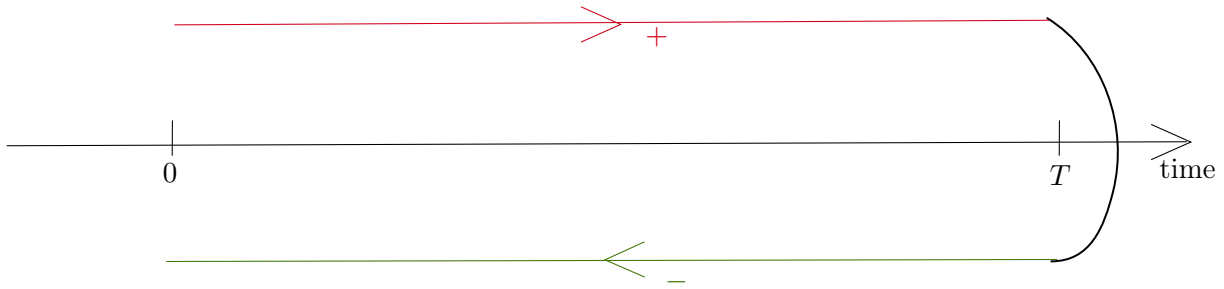


Figure 1: Closed-time contour with $+$ denoting the forward channel and $-$ indicating the backward channel.

The factor $e^{-\frac{iHT}{\hbar}}$ corresponds to the evolution along the forward contour (ket, $+$), while the factor $e^{\frac{iHT}{\hbar}}$ corresponds to the evolution along the backward contour (bra, $-$).

Note. An intuitive way to understand the closed-time contour [32] is to realize that the expectation value of an operator in real time is given by:

$$\langle O(T) \rangle = \text{Tr} \left(e^{\frac{iHT}{\hbar}} O e^{-\frac{iHT}{\hbar}} \rho(0) \right). \quad (11)$$

Our first task is to express the partition function as a functional integral and subsequently apply the bosonization formula (7).

Step 1: Time Discretization

The initial step is to divide the total time T into M discrete time slices:

$$T = M\Delta t. \quad (12)$$

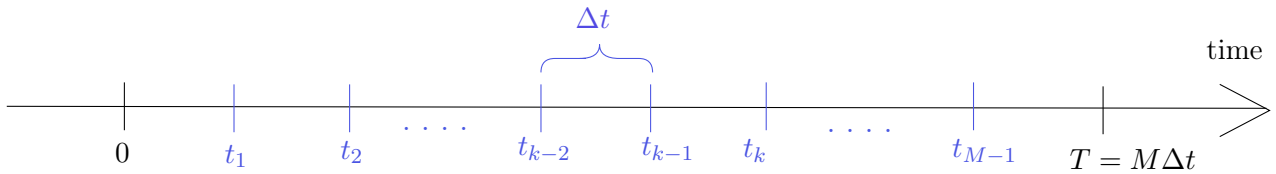


Figure 2: Discretization of time T into M discrete intervals.

Different time slices are indexed by t_k , where $k = 1, 2, \dots, M$. The time interval between two consecutive time slices is denoted by $\Delta t = t_{k-1} - t_{k-2}$.

In this context, we are working within the density matrix path-integral formalism. It is essential to perform time discretization for both factors in the expression for the partition function Z : the forward evolution operator e^{-iHT} (discretized on the forward or $+$ channel), and the backward evolution operator e^{iHT} (discretized on the backward or $-$ channel), as shown below:

$$\begin{aligned} Z &= \text{Tr} \left(e^{-\frac{iTH}{\hbar}} \rho(0) e^{\frac{iTH}{\hbar}} \right) \\ &= \text{Tr} \left(\underbrace{e^{-\frac{i\Delta t H}{\hbar}} \dots e^{-\frac{i\Delta t H}{\hbar}}}_{M \text{ factors}} \rho(0) \underbrace{e^{\frac{i\Delta t H}{\hbar}} \dots e^{\frac{i\Delta t H}{\hbar}}}_{M \text{ factors}} \right). \end{aligned} \quad (13)$$

Step 2: Insertion of Resolution of Identity and Replacement of Operators by Grassmann Fields

The next step is to insert coherent-state resolutions of identity into the time-slice dissection of Z :

$$Z = \text{Tr} \left(e^{\frac{iH\Delta t}{\hbar}} \dots e^{\frac{iH\Delta t}{\hbar}} I e^{-\frac{iH\Delta t}{\hbar}} \dots e^{-\frac{iH\Delta t}{\hbar}} \rho(0) \right) \quad (14)$$

where I denotes the identity operator, and  indicates the insertion of the resolution of identity.

Following this, we examine the contribution from a single block $t_{k-1} \rightarrow t_k$ to the partition function⁶:

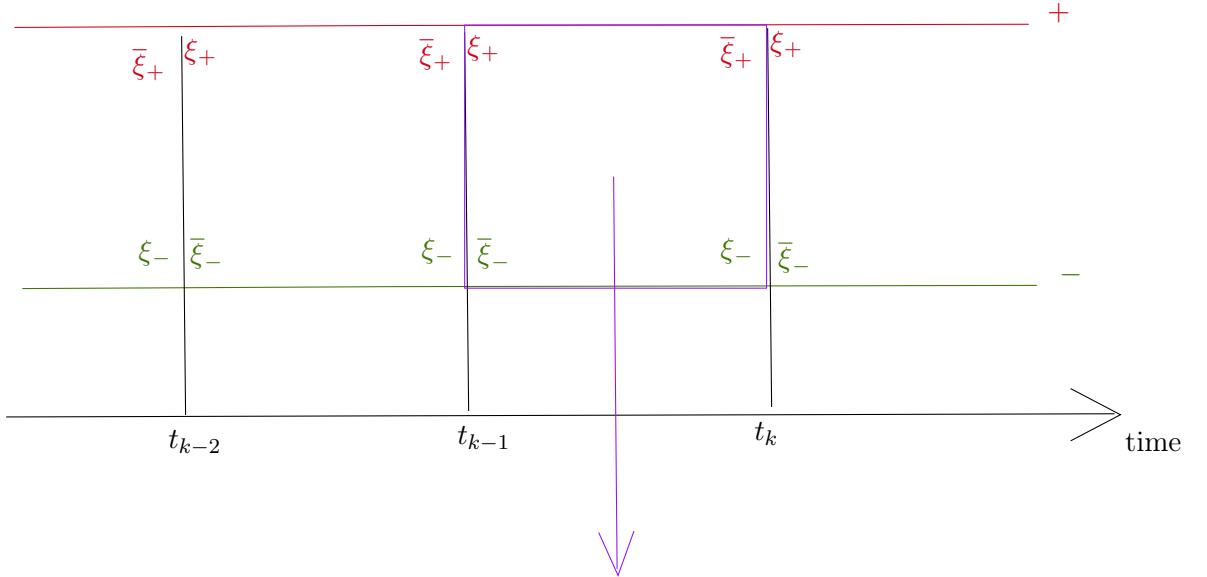


Figure 3: The purple block $t_{k-1} \rightarrow t_k$, whose contribution to the partition function is examined below.

⁶Some steps in the coherent-state path integral construction have been omitted in this discussion. Nevertheless, this method is a common tool in quantum field theory and is widely covered in the literature. For those interested, we mention a few references here [29, 9, 30].

$$\begin{aligned}
 & \prod_{\sigma=1}^n \prod_{r=1}^R \frac{\partial^2}{\partial \bar{\xi}_{+, \sigma}^r(t_k) \partial \xi_{r, +, \sigma}(t_{k-1})} \frac{\partial^2}{\partial \bar{\xi}_{-, \sigma}^r(t_{k-1}) \partial \xi_{r, -, \sigma}(t_k)} \\
 & \exp \left\{ \sum_{\sigma} \bar{\xi}_{+, \sigma}^r(t_k) \xi_{r, +, \sigma}(t_{k-1}) - \frac{i \Delta t}{\hbar} H(\bar{\xi}_{+, \sigma_1}^r(t_k) \xi_{r, +, \sigma_2}(t_{k-1})) \right\} \\
 & \exp \left\{ - \sum_{\sigma} \left(\bar{\xi}_{+, \sigma}^r(t_k) \xi_{r, +, \sigma}(t_k) + \bar{\xi}_{+, \sigma}^r(t_{k-1}) \xi_{r, +, \sigma}(t_{k-1}) \right) \right\} \quad (15) \\
 & \exp \left\{ \sum_{\sigma} \bar{\xi}_{-, \sigma}^r(t_{k-1}) \xi_{r, -, \sigma}(t_k) + \frac{i \Delta t}{\hbar} H(\bar{\xi}_{-, \sigma_1}^r(t_{k-1}) \xi_{r, -, \sigma_2}(t_k)) \right\} \\
 & \exp \left\{ - \sum_{\sigma} \left(\bar{\xi}_{-, \sigma}^r(t_k) \xi_{r, -, \sigma}(t_k) + \bar{\xi}_{-, \sigma}^r(t_{k-1}) \xi_{r, -, \sigma}(t_{k-1}) \right) \right\}.
 \end{aligned}$$

A word on the equation. We outline several points to elaborate on the equation above (15).

1. The variables $\bar{\xi}_{c, \sigma}^r$ and $\xi_{r, c, \sigma}$ represent Grassmann fields introduced during the construction of the coherent state path integral. Here, $r = 1, 2, \dots, R$ signifies the “color” space \mathbb{C}^R , while $c = +, -$ and $\sigma = 1, 2, \dots, n$ indicate the enlarged “flavor” space $\mathbb{C}^{2n} = \mathbb{C}^2 \otimes \mathbb{C}^n$.
2. We have included all the terms in the partition function that contain the fields $\bar{\xi}_{+, \sigma}^r(t_k)$, $\xi_{r, +, \sigma}(t_{k-1})$, $\bar{\xi}_{-, \sigma}^r(t_{k-1})$, and $\xi_{r, -, \sigma}(t_k)$.
3. The terms in the second and third lines of equation (15) represent contributions to the partition function from the $+$ contour, while the terms in the fourth and fifth lines represent contributions from the $-$ contour. Given the assumed form of the Hamiltonian (9), and by replacing the operators (c^\dagger, c) with Grassmann fields $(\bar{\xi}, \xi)$ in the coherent-state path integral, we can elucidate the following terms in equation (15):

$$\begin{aligned}
 H & \equiv : H(c_{\sigma_1}^{\dagger r}, c_{r, \sigma_2}) : \rightarrow H(\bar{\xi}_{+, \sigma_1}^r(t_k), \xi_{r, +, \sigma_2}(t_{k-1})) = H(\bar{\xi}_{+, \sigma_1}^r(t_k) \xi_{r, +, \sigma_2}(t_{k-1})) \text{ on the } + \text{ contour,} \\
 H & \equiv : H(c_{\sigma_1}^{\dagger r}, c_{r, \sigma_2}) : \rightarrow H(\bar{\xi}_{-, \sigma_1}^r(t_{k-1}), \xi_{r, +, \sigma_2}(t_k)) = H(\bar{\xi}_{-, \sigma_1}^r(t_{k-1}) \xi_{r, -, \sigma_2}(t_k)) \text{ on the } - \text{ contour,}
 \end{aligned} \quad (16)$$

where $: H(c_{\sigma_1}^{\dagger r}, c_{r, \sigma_2}) :$ denotes the normal-ordered Hamiltonian. The final equality in both lines of equation (16) arises because each term in the Hamiltonian (9) can be expressed as $\bar{\xi}_{+, \sigma_1}^r(t_k) \xi_{r, +, \sigma_2}(t_{k-1})$ on the $+$ contour, and $\bar{\xi}_{-, \sigma_1}^r(t_{k-1}) \xi_{r, -, \sigma_2}(t_k)$ on the $-$ contour. We demonstrate this below for the $+$ contour, and a similar verification

can be performed for the $-$ contour.

$$\begin{aligned}
 & \sum_{\sigma, \sigma'} c_{\sigma}^{\dagger r} c_{r, \sigma'} + \sum_{\sigma, \sigma', \sigma'', \sigma'''} c_{\sigma}^{\dagger r'} c_{\sigma'}^{\dagger r} c_{r, \sigma''} c_{r', \sigma'''} \\
 & \equiv: H(c_{\sigma_1}^{\dagger r}, c_{r, \sigma_2}) : \\
 & \rightarrow H(\bar{\xi}_{+, \sigma_1}^r(t_k), \xi_{r, +, \sigma_2}(t_{k-1})) \\
 & = \sum_{\sigma, \sigma'} \bar{\xi}_{+, \sigma}^r(t_k) \xi_{r, +, \sigma'}(t_{k-1}) + \sum_{\sigma, \sigma', \sigma'', \sigma'''} \bar{\xi}_{+, \sigma}^{r'}(t_k) \bar{\xi}_{+, \sigma'}^r(t_k) \xi_{r, +, \sigma''}(t_{k-1}) \xi_{r', +, \sigma'''}(t_{k-1}) \\
 & = \sum_{\sigma, \sigma'} \left(\bar{\xi}_{+, \sigma}^r(t_k) \xi_{r, +, \sigma'}(t_{k-1}) \right) + \sum_{\sigma, \sigma', \sigma'', \sigma'''} \left(\bar{\xi}_{+, \sigma}^{r'}(t_k) \xi_{r', +, \sigma'''}(t_{k-1}) \right) \left(\bar{\xi}_{+, \sigma'}^r(t_k) \xi_{r, +, \sigma''}(t_{k-1}) \right) \\
 & = H(\bar{\xi}_{+, \sigma_1}^r(t_k) \xi_{r, +, \sigma_2}(t_{k-1})).
 \end{aligned} \tag{17}$$

4. The third and fifth lines of equation (15), marked in blue, contain terms that are “diagonal in time”, specifically of the form $\bar{\xi}_{c, \sigma}^r(t_k) \xi_{r, c, \sigma}(t_k)$. In contrast, the second and fourth line of the equation (15), highlighted in brown, include terms referred to as “off-diagonal in time”, such as $\bar{\xi}_{+, \sigma_1}^r(t_k) \xi_{r, +, \sigma_2}(t_{k-1})$, or $\bar{\xi}_{-, \sigma_1}^r(t_{k-1}) \xi_{r, -, \sigma_2}(t_k)$.

Step 3: Bosonization

The third and final step is the most important in our formalism. Here, we deviate from the usual strategy of using the Hubbard-Stratonovich transformation to decouple the fermion interaction term with a local bosonic field. Instead, we apply the bosonization identity (7).

The main idea behind the bosonization method is to rewrite the theory of fermions in terms of $U(R)$ -invariant “color singlets” formed using the fermionic fields. Referring to the expression (15) above, there are two choices for forming “color singlets”:

$$\begin{pmatrix} \bar{\xi}_{+, \sigma}^r(t_k) \\ \bar{\xi}_{-, \sigma}^r(t_{k-1}) \end{pmatrix} \begin{pmatrix} \xi_{r, +, \sigma'}(t_{k-1}) & \xi_{r, -, \sigma'}(t_k) \end{pmatrix}, \tag{18}$$

OR

$$\begin{pmatrix} \bar{\xi}_{+, \sigma}^r(t_k) \\ \bar{\xi}_{-, \sigma}^r(t_k) \end{pmatrix} \begin{pmatrix} \xi_{r, +, \sigma'}(t_k) & \xi_{r, -, \sigma'}(t_k) \end{pmatrix}. \tag{19}$$

Notice that the two different choices arise from the difference in the time arguments of the fields. Out of these two options, we choose the first one to form color singlets.⁷

Using the bosonization formula (7), we want to express the chosen “color-singlets” (18) as a $U(2n)$ unitary matrix $Q(t_k)$ in the $\mathbb{C}^2 \otimes \mathbb{C}^n$ “flavor” space. Let us take a moment to explain the $Q(t_k)$ matrix.

⁷We choose this option since this combination of fields appears in the terms of the partition function originating from the Hamiltonian, as shown in equation (16).

Components of the $Q(t_k)$ Matrix

The $Q(t_k)$ matrix is defined as a $2n \times 2n$ unitary matrix in $\mathbb{C}^2 \otimes \mathbb{C}^n$ “flavor” space. The components of the matrix can be understood as follows:

$$Q(t_k) = \begin{bmatrix} Q_{++}(t_k) & Q_{+-}(t_k) \\ Q_{-+}(t_k) & Q_{--}(t_k) \end{bmatrix}, \quad (20)$$

where each block in the above matrix is a $n \times n$ matrix. The components of the matrix $Q(t_k)$ in terms of the fermionic fields are defined below:

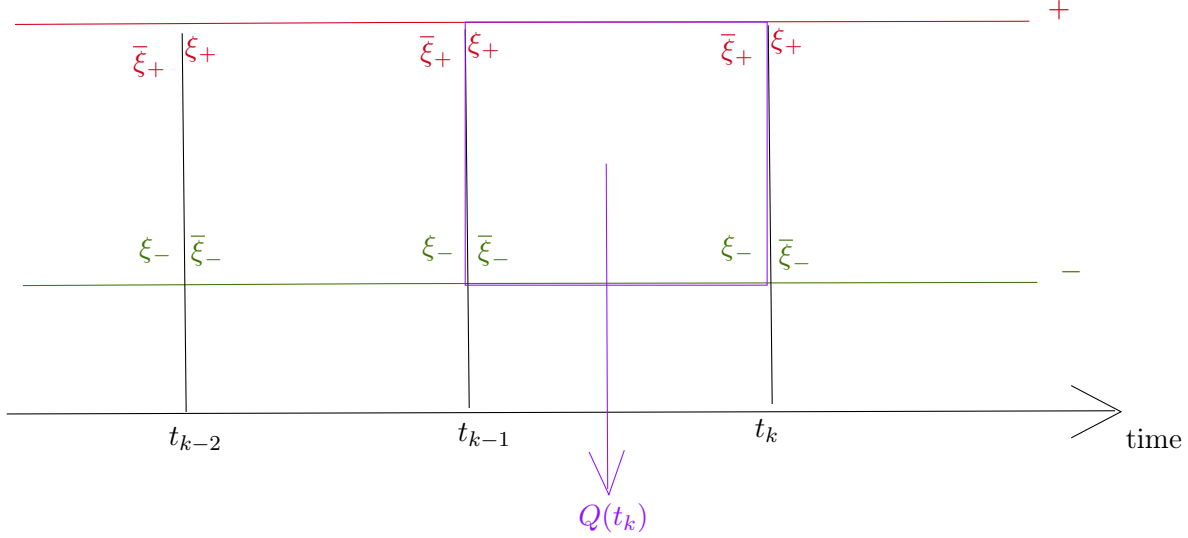


Figure 4: The fields within the purple block are used to define the field $Q(t_k)$, as demonstrated below.

$$\begin{aligned} (Q_{++})_{\sigma\sigma'}(t_k) &= \bar{\xi}_{+,\sigma}^r(t_k)\xi_{r,+,\sigma'}(t_{k-1}), \\ (Q_{+-})_{\sigma\sigma'}(t_k) &= \bar{\xi}_{+,\sigma}^r(t_k)\xi_{r,-,\sigma'}(t_k), \\ (Q_{-+})_{\sigma\sigma'}(t_k) &= \bar{\xi}_{-,\sigma}^r(t_{k-1})\xi_{r,+,\sigma'}(t_{k-1}), \\ (Q_{--})_{\sigma\sigma'}(t_k) &= \bar{\xi}_{-,\sigma}^r(t_{k-1})\xi_{r,-,\sigma'}(t_k). \end{aligned} \quad (21)$$

We are now almost in a position to reformulate the partition function (15) using the matrix Q . However, one major obstacle remains: there are a few terms in the partition function

$$\begin{aligned} &\exp \left\{ - \sum_{\sigma} \left(\bar{\xi}_{+,\sigma}^r(t_k)\xi_{r,+,\sigma}(t_k) + \bar{\xi}_{+,\sigma}^r(t_{k-1})\xi_{r,+,\sigma}(t_{k-1}) \right) \right\}, \\ &\exp \left\{ - \sum_{\sigma} \left(\bar{\xi}_{-,\sigma}^r(t_k)\xi_{r,-,\sigma}(t_k) + \bar{\xi}_{-,\sigma}^r(t_{k-1})\xi_{r,-,\sigma}(t_{k-1}) \right) \right\}, \end{aligned} \quad (22)$$

that cannot be expressed in terms of the $U(R)$ -invariant Q field. The question arises: how should we handle these terms? A possible solution to this issue is to employ a trick involving local $U(R)$ -transformations (where “local” refers to transformations that are local in time). We demonstrate below how this method works.

Step 3.1: Local $U(R)$ -Transformations and Linked Cluster Expansion

To express all terms in the partition function in terms of the Q field, we apply the following local $U(R)$ -transformations:

\times : local $U(R)$ – transformation $g(\cdot)$.

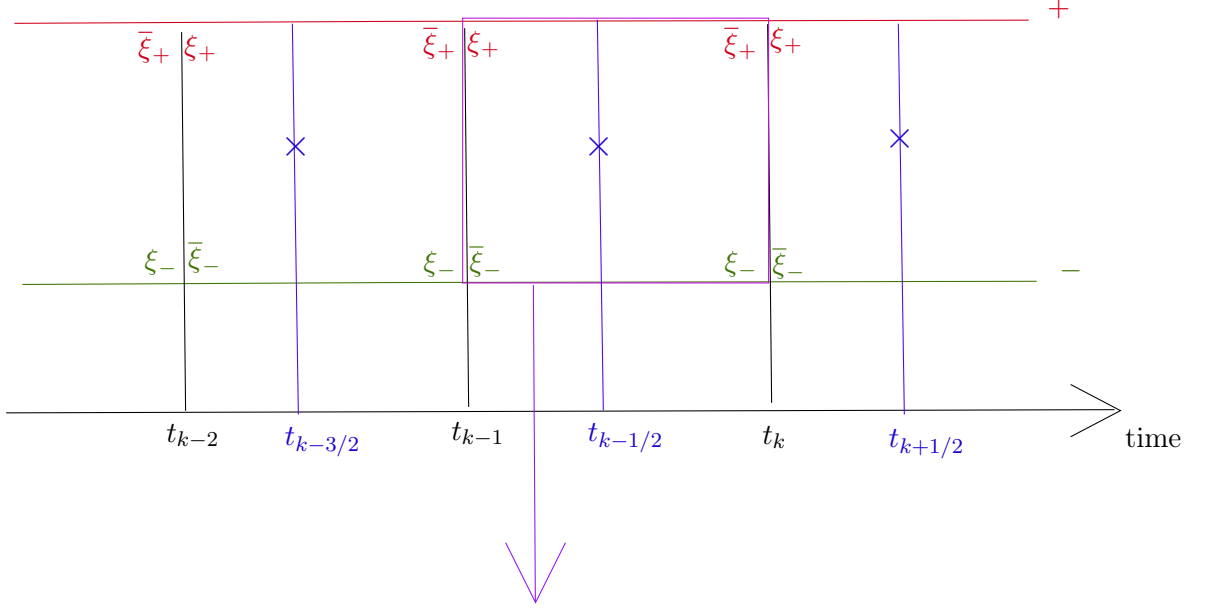


Figure 5: Local $U(R)$ -transformations applied to the fields, as illustrated below for those within the purple block.

$$\begin{aligned}
 \bar{\xi}_{+,\sigma}^r(t_k) &\rightarrow \bar{\xi}_{+,\sigma}^{r_1}(t_k) g^{-1}(t_{k-\frac{1}{2}})_{r_1}^r, \\
 \xi_{r,+,\sigma}(t_{k-1}) &\rightarrow g(t_{k-\frac{1}{2}})_{r_1}^{r_2} \xi_{r_2,+,\sigma}(t_{k-1}), \\
 \bar{\xi}_{-,\sigma}^r(t_{k-1}) &\rightarrow \bar{\xi}_{-,\sigma}^{r_1}(t_{k-1}) g^{-1}(t_{k-\frac{1}{2}})_{r_1}^r, \\
 \xi_{r,-,\sigma}(t_k) &\rightarrow g(t_{k-\frac{1}{2}})_{r_1}^{r_2} \xi_{r_2,-,\sigma}(t_k).
 \end{aligned} \tag{23}$$

Here, $g(t_{k-\frac{1}{2}})$ represents a $U(R)$ matrix, and the Einstein summation convention is applied.

The next step is to perform an average over the $U(R)$ -transformations under the Berezin integral sign, $(\int_{\bar{\xi},\xi})$:

$$\begin{aligned}
 &\int_{U(R)} \prod_t dg(t) \exp \left\{ - \sum_{\sigma} \left(\bar{\xi}_{+,\sigma}^{r_1}(t_k) g^{-1}(t_{k-\frac{1}{2}})_{r_1}^r g(t_{k+\frac{1}{2}})_{r_1}^{r_2} \xi_{r_2,+,\sigma}(t_k) \right. \right. \\
 &\quad \left. \left. + \bar{\xi}_{+,\sigma}^{r_1}(t_{k-1}) g^{-1}(t_{k-\frac{3}{2}})_{r_1}^r g(t_{k-\frac{1}{2}})_{r_1}^{r_2} \xi_{r_2,+,\sigma}(t_{k-1}) \right) \right\} \\
 &\exp \left\{ - \sum_{\sigma} \left(\bar{\xi}_{-,\sigma}^{r_1}(t_k) g^{-1}(t_{k+\frac{1}{2}})_{r_1}^r g(t_{k-\frac{1}{2}})_{r_1}^{r_2} \xi_{r_2,-,\sigma}(t_k) \right. \right. \\
 &\quad \left. \left. + \bar{\xi}_{-,\sigma}^{r_1}(t_{k-1}) g^{-1}(t_{k-\frac{1}{2}})_{r_1}^r g(t_{k-\frac{3}{2}})_{r_1}^{r_2} \xi_{r_2,-,\sigma}(t_{k-1}) \right) \right\} \\
 &\equiv e^{-S_c},
 \end{aligned} \tag{24}$$

to obtain the contribution S_c from the terms in equation (22) to the partition function. Here, $dg(t)$ denotes the Haar measure on $U(R)$. By construction, S_c can be expressed in terms of the ‘‘color-singlet’’ in (18), which is used to define the $Q(t_k)$ field. It admits a linked-cluster expansion, organized by powers of $\frac{1}{R}$.⁸ Using the following properties of the $U(R)$ -Haar integrals [33]⁹:

$$\begin{aligned} \int_{U(R)} \prod_t dg(t) g^{-1}(t_p)_{r_2}^{r_1} g(t_q)_{r'_1}^{r'_2} &= \frac{\delta_{t_p, t_q}}{R} \delta_{r'_1}^{r_1} \delta_{r_2}^{r'_2}, \\ \int_{U(R)} \prod_t dg(t) g^{-1}(t_{p-\frac{1}{2}})_{r_2}^{r_1} g(t_{p-\frac{1}{2}})_{r'_1}^{r'_2} g^{-1}(t_{p+\frac{1}{2}})_{r_4}^{r_3} g(t_{p+\frac{1}{2}})_{r'_3}^{r'_4} &= \frac{1}{R^2 - 1} \delta_{r'_1}^{r_1} \delta_{r'_2}^{r_2} \delta_{r'_3}^{r_3} \delta_{r'_4}^{r_4}, \end{aligned} \quad (25)$$

we find that the first term $S_c^{(1)}$ of the linked-cluster expansion contributes zero, while the first non-zero contribution arises from the second term $S_c^{(2)}$ of the linked-cluster expansion:

$$\begin{aligned} S_c^{(2)} = \frac{1}{R^2 - 1} \sum_{\sigma_1, \sigma_2} &\left(\bar{\xi}_{+, \sigma_1}^{r_1}(t_k) \xi_{r_1, -, \sigma_2}(t_k) \bar{\xi}_{-, \sigma_2}^{r_2}(t_k) \xi_{r_2, +, \sigma_1}(t_k) \right. \\ &\left. + \bar{\xi}_{+, \sigma_1}^{r_1}(t_{k-1}) \xi_{r_1, -, \sigma_2}(t_{k-1}) \bar{\xi}_{-, \sigma_2}^{r_2}(t_{k-1}) \xi_{r_2, +, \sigma_1}(t_{k-1}) \right). \end{aligned} \quad (26)$$

Note. Here, we perform a linked-cluster expansion in powers of $\frac{1}{R}$, assuming $R \gg 1$. However, it is important to note that we will relax this assumption in our later analysis and employ a different expansion parameter for the linked-cluster expansion. When applying this formalism to various systems, we will utilize the fact that we are dealing with strongly interacting systems and conduct the linked-cluster expansion in a manner that remains valid in the strong-interaction limit.

For example, when considering the strongly interacting Hubbard model, we will expand in terms of $\frac{\tau_h}{U}$, where U represents the interaction strength, and τ_h denotes the hopping parameter. In the strong interaction regime, characterized by $U \gg \tau_h$, $\frac{\tau_h}{U}$ serves as a suitable parameter for expansion.

We previously mentioned that we would explain the reason for using a closed-time contour soon. Now, we take a moment to discuss why this approach is necessary. Our goal is to convert the complete set of Grassmann fields into a bosonic field $Q(t_k)$, as described in equation (21), which is ‘‘local’’ in time. However, we face a challenge: not all terms in the partition function can be directly expressed in terms of this bosonic field.

For example, consider the term $\bar{\xi}_{+, \sigma}^r(t_k) \xi_{r, +, \sigma}(t_k)$. To address this issue, we perform a local $U(R)$ -transformation and employ a linked-cluster expansion. Without the closed-time contour, it is not immediately clear how to pair this term with others in the linked-cluster expansion to express their product in terms of $Q(t_k)$. The additional channel allows us to pair this term with $\bar{\xi}_{-, \sigma}^r(t_k) \xi_{r, -, \sigma}(t_k)$ in the linked-cluster expansion (as demonstrated in equation (26)), facilitating the expression of the combination in terms of $Q(t_k)$. This operational reason explains why we use a closed-time contour to bosonize the complete set of Grassmann fields into a ‘‘time-local’’ bosonic field.

⁸A brief overview of the linked-cluster expansion used in this context is provided in Appendix A.

⁹In general, the values of such integrals are expressed in terms of the Weingarten function [33].

In future analyses, particularly in the next chapter, if we relax the condition that the bosonic field needs to be “local” in time or if we only bosonize a subset of Grassmann fields, we may not need the closed-time contour.

Now that we have addressed this point, we are ready to proceed with the bosonization step. The partition function, in terms of the field Q after bosonization, is given by:

$$\begin{aligned}
 & \int_{U(2n)} dQ(t_k) \text{Det}^{-R}(Q(t_k)) \\
 & \exp \left\{ \sum_{\sigma} (Q_{++})_{\sigma\sigma}(t_k) - \frac{i\Delta t}{\hbar} H(Q_{++}(t_k)) \right\} \\
 & \exp \left\{ \sum_{\sigma} (Q_{--})_{\sigma\sigma}(t_k) + \frac{i\Delta t}{\hbar} H(Q_{--}(t_k)) \right\} \\
 & \exp \left\{ -\frac{1}{R^2 - 1} \sum_{\sigma_1, \sigma_2} \left((Q_{+-})_{\sigma_1\sigma_2}(t_k) (Q_{-+})_{\sigma_2\sigma_1}(t_{k+1}) + (Q_{+-})_{\sigma_1\sigma_2}(t_{k-1}) (Q_{-+})_{\sigma_2\sigma_1}(t_k) \right) \right\}.
 \end{aligned} \tag{27}$$

This completes our three-step procedure for reformulating the partition function, originally expressed in terms of fermionic fields, in terms of a $U(2n)$ bosonic¹⁰ field.

¹⁰By “bosonic”, we mean that the components of the $U(2n)$ matrix have commuting variables as entries because they are formed by the product of two Grassmann fields.

2.2 Summary

Let us summarize what we have accomplished thus far through a flowchart.

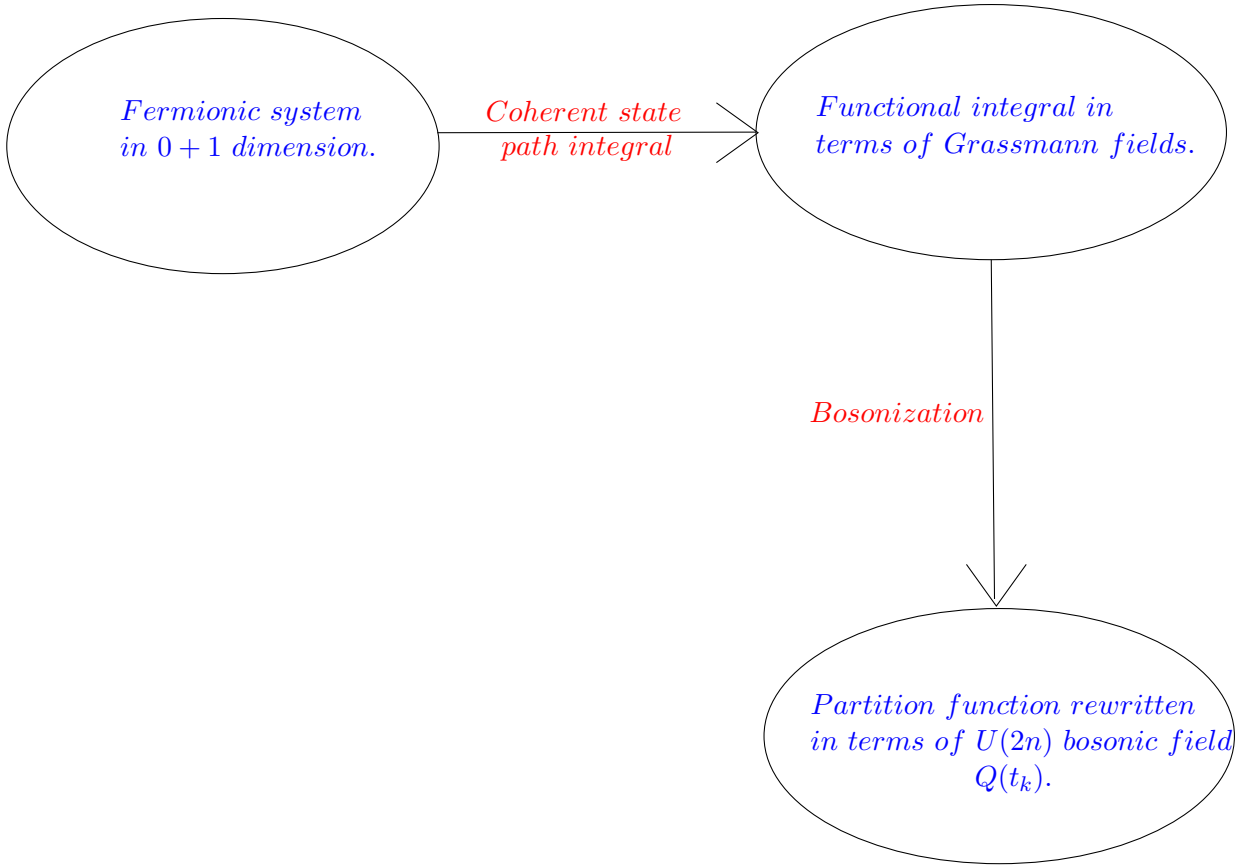


Figure 6: Flowchart illustrating the outcomes of the formalism.

By employing the functional integral bosonization technique, we have successfully expressed the partition function as an integral over a $U(2n)$ bosonic field, thereby bosonizing the fermionic system. While this approach may initially appear straightforward, it is essential to note an important caveat. Specifically, we will encounter a technical challenge related to taking the continuum limit in time during our subsequent analysis, which will begin in the next chapter. Having established this formalism, we will now focus on applying it to a specific model in the following chapter.

3 Application: Functional Integral Bosonization Approach to the Strongly Interacting One-Dimensional Hubbard Model at Half-Filling

In this chapter, we apply the functional integral bosonization technique, as developed in the preceding chapter, to the strongly interacting Hubbard model at half-filling in 1+1 space-time dimensions. Our primary objective is to validate this approach by reproducing well-established results of the Hubbard model. Before proceeding with the analysis, we will briefly revisit some essential features of the Hubbard model, drawing on [9, 34, 35] to provide necessary context.

3.1 The Hubbard Model

The Hubbard model is an excellent starting point for studying strongly correlated electron systems due to its simplicity. Despite its apparent simplicity, the Hubbard model can exhibit a rich phase diagram with a plethora of interesting phases such as antiferromagnetic Mott insulator, charge density wave (CDW), spin density wave (SDW), superconductor, and more. Let us begin our brief review of the Hubbard model by specifying its Hamiltonian.

The Hamiltonian of the one-band Hubbard model is given by:

$$\begin{aligned}
 H = & -\tau_h \sum_{x,\sigma} (c_\sigma^\dagger(x+a)c_\sigma(x) + c_\sigma^\dagger(x)c_\sigma(x+a)) \\
 & + U \sum_x c_\uparrow^\dagger(x)c_\downarrow^\dagger(x)c_\downarrow(x)c_\uparrow(x) - \mu \sum_{x,\sigma} c_\sigma^\dagger(x)c_\sigma(x),
 \end{aligned} \tag{28}$$

where $c_\sigma^\dagger(x)$ creates an electron at site x with spin σ , and a denotes the lattice constant. The first term in the Hamiltonian represents hopping of electrons between nearest neighboring sites with hopping parameter τ_h . The second term represents the on-site repulsive interaction term between electrons, with interaction strength $U > 0$, and the last term represents the chemical potential term with μ denoting the chemical potential. At half-filling $\nu = \frac{1}{2}$, the chemical potential μ is equal to $\frac{U}{2}$.

Remark. We denote the hopping parameter as τ_h instead of the commonly used symbol t , which we reserve to represent time.

We now outline several prominent features of the Hubbard model.

1. The Hubbard model Hamiltonian is invariant under the following $U(1)$ transformation:

$$\begin{aligned}
 c_\sigma(x) & \rightarrow e^{i\theta} c_\sigma(x), \\
 c_\sigma^\dagger(x) & \rightarrow c_\sigma^\dagger(x) e^{-i\theta}.
 \end{aligned} \tag{29}$$

This invariance corresponds to charge conservation.

2. The Hubbard model Hamiltonian is spin-rotation invariant, meaning it remains

unchanged under the following $SU(2)$ transformation:

$$\begin{aligned} c_\sigma(x) &\rightarrow \sum_{\sigma'} U_{\sigma\sigma'} c_{\sigma'}(x), \\ c_\sigma^\dagger(x) &\rightarrow \sum_{\sigma'} c_{\sigma'}^\dagger(x) U_{\sigma'\sigma}^{-1}, \end{aligned} \quad (30)$$

where $U \in SU(2)$.

3. In the strong interaction limit ($U \gg \tau_h$), and at half-filling $\nu = \frac{1}{2}$, the Hubbard model maps to the spin- $\frac{1}{2}$ quantum Heisenberg antiferromagnet. Using Brillouin-Wigner perturbation theory [9], one can derive the effective Hamiltonian:

$$H_{\text{eff}} = \frac{J}{\hbar^2} \sum_x \sum_{j=1,2,3} S^j(x) S^j(x+a), \quad (31)$$

where $S^j(x) = \frac{\hbar}{2} \sum_{\sigma,\sigma'} c_\sigma^\dagger(x) \boldsymbol{\tau}_{\sigma\sigma'}^j c_{\sigma'}(x)$ represents the three components of the spin operator, and $\boldsymbol{\tau}^j$ denotes the standard Pauli matrices. The exchange coupling J is given by $\frac{2\tau_h^2}{U}$. This implies that, at half-filling, the charge degrees of freedom are gapped in the strong interaction limit, leaving the spin degrees of freedom as the dominant low-energy excitations.

Using a semiclassical treatment [35, 9], one can demonstrate that the system's low-energy excitations are spin waves characterized by a linear dispersion relation:

$$\omega(\tilde{k}) = \frac{J}{\hbar} \left(\frac{\tilde{k}a}{2} \right). \quad (32)$$

Remark. To avoid confusion with the time-slice label used in the coherent-state path integral construction, we use \tilde{k} to denote the wave-number instead of k .

4. Away from half-filling ($\nu < \frac{1}{2}$), the effective Hamiltonian takes the form:

$$\begin{aligned} H &= -\tau_h \sum_{x,\sigma} (c_\sigma^\dagger(x+a) c_\sigma(x) + c_\sigma^\dagger(x) c_\sigma(x+a)) \\ &+ \frac{J}{\hbar^2} \sum_x \sum_{j=1,2,3} S^j(x) S^j(x+a) \end{aligned} \quad (33)$$

with the constraint

$$\sum_\sigma c_\sigma^\dagger(x) c_\sigma(x) = 0 \text{ or } 1, \quad (34)$$

which eliminates doubly occupied sites.

That concludes our brief overview of the Hubbard model. In our analysis, we will primarily focus on the third aspect (32) and aim to rederive the result using our formalism. The outcome is summarized in the flowchart below.

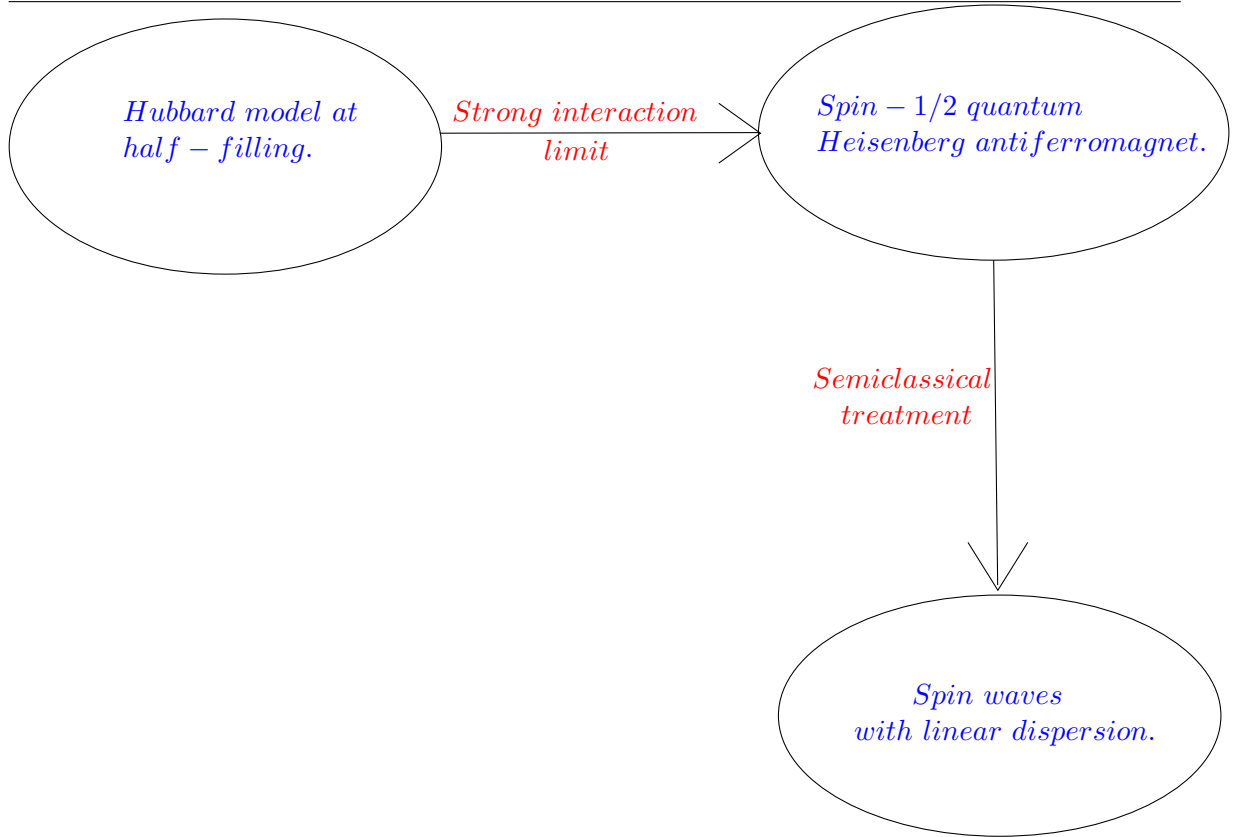


Figure 7: Flowchart summarizing the results of the Hubbard model relevant to our analysis below.

3.2 Attempt I: Reformulation of the Partition Function Using the $Q(x, t_k) \in U(4)$ Field

We now begin our study of the Hubbard model using the functional integral bosonization method. In this section, our objective is to derive spin-wave solutions as the low-energy excitations of the system in the strong interaction limit.

First, we note that we are working with a one-band Hubbard model, meaning that $R = 1$ (single “color” degree of freedom). The enlarged “flavor” space for this problem is $\mathbb{C}_{\text{contour}}^2 \otimes \mathbb{C}_{\text{spin}}^2$, where $\mathbb{C}_{\text{contour}}^2$ refers to the two channels (+/-) on the closed-time contour, and $\mathbb{C}_{\text{spin}}^2$ refers to the spin.

Next, we apply the three steps of the technique outlined in Section 2.1 to the Hubbard model. Our goal is to rewrite the partition function in terms of a “local” bosonic field $Q(x, t)$, which is “local” in both space and time.

The initial step of time discretization remains unchanged. However, there is a noticeable change in the second step. We retain terms up to order $(\Delta t)^2$ in the partition function. Let us explain the rationale behind doing that. Consider the terms in the Hamiltonian of the Hubbard model. The interaction term is spatially “local”, meaning all fields in the term are defined at the same spatial point, whereas the hopping term is “non-local” in space. To express the contribution from the hopping term to the partition function in terms of the

3 APPLICATION: FUNCTIONAL INTEGRAL BOSONIZATION APPROACH TO THE STRONGLY INTERACTING ONE-DIMENSIONAL HUBBARD MODEL AT HALF-FILLING

bosonic field $Q(x, t)$, which is defined to be “local” in space, we encounter a difficulty. To address this issue, we employ the technique of local $U(1)$ phase rotations. This will result in a term of order $(\Delta t)^2$. Therefore, in order to be consistent, we include terms up to order $(\Delta t)^2$ in the expression for the partition function.

We will now express the contribution from the block $(x, t_{k-1}) \rightarrow (x, t_k)$ to the partition function:

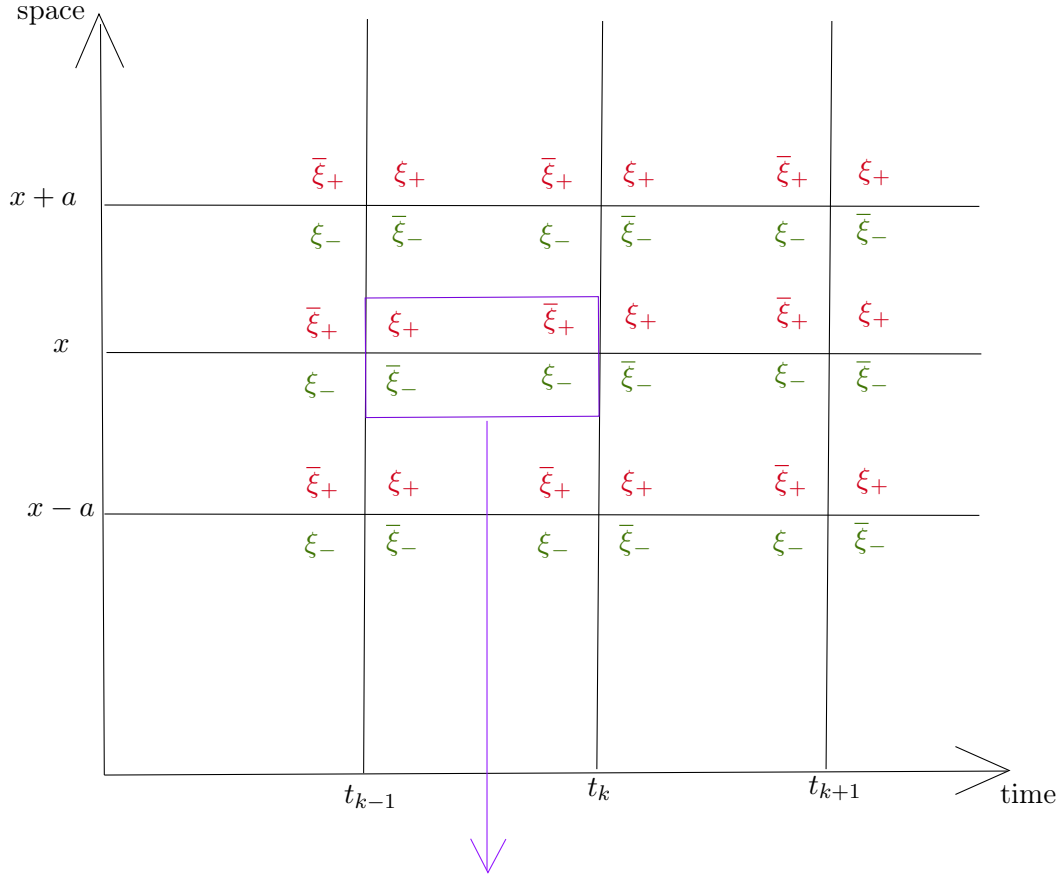


Figure 8: The purple block $(x, t_{k-1}) \rightarrow (x, t_k)$, whose contribution to the partition function is examined below.

$$\begin{aligned}
& \prod_{\sigma=\uparrow,\downarrow} \frac{\partial^2}{\partial \bar{\xi}_{+,\sigma}(x, t_k) \partial \xi_{+,\sigma}(x, t_{k-1})} \frac{\partial^2}{\partial \bar{\xi}_{-,\sigma}(x, t_{k-1}) \partial \xi_{-,\sigma}(x, t_k)} \\
& \exp \left\{ \sum_{\sigma} \bar{\xi}_{+,\sigma}(x, t_k) \xi_{+,\sigma}(x, t_{k-1}) - \left(\frac{iU\Delta t}{\hbar} \right) \bar{\xi}_{+,\uparrow}(x, t_k) \bar{\xi}_{+,\downarrow}(x, t_k) \xi_{+,\downarrow}(x, t_{k-1}) \xi_{+,\uparrow}(x, t_{k-1}) \right. \\
& + \left(\frac{iU\Delta t}{2\hbar} \right) \sum_{\sigma} \bar{\xi}_{+,\sigma}(x, t_k) \xi_{+,\sigma}(x, t_{k-1}) + \left(\frac{U\Delta t}{\hbar} \right)^2 \bar{\xi}_{+,\uparrow}(x, t_k) \bar{\xi}_{+,\downarrow}(x, t_k) \xi_{+,\downarrow}(x, t_{k-1}) \xi_{+,\uparrow}(x, t_{k-1}) \\
& \left. - \left(\frac{U\Delta t}{2\hbar} \right)^2 \sum_{\sigma} \bar{\xi}_{+,\sigma}(x, t_k) \xi_{+,\sigma}(x, t_{k-1}) - \left(\frac{\tau_h \Delta t}{\hbar} \right)^2 \sum_{\sigma} \bar{\xi}_{+,\sigma}(x, t_k) \xi_{+,\sigma}(x, t_{k-1}) \right\} \\
& \exp \left\{ - \sum_{\sigma} \bar{\xi}_{+,\sigma}(x, t_k) \xi_{+,\sigma}(x, t_k) - \sum_{\sigma} \bar{\xi}_{+,\sigma}(x, t_{k-1}) \xi_{+,\sigma}(x, t_{k-1}) \right. \\
& \left. + \left(\frac{i\tau_h \Delta t}{\hbar} \right) \sum_{\sigma, y=x+a, x-a} \bar{\xi}_{+,\sigma}(x, t_k) \xi_{+,\sigma}(y, t_{k-1}) + \bar{\xi}_{+,\sigma}(y, t_k) \xi_{+,\sigma}(x, t_{k-1}) \right\} \\
& \exp \left\{ \sum_{\sigma} \bar{\xi}_{-,\sigma}(x, t_{k-1}) \xi_{-,\sigma}(x, t_k) + \left(\frac{iU\Delta t}{\hbar} \right) \bar{\xi}_{-,\uparrow}(x, t_{k-1}) \bar{\xi}_{-,\downarrow}(x, t_{k-1}) \xi_{-,\downarrow}(x, t_k) \xi_{-,\uparrow}(x, t_k) \right. \\
& - \left(\frac{iU\Delta t}{2\hbar} \right) \sum_{\sigma} \bar{\xi}_{-,\sigma}(x, t_{k-1}) \xi_{-,\sigma}(x, t_k) + \left(\frac{U\Delta t}{\hbar} \right)^2 \bar{\xi}_{-,\uparrow}(x, t_{k-1}) \bar{\xi}_{-,\downarrow}(x, t_{k-1}) \xi_{-,\downarrow}(x, t_k) \xi_{-,\uparrow}(x, t_k) \\
& \left. - \left(\frac{U\Delta t}{2\hbar} \right)^2 \sum_{\sigma} \bar{\xi}_{-,\sigma}(x, t_{k-1}) \xi_{-,\sigma}(x, t_k) - \left(\frac{\tau_h \Delta t}{\hbar} \right)^2 \sum_{\sigma} \bar{\xi}_{-,\sigma}(x, t_{k-1}) \xi_{-,\sigma}(x, t_k) \right\} \\
& \exp \left\{ - \sum_{\sigma} \bar{\xi}_{-,\sigma}(x, t_k) \xi_{-,\sigma}(x, t_k) - \sum_{\sigma} \bar{\xi}_{-,\sigma}(x, t_{k-1}) \xi_{-,\sigma}(x, t_{k-1}) \right. \\
& \left. - \left(\frac{i\tau_h \Delta t}{\hbar} \right) \sum_{\sigma, y=x+a, x-a} \bar{\xi}_{-,\sigma}(x, t_{k-1}) \xi_{-,\sigma}(y, t_k) + \bar{\xi}_{-,\sigma}(y, t_{k-1}) \xi_{-,\sigma}(x, t_k) \right\}.
\end{aligned} \tag{35}$$

A word on the equation. We present several points to elaborate on the equation above (35):

1. We retain terms up to order $(\Delta t)^2$ in the coherent-state path integral construction. However, certain terms of this order that we have omitted from the expression for the partition function (35) are considered “non-local” in space. The rationale for their exclusion is that, as our analysis progresses, these terms will drop out and will not influence the final expression.
2. The terms highlighted in blue can be classified into two categories: those that are “local” in space and “diagonal in time”, such as $\bar{\xi}_{+,\sigma}(x, t_k) \xi_{+,\sigma}(x, t_k)$, and those that are “non-local” in space and “off-diagonal in time”, such as $\bar{\xi}_{-,\sigma}(x, t_{k-1}) \xi_{-,\sigma}(y, t_k)$. In contrast, the terms highlighted in brown are “local” in space and “off-diagonal in time”, exemplified by $\bar{\xi}_{+,\sigma}(x, t_k) \xi_{+,\sigma}(x, t_{k-1})$.

We aim to express the above equation (35) in terms of the field $Q(x, t_k)$ defined as follows:

3 APPLICATION: FUNCTIONAL INTEGRAL BOSONIZATION APPROACH TO THE STRONGLY INTERACTING ONE-DIMENSIONAL HUBBARD MODEL AT HALF-FILLING

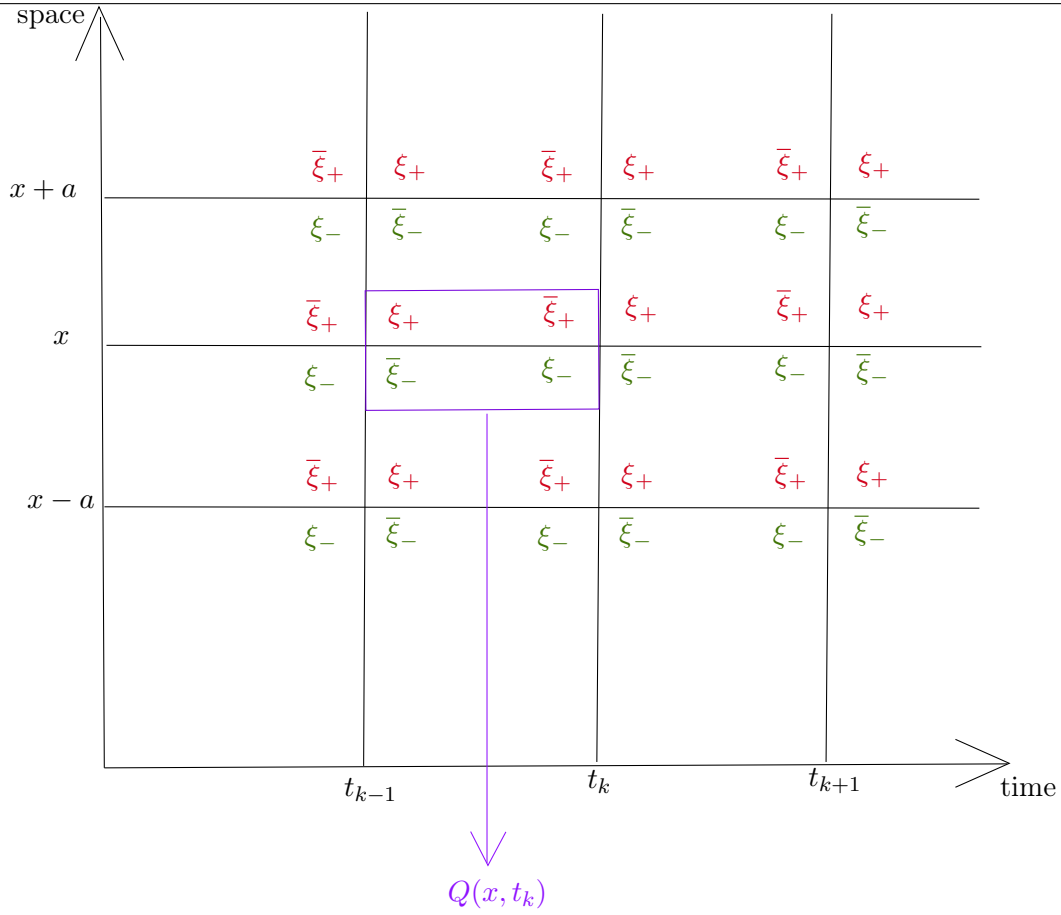


Figure 9: The fields within the purple block are used to define the field $Q(x, t_k)$, as demonstrated below.

$$\begin{aligned}
(Q_{++})_{\sigma_1\sigma_2}(x, t_k) &= \bar{\xi}_{+, \sigma_1}(x, t_k)\xi_{+, \sigma_2}(x, t_{k-1}), \\
(Q_{+-})_{\sigma_1\sigma_2}(x, t_k) &= \bar{\xi}_{+, \sigma_1}(x, t_k)\xi_{-, \sigma_2}(x, t_k), \\
(Q_{-+})_{\sigma_1\sigma_2}(x, t_k) &= \bar{\xi}_{-, \sigma_1}(x, t_{k-1})\xi_{+, \sigma_2}(x, t_{k-1}), \\
(Q_{--})_{\sigma_1\sigma_2}(x, t_k) &= \bar{\xi}_{-, \sigma_1}(x, t_{k-1})\xi_{-, \sigma_2}(x, t_k).
\end{aligned} \tag{36}$$

However, the terms highlighted in blue in the partition function (35) cannot be directly expressed in terms of the field $Q(x, t_k)$. To account for the contributions from these terms, we perform local $U(1)$ phase rotations. Before doing so, we first rescale all fields by a factor of $(\frac{\tau_h}{U})^{\frac{1}{4}}$:

$$\begin{aligned}
\forall (x, t_k), \quad \bar{\xi}_{c, \sigma}(x, t_k) &\rightarrow \left(\frac{\tau_h}{U}\right)^{\frac{1}{4}} \bar{\xi}_{c, \sigma}(x, t_k), \\
\xi_{c, \sigma}(x, t_k) &\rightarrow \left(\frac{\tau_h}{U}\right)^{\frac{1}{4}} \xi_{c, \sigma}(x, t_k),
\end{aligned} \tag{37}$$

where $c \in \{+, -\}$, and $\sigma \in \{\uparrow, \downarrow\}$.

The purpose of the rescaling is due to our work in the strong interaction limit ($U \gg \tau_h$). In this context, the factor $(\frac{\tau_h}{U})$ serves as an appropriate parameter for the linked-cluster

expansion that we will carry out after performing the local phase rotations.

Next, we will perform the following local $U(1)$ phase rotations:

\times : local $U(1)$ phase rotations $e^{i\alpha(\cdot,\cdot)}$.

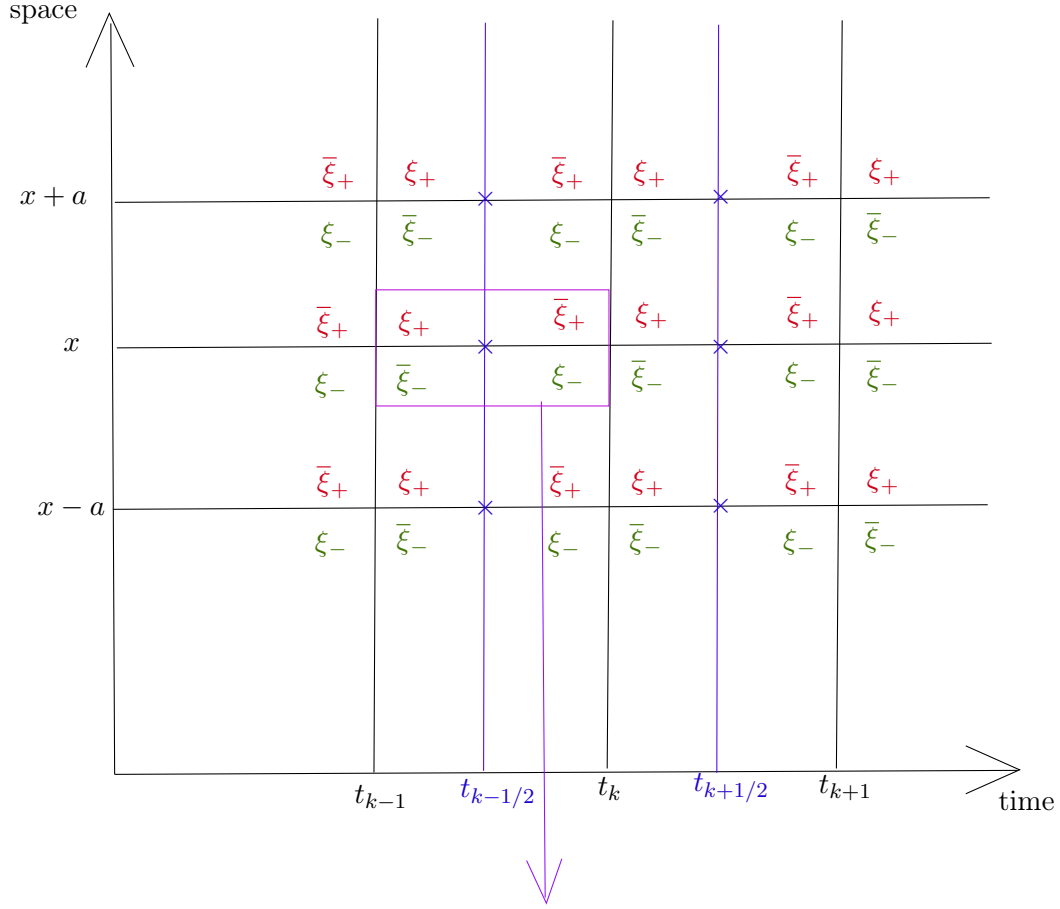


Figure 10: Local $U(1)$ phase rotations applied to the fields, as illustrated below for those within the purple block.

$$\begin{aligned}
 \bar{\xi}_{+, \sigma_1}(x, t_k) &\rightarrow \bar{\xi}_{+, \sigma_1}(x, t_k) e^{-i\alpha(x, t_{k-1/2})}, \\
 \xi_{-, \sigma_2}(x, t_k) &\rightarrow e^{i\alpha(x, t_{k-1/2})} \xi_{-, \sigma_2}(x, t_k), \\
 \bar{\xi}_{-, \sigma_1}(x, t_{k-1}) &\rightarrow \bar{\xi}_{-, \sigma_1}(x, t_{k-1}) e^{-i\alpha(x, t_{k-1/2})}, \\
 \xi_{+, \sigma_2}(x, t_{k-1}) &\rightarrow e^{i\alpha(x, t_{k-1/2})} \xi_{+, \sigma_2}(x, t_{k-1}).
 \end{aligned} \tag{38}$$

The next step is to integrate over all possible phase rotations using the following property of $U(1)$ integrals:

$$\int_0^{2\pi} \prod_{x,t} \frac{d\alpha(x,t)}{2\pi} e^{-i\alpha(x_1, t_1)} e^{i\alpha(x_2, t_2)} = \delta_{x_1, x_2} \delta_{t_1, t_2}, \tag{39}$$

and subsequently carry out the linked-cluster expansion. This expansion can be organized by powers of $\frac{\hbar}{U}$, which serves as an appropriate expansion parameter in the strong interaction limit. Here, we conduct the linked-cluster expansion up to second order, yielding

the resulting expression for the partition function after completing these steps¹¹:

$$\begin{aligned}
& \prod_{\sigma=\uparrow,\downarrow} \frac{\partial^2}{\partial \bar{\xi}_{+,\sigma}(x, t_k) \partial \xi_{+,\sigma}(x, t_{k-1})} \frac{\partial^2}{\partial \bar{\xi}_{-,\sigma}(x, t_{k-1}) \partial \xi_{-,\sigma}(x, t_k)} \\
& \exp \left\{ \left(\frac{\tau_h}{U} \right)^{\frac{1}{2}} \sum_{\sigma} \bar{\xi}_{+,\sigma}(x, t_k) \xi_{+,\sigma}(x, t_{k-1}) - \left(\frac{i\tau_h \Delta t}{\hbar} \right) \bar{\xi}_{+,\uparrow}(x, t_k) \bar{\xi}_{+,\downarrow}(x, t_k) \xi_{+,\downarrow}(x, t_{k-1}) \xi_{+,\uparrow}(x, t_{k-1}) + \right. \\
& \left(\frac{U}{\tau_h} \right)^{\frac{1}{2}} \left(\frac{i\tau_h \Delta t}{2\hbar} \right) \sum_{\sigma} \bar{\xi}_{+,\sigma}(x, t_k) \xi_{+,\sigma}(x, t_{k-1}) + \left(\frac{U}{\tau_h} \right) \left(\frac{\tau_h \Delta t}{\hbar} \right)^2 \bar{\xi}_{+,\uparrow}(x, t_k) \bar{\xi}_{+,\downarrow}(x, t_k) \xi_{+,\downarrow}(x, t_{k-1}) \xi_{+,\uparrow}(x, t_{k-1}) \\
& \left. - \left(\frac{U}{\tau_h} \right)^{\frac{3}{2}} \left(\frac{\tau_h \Delta t}{2\hbar} \right)^2 \sum_{\sigma} \bar{\xi}_{+,\sigma}(x, t_k) \xi_{+,\sigma}(x, t_{k-1}) - \left(\frac{\tau_h}{U} \right)^{\frac{1}{2}} \left(\frac{\tau_h \Delta t}{\hbar} \right)^2 \sum_{\sigma} \bar{\xi}_{+,\sigma}(x, t_k) \xi_{+,\sigma}(x, t_{k-1}) \right\} \\
& \exp \left\{ \left(\frac{\tau_h}{U} \right)^{\frac{1}{2}} \sum_{\sigma} \bar{\xi}_{-,\sigma}(x, t_{k-1}) \xi_{-,\sigma}(x, t_k) + \left(\frac{i\tau_h \Delta t}{\hbar} \right) \bar{\xi}_{-,\uparrow}(x, t_{k-1}) \bar{\xi}_{-,\downarrow}(x, t_{k-1}) \xi_{-,\downarrow}(x, t_k) \xi_{-,\uparrow}(x, t_k) - \right. \\
& \left(\frac{U}{\tau_h} \right)^{\frac{1}{2}} \left(\frac{i\tau_h \Delta t}{2\hbar} \right) \sum_{\sigma} \bar{\xi}_{-,\sigma}(x, t_{k-1}) \xi_{-,\sigma}(x, t_k) + \left(\frac{U}{\tau_h} \right) \left(\frac{\tau_h \Delta t}{\hbar} \right)^2 \bar{\xi}_{-,\uparrow}(x, t_{k-1}) \bar{\xi}_{-,\downarrow}(x, t_{k-1}) \xi_{-,\downarrow}(x, t_k) \xi_{-,\uparrow}(x, t_k) \\
& \left. - \left(\frac{U}{\tau_h} \right)^{\frac{3}{2}} \left(\frac{\tau_h \Delta t}{2\hbar} \right)^2 \sum_{\sigma} \bar{\xi}_{-,\sigma}(x, t_{k-1}) \xi_{-,\sigma}(x, t_k) - \left(\frac{\tau_h}{U} \right)^{\frac{1}{2}} \left(\frac{\tau_h \Delta t}{\hbar} \right)^2 \sum_{\sigma} \bar{\xi}_{-,\sigma}(x, t_{k-1}) \xi_{-,\sigma}(x, t_k) \right\} \\
& \exp \left\{ \left(\frac{\tau_h}{U} \right) \left(\frac{\tau_h \Delta t}{\hbar} \right)^2 \sum_{\sigma_1, \sigma_2} \sum_{y=x+a, x-a} \left(\bar{\xi}_{+,\sigma_1}(x, t_k) \xi_{+,\sigma_2}(x, t_{k-1}) \bar{\xi}_{+,\sigma_2}(y, t_k) \xi_{+,\sigma_1}(y, t_{k-1}) \right. \right. \\
& \quad \left. \left. + \bar{\xi}_{-,\sigma_1}(x, t_{k-1}) \xi_{-,\sigma_2}(x, t_k) \bar{\xi}_{-,\sigma_2}(y, t_{k-1}) \xi_{-,\sigma_1}(y, t_k) \right. \right. \\
& \quad \left. \left. - \bar{\xi}_{+,\sigma_1}(x, t_k) \xi_{-,\sigma_2}(x, t_k) \bar{\xi}_{-,\sigma_2}(y, t_{k-1}) \xi_{+,\sigma_1}(y, t_{k-1}) \right. \right. \\
& \quad \left. \left. - \bar{\xi}_{-,\sigma_1}(x, t_{k-1}) \xi_{+,\sigma_2}(x, t_{k-1}) \bar{\xi}_{+,\sigma_2}(y, t_k) \xi_{-,\sigma_1}(y, t_k) \right) \right\} \\
& \exp \left\{ - \left(\frac{\tau_h}{U} \right) \sum_{\sigma_1, \sigma_2} \left(\bar{\xi}_{+,\sigma_1}(x, t_k) \xi_{-,\sigma_2}(x, t_k) \bar{\xi}_{-,\sigma_1}(x, t_k) \xi_{+,\sigma_2}(x, t_k) \right. \right. \\
& \quad \left. \left. + \bar{\xi}_{+,\sigma_1}(x, t_{k-1}) \xi_{-,\sigma_2}(x, t_{k-1}) \bar{\xi}_{-,\sigma_1}(x, t_{k-1}) \xi_{+,\sigma_2}(x, t_{k-1}) \right) \right\}.
\end{aligned} \tag{40}$$

With all preparations complete, we are now ready to execute the bosonization step. The

¹¹The rescaling factor $\frac{\tau_h}{U}$ from equation (37) is implicitly included in the integration measure that follows, though it is not explicitly shown in the expression.

partition function, expressed in terms of the field Q after bosonization, is given by:

$$\begin{aligned}
& \int_{U(4)} dQ(x, t_k) \text{Det}^{-1}(Q(x, t_k)) \\
& \exp \left\{ \left(\frac{\tau_h}{U} \right)^{\frac{1}{2}} \sum_{\sigma} (Q_{++})_{\sigma\sigma}(x, t_k) - \left(\frac{i\tau_h \Delta t}{\hbar} \right) (Q_{++})_{\uparrow\uparrow}(x, t_k) (Q_{++})_{\downarrow\downarrow}(x, t_k) \right. \\
& + \left(\frac{U}{\tau_h} \right)^{\frac{1}{2}} \left(\frac{i\tau_h \Delta t}{2\hbar} \right) \sum_{\sigma} (Q_{++})_{\sigma\sigma}(x, t_k) + \left(\frac{U}{\tau_h} \right) \left(\frac{\tau_h \Delta t}{\hbar} \right)^2 (Q_{++})_{\uparrow\uparrow}(x, t_k) (Q_{++})_{\downarrow\downarrow}(x, t_k) \\
& \left. - \left(\frac{U}{\tau_h} \right)^{\frac{3}{2}} \left(\frac{\tau_h \Delta t}{2\hbar} \right)^2 \sum_{\sigma} (Q_{++})_{\sigma\sigma}(x, t_k) - \left(\frac{\tau_h}{U} \right)^{\frac{1}{2}} \left(\frac{\tau_h \Delta t}{\hbar} \right)^2 \sum_{\sigma} (Q_{++})_{\sigma\sigma}(x, t_k) \right\} \\
& \exp \left\{ \left(\frac{\tau_h}{U} \right)^{\frac{1}{2}} \sum_{\sigma} (Q_{--})_{\sigma\sigma}(x, t_k) + \left(\frac{i\tau_h \Delta t}{\hbar} \right) (Q_{--})_{\uparrow\uparrow}(x, t_k) (Q_{--})_{\downarrow\downarrow}(x, t_k) \right. \\
& - \left(\frac{U}{\tau_h} \right)^{\frac{1}{2}} \left(\frac{i\tau_h \Delta t}{2\hbar} \right) \sum_{\sigma} (Q_{--})_{\sigma\sigma}(x, t_k) + \left(\frac{U}{\tau_h} \right) \left(\frac{\tau_h \Delta t}{\hbar} \right)^2 (Q_{--})_{\uparrow\uparrow}(x, t_k) (Q_{--})_{\downarrow\downarrow}(x, t_k) \\
& \left. - \left(\frac{U}{\tau_h} \right)^{\frac{3}{2}} \left(\frac{\tau_h \Delta t}{2\hbar} \right)^2 \sum_{\sigma} (Q_{--})_{\sigma\sigma}(x, t_k) - \left(\frac{\tau_h}{U} \right)^{\frac{1}{2}} \left(\frac{\tau_h \Delta t}{\hbar} \right)^2 \sum_{\sigma} (Q_{--})_{\sigma\sigma}(x, t_k) \right\} \quad (41) \\
& \exp \left\{ \left(\frac{\tau_h}{U} \right) \left(\frac{\tau_h \Delta t}{\hbar} \right)^2 \sum_{\sigma_1, \sigma_2} \sum_{y=x+a, x-a} \left((Q_{++})_{\sigma_1 \sigma_2}(x, t_k) (Q_{++})_{\sigma_2 \sigma_1}(y, t_k) \right. \right. \\
& \quad + (Q_{--})_{\sigma_1 \sigma_2}(x, t_k) (Q_{--})_{\sigma_2 \sigma_1}(y, t_k) \\
& \quad - (Q_{+-})_{\sigma_1 \sigma_2}(x, t_k) (Q_{-+})_{\sigma_2 \sigma_1}(y, t_k) \\
& \quad \left. \left. - (Q_{-+})_{\sigma_1 \sigma_2}(x, t_k) (Q_{+-})_{\sigma_2 \sigma_1}(y, t_k) \right) \right\} \\
& \exp \left\{ - \left(\frac{\tau_h}{U} \right) \sum_{\sigma_1, \sigma_2} \left((Q_{+-})_{\sigma_1 \sigma_2}(x, t_k) (Q_{-+})_{\sigma_2 \sigma_1}(x, t_{k+1}) \right. \right. \\
& \quad \left. \left. + (Q_{+-})_{\sigma_1 \sigma_2}(x, t_{k-1}) (Q_{-+})_{\sigma_2 \sigma_1}(x, t_k) \right) \right\} \\
& \equiv \int_{U(4)} dQ(x, t_k) \exp \left(\frac{iS_{\text{eff}}[Q(x, t_k)]}{\hbar} \right).
\end{aligned}$$

Before proceeding, let us summarize the steps we have undertaken thus far.

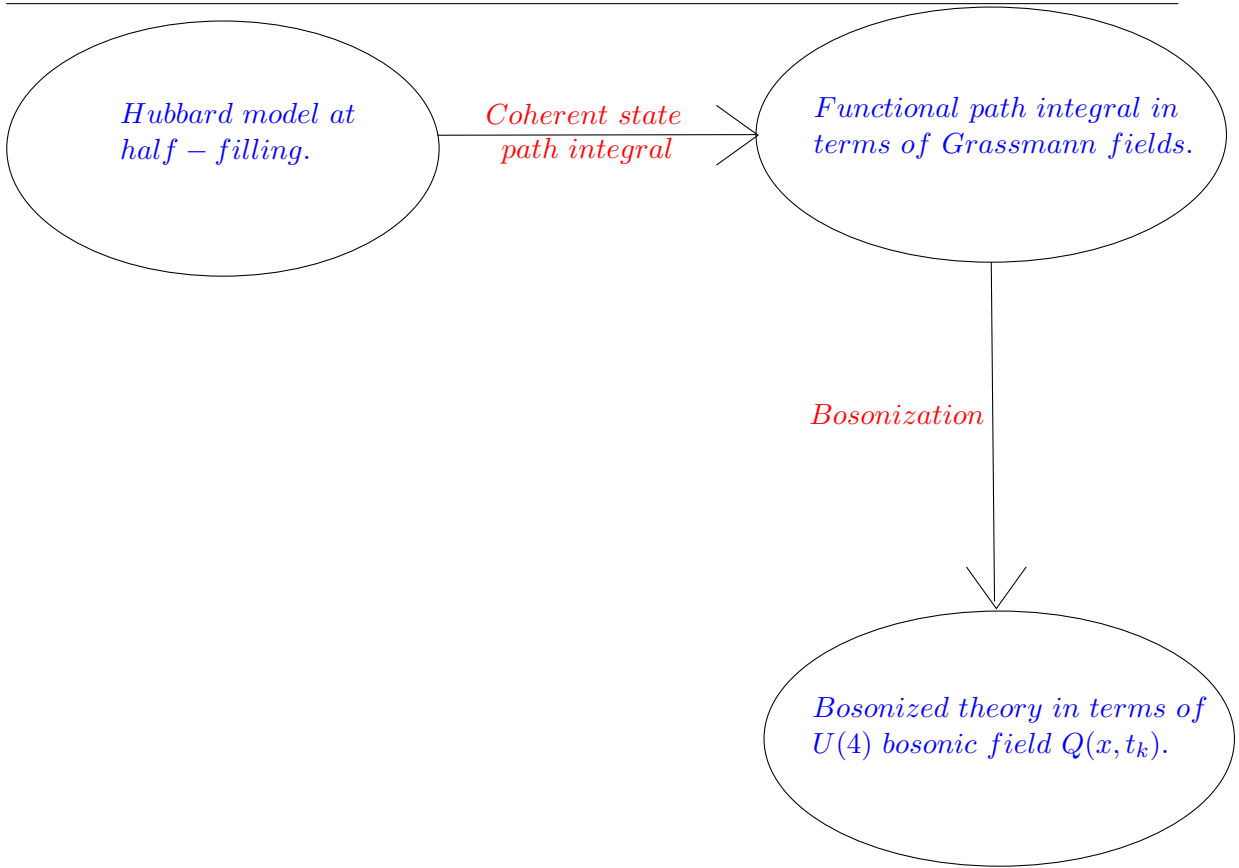


Figure 11: Flowchart summarizing the analysis conducted thus far.

We have reformulated the partition function in terms of the $U(4)$ bosonic field $Q(x, t_k)$. Our next objective is to take the continuum limit in time by letting $\Delta t \rightarrow 0$. However, as observed in equation (41), it remains unclear how to proceed with the continuum limit, particularly regarding the treatment of the determinant term in the partition function. Furthermore, terms of order $(\Delta t)^2$ vanish in the straightforward continuum limit as $\Delta t \rightarrow 0$.¹²

In light of the difficulties associated with handling the continuum limit at the level of the action, we refer to the following diagram:

¹²To clarify, it is important to recognize that the determinant term and the other components of the action should not be treated separately while taking the continuum limit in time. To illustrate this point, consider the simpler example of non-interacting fermions at half-filling in one dimension [9]. In this scenario, the continuum limit in space yields an effective description characterized by a Dirac-like Hamiltonian; however, this limit is applicable only near the Fermi points. Returning to our original problem, based on insights from this example, we propose that the determinant term may be interpreted as setting the chemical potential. This interpretation emphasizes the necessity of viewing S_{eff} as a unified entity when taking the continuum limit.

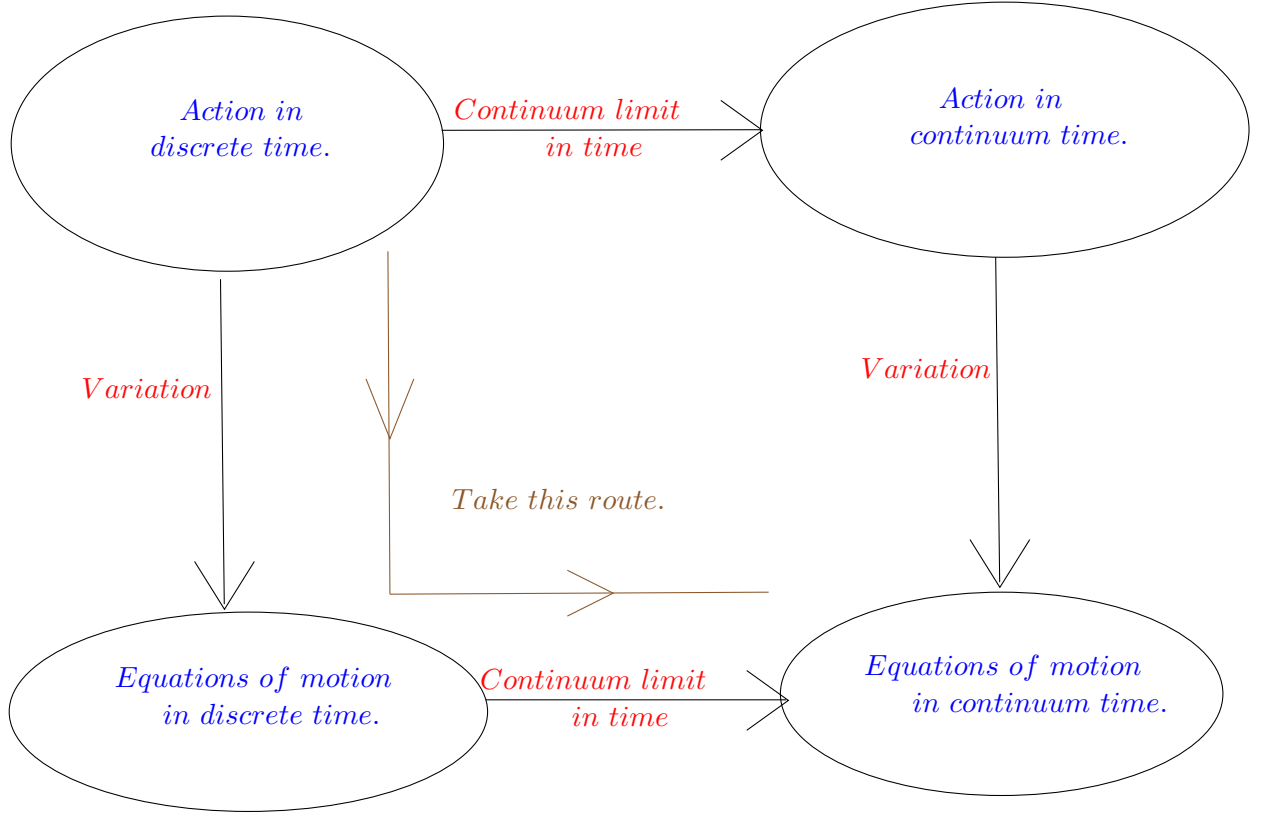


Figure 12: Flow diagram depicting the transition from the action to the equations of motion to facilitate the continuum limit in time.

We now shift our focus to analyzing the equations of motion. We assume that the continuum limit in time exists, even though the specific approach to applying this limit to the action is not immediately clear. Additionally, we assume that the diagram above is “commutative” in the low-energy limit, allowing us to consider an alternative path, indicated in brown in Figure 12.

Equations of motion

To derive the equations of motion for (41), we utilize a key property of the Haar measure [33] associated with the unitary group, which is as follows:

$$\int_{U(4)} dQ F(g_L Q) = \int_{U(4)} dQ F(Q) = \int_{U(4)} dQ F(Q g_R), \quad g_L, g_R \in U(4). \quad (42)$$

This property indicates that the Haar measure on the unitary group is invariant under both left and right multiplication. Here, $F(Q)$ denotes a function of Q . Based on this property, the equations of motion are given as follows¹³:

$$\left. \frac{d}{d\lambda} \right|_{\lambda=0} S_{\text{eff}}[e^{\lambda X} Q(x, t_k)] = 0 = \left. \frac{d}{d\lambda} \right|_{\lambda=0} S_{\text{eff}}[Q(x, t_k) e^{\lambda X}], \quad (43)$$

where X represents the generators of the Lie algebra $u(4)$.

¹³The motivation for deriving the equations of motion from the invariance of the Haar measure is detailed in Appendix B.

Using equation (43), we proceed to write down the equations of motion for the matrix elements of the field Q and attempt to take the continuum limit, $\Delta t \rightarrow 0$. This can be accomplished in the following three steps:

1. Choose one of the 16 generators of the Lie algebra $u(4)$, denoted by X .
2. Substitute the chosen X in equation (43):

$$\begin{aligned} L|_{x,t_k} &\equiv \left. \frac{d}{d\lambda} \right|_{\lambda=0} S_{\text{eff}}[e^{\lambda X} Q(x, t_k)] = 0, \\ R|_{x,t_k} &\equiv \left. \frac{d}{d\lambda} \right|_{\lambda=0} S_{\text{eff}}[Q(x, t_k) e^{\lambda X}] = 0, \end{aligned} \tag{44}$$

where $L|_{x,t_k}$ denotes the equation of motion obtained using the left invariance of the Haar measure, and $R|_{x,t_k}$ denotes the equation of motion obtained using the right invariance of the Haar measure.

3. Send $t_k \rightarrow t_{k+1}$ in $R|_{x,t_k}$, and subtract this from $L|_{x,t_k}$. Finally, we take the continuum limit $\Delta t \rightarrow 0$.

After executing the three steps outlined above, we observe that the contribution to the equations of motion from the hopping term vanishes in the continuum limit.¹⁴ This outcome raises concerns, as the presence of the hopping term is crucial for deriving spin waves as low-energy excitations. Consequently, there exists an inconsistency that must be resolved.

To retain the contribution from the hopping term in the continuum limit, we will explore an alternative approach in the next section by mapping to a different bosonic field using the bosonization method.

3.3 Attempt II: Reformulation of the Partition Function Using the $Q(x) \in U(2M)$ Field

As previously mentioned, we aim to reattempt the bosonization of the strongly interacting Hubbard model at filling factor $\nu = \frac{1}{2}$. Based on our earlier analysis, certain adjustments are necessary. In this iteration, we will express the theory in terms of a bosonic field $Q(x)$, which is “local” in space but not in time. As discussed in Section 2.1, this allows us to bypass the requirement of working on a closed-time contour.

Our next task is to formulate the partition function as a functional integral over a single time channel, specifically the forward channel only. The partition function can be expressed mathematically as follows:

$$Z = \text{Tr} \left(e^{-\frac{iTH}{\hbar}} \right), \tag{45}$$

where Tr denotes the trace over the Fock space, H is the Hamiltonian of the system, and T

¹⁴We do not provide the explicit calculations here. For detailed calculations, please refer to Appendix C.

represents the time period of evolution.

The initial two steps of the formalism remain unchanged; the only difference, as previously noted, is that we now work with a single time channel instead of the previously used closed-time contour. Next, let us write down the contribution to the partition function from the block depicted in Figure 13:

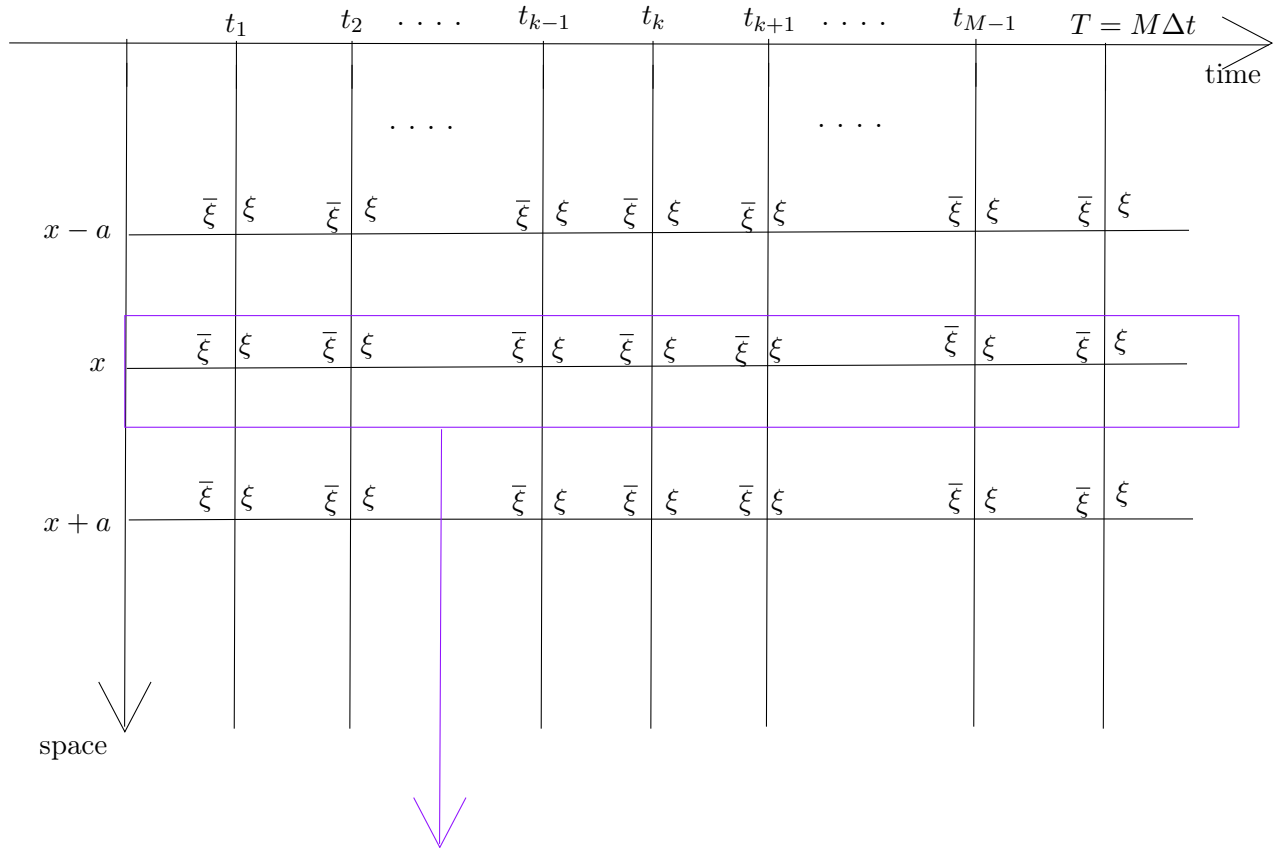


Figure 13: The contribution of the purple block to the partition function is analyzed below.

$$\begin{aligned}
& \prod_{k=1}^M \prod_{\sigma=\uparrow,\downarrow} \frac{\partial^2}{\partial \bar{\xi}_\sigma(x, t_k) \partial \xi_\sigma(x, t_k)} \\
& \exp \left\{ \sum_{k=2}^M \left(\sum_{\sigma} (\bar{\xi}_\sigma(x, t_k) \xi_\sigma(x, t_{k-1}) - \bar{\xi}_\sigma(x, t_{k-1}) \xi_\sigma(x, t_{k-1})) \right. \right. \\
& \quad - \left(\frac{iU\Delta t}{\hbar} \right) \bar{\xi}_\uparrow(x, t_k) \bar{\xi}_\downarrow(x, t_k) \xi_\downarrow(x, t_{k-1}) \xi_\uparrow(x, t_{k-1}) \\
& \quad + \left(\frac{iU\Delta t}{2\hbar} \right) \sum_{\sigma} \bar{\xi}_\sigma(x, t_k) \xi_\sigma(x, t_{k-1}) + \left(\frac{U\Delta t}{\hbar} \right)^2 \bar{\xi}_\uparrow(x, t_k) \bar{\xi}_\downarrow(x, t_k) \xi_\downarrow(x, t_{k-1}) \xi_\uparrow(x, t_{k-1}) \\
& \quad \left. \left. - \left(\frac{U\Delta t}{2\hbar} \right)^2 \sum_{\sigma} \bar{\xi}_\sigma(x, t_k) \xi_\sigma(x, t_{k-1}) - \left(\frac{\tau_h \Delta t}{\hbar} \right)^2 \sum_{\sigma} \bar{\xi}_\sigma(x, t_k) \xi_\sigma(x, t_{k-1}) \right) \right\} \\
& \exp \left\{ \sum_{k=2}^M \left(\frac{i\tau_h \Delta t}{\hbar} \right) \sum_{\sigma, y=x+a, x-a} \bar{\xi}_\sigma(x, t_k) \xi_\sigma(y, t_{k-1}) + \bar{\xi}_\sigma(y, t_k) \xi_\sigma(x, t_{k-1}) \right\} \\
& \exp \left\{ \left(\sum_{\sigma} (\bar{\xi}_\sigma(x, t_1) (-\xi_\sigma(x, t_M)) - \bar{\xi}_\sigma(x, t_M) \xi_\sigma(x, t_M)) \right. \right. \\
& \quad - \left(\frac{iU\Delta t}{\hbar} \right) \bar{\xi}_\uparrow(x, t_1) \bar{\xi}_\downarrow(x, t_1) (-\xi_\downarrow(x, t_M)) (-\xi_\uparrow(x, t_M)) \\
& \quad + \left(\frac{iU\Delta t}{2\hbar} \right) \sum_{\sigma} \bar{\xi}_\sigma(x, t_1) (-\xi_\sigma(x, t_M)) + \left(\frac{U\Delta t}{\hbar} \right)^2 \bar{\xi}_\uparrow(x, t_1) \bar{\xi}_\downarrow(x, t_1) (-\xi_\downarrow(x, t_M)) (-\xi_\uparrow(x, t_M)) \\
& \quad \left. \left. - \left(\frac{U\Delta t}{2\hbar} \right)^2 \sum_{\sigma} \bar{\xi}_\sigma(x, t_1) (-\xi_\sigma(x, t_M)) - \left(\frac{\tau_h \Delta t}{\hbar} \right)^2 \sum_{\sigma} \bar{\xi}_\sigma(x, t_1) (-\xi_\sigma(x, t_M)) \right) \right\} \\
& \exp \left\{ \left(\frac{i\tau_h \Delta t}{\hbar} \right) \sum_{\sigma, y=x+a, x-a} \bar{\xi}_\sigma(x, t_1) (-\xi_\sigma(y, t_M)) + \bar{\xi}_\sigma(y, t_1) (-\xi_\sigma(x, t_M)) \right\}.
\end{aligned} \tag{46}$$

A word on the equation. *It is important to note that the boundary terms in the construction of the coherent state path integral for fermions exhibit a relative minus sign, as demonstrated in the last five lines of equation (46).*

We aim to reformulate the partition function (46) using the $Q(x)$ field, which is represented as a $2M \times 2M$ unitary matrix. This matrix can be expressed in block form as follows:

$$Q(x) = \begin{bmatrix} Q_{\uparrow\uparrow}(x) & Q_{\uparrow\downarrow}(x) \\ Q_{\downarrow\uparrow}(x) & Q_{\downarrow\downarrow}(x) \end{bmatrix}, \tag{47}$$

where each block in this matrix is an $M \times M$ matrix. The components of $Q(x)$ in relation to the fermionic fields are defined as follows:

3 APPLICATION: FUNCTIONAL INTEGRAL BOSONIZATION APPROACH TO THE
STRONGLY INTERACTING ONE-DIMENSIONAL HUBBARD MODEL AT
HALF-FILLING

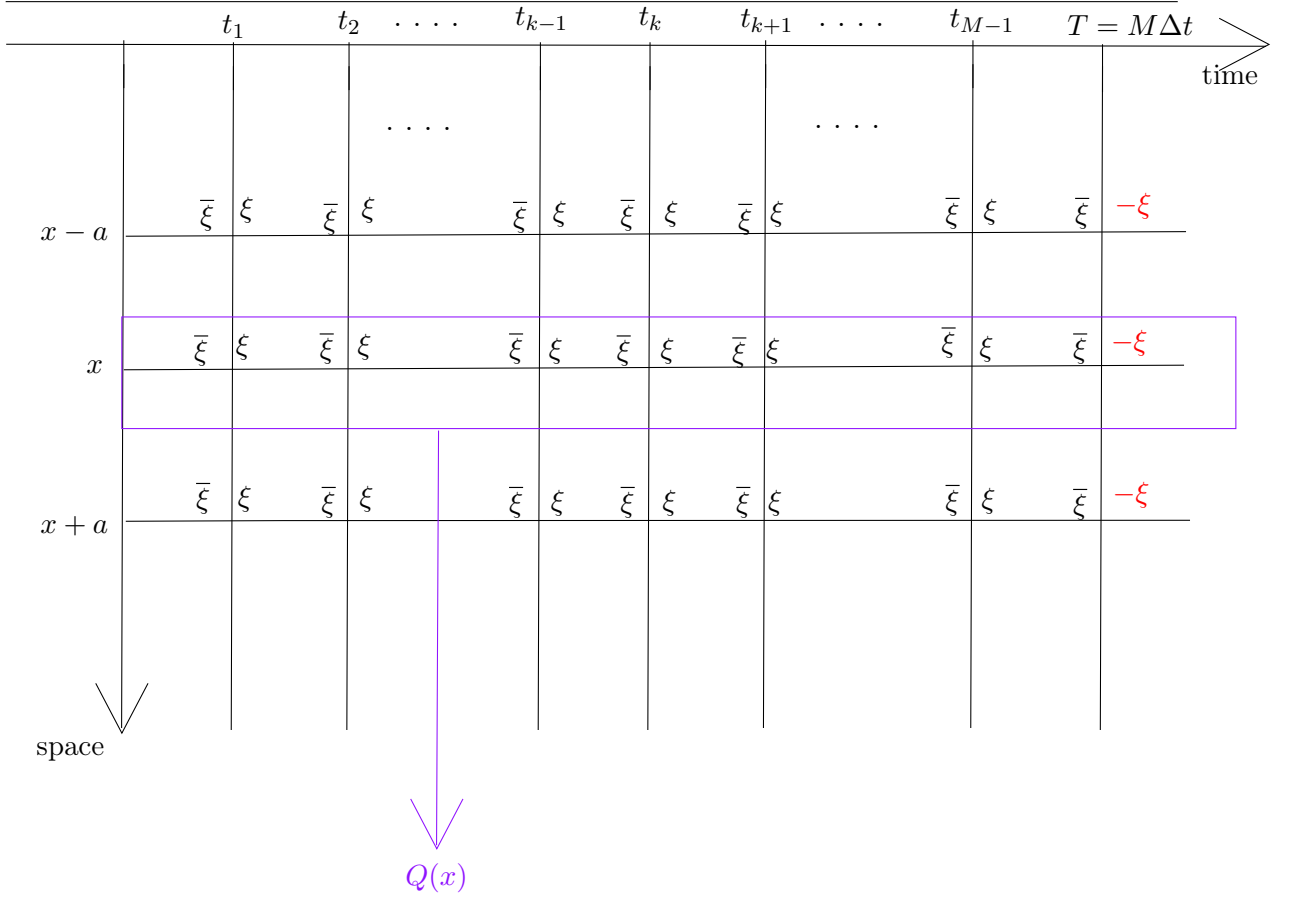


Figure 14: The fields within the purple block are used to define the field $Q(x)$, as demonstrated below.

$$\begin{aligned}
 Q_{\sigma_1\sigma_2}(x; t_k, t_{k'}) &= \bar{\xi}_{\sigma_1}(x, t_k)\xi_{\sigma_2}(x, t_{k'}), \quad k \in \{1, 2, \dots, M\}, \quad k' \in \{1, 2, \dots, M-1\}, \\
 Q_{\sigma_1\sigma_2}(x; t_k, t_M) &= \bar{\xi}_{\sigma_1}(x, t_k)(-\xi_{\sigma_2}(x, t_M)), \quad k \in \{1, 2, \dots, M\}.
 \end{aligned} \tag{48}$$

As before, the terms highlighted in blue in the partition function (46) cannot be directly expressed in terms of the field $Q(x)$. To resolve this, we perform local $U(1)$ phase rotations (“localized” only in space) to incorporate the contributions from these terms. Prior to continuing, we do the same rescaling step as before:

$$\begin{aligned}
 \forall (x, t_k), \quad \bar{\xi}_\sigma(x, t_k) &\rightarrow \left(\frac{\tau_h}{U}\right)^{\frac{1}{4}} \bar{\xi}_\sigma(x, t_k), \\
 \xi_\sigma(x, t_k) &\rightarrow \left(\frac{\tau_h}{U}\right)^{\frac{1}{4}} \xi_\sigma(x, t_k),
 \end{aligned} \tag{49}$$

where $\sigma \in \{\uparrow, \downarrow\}$.

Next, we perform the following local $U(1)$ phase rotations:

3 APPLICATION: FUNCTIONAL INTEGRAL BOSONIZATION APPROACH TO THE STRONGLY INTERACTING ONE-DIMENSIONAL HUBBARD MODEL AT HALF-FILLING

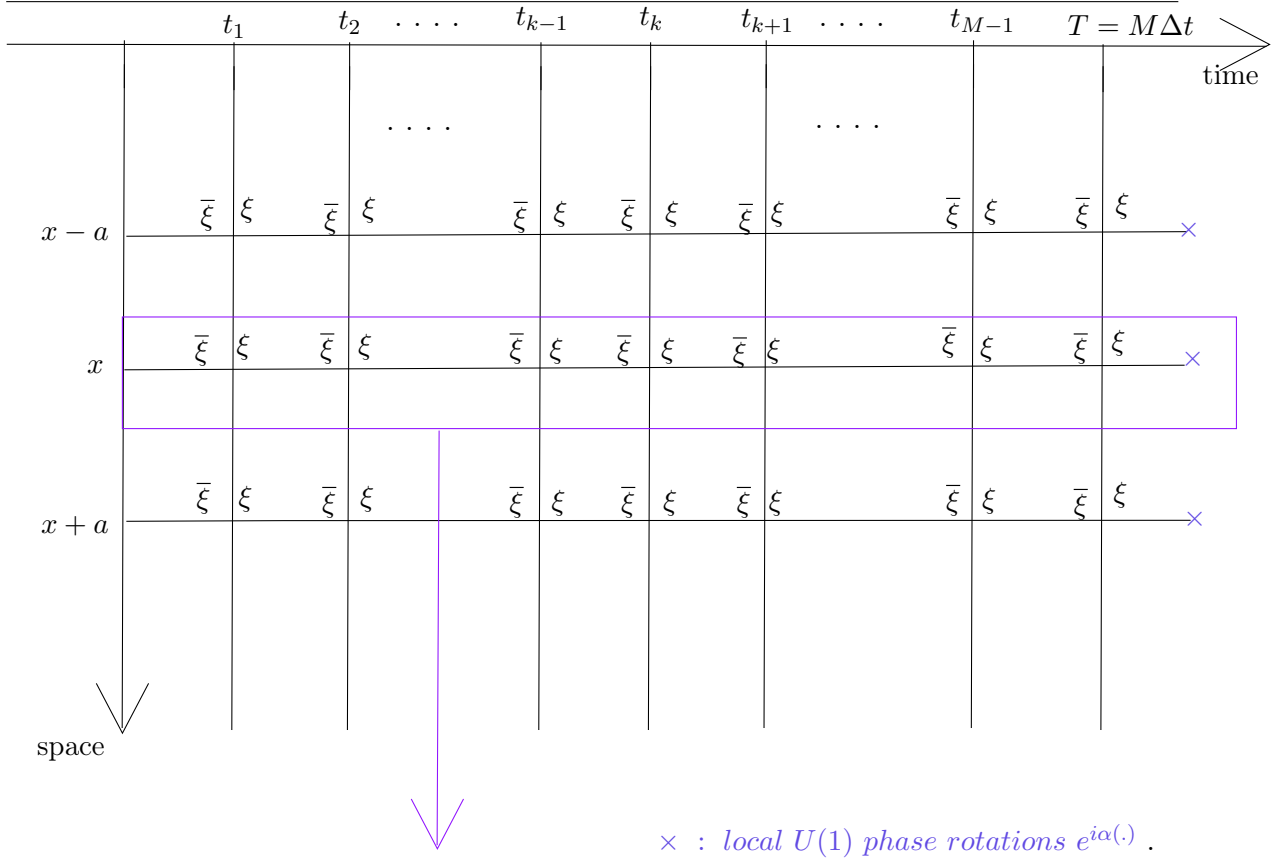


Figure 15: Local $U(1)$ phase rotations applied to the fields, as illustrated below for those within the purple block.

$$\begin{aligned} \forall t_k, \quad \bar{\xi}_\sigma(x, t_k) &\rightarrow \bar{\xi}_\sigma(x, t_k) e^{-i\alpha(x)}, \\ \xi_\sigma(x, t_k) &\rightarrow e^{i\alpha(x)} \xi_\sigma(x, t_k). \end{aligned} \tag{50}$$

Building on the previous analysis, the next step is to integrate over all possible phase rotations and perform the linked-cluster expansion. We will also expand up to second order in this case. The resulting expression for the partition function, after completing these steps,

is:

$$\begin{aligned}
& \prod_{k=1}^M \prod_{\sigma=\uparrow,\downarrow} \frac{\partial^2}{\partial \bar{\xi}_\sigma(x, t_k) \partial \xi_\sigma(x, t_k)} \\
& \exp \left\{ \sum_{k=2}^M \left(\left(\frac{\tau_h}{U} \right)^{\frac{1}{2}} \sum_{\sigma} (\bar{\xi}_\sigma(x, t_k) \xi_\sigma(x, t_{k-1}) - \bar{\xi}_\sigma(x, t_{k-1}) \xi_\sigma(x, t_k)) \right. \right. \\
& \quad - \left(\frac{\tau_h}{U} \right) \left(\frac{iU\Delta t}{\hbar} \right) \bar{\xi}_\uparrow(x, t_k) \bar{\xi}_\downarrow(x, t_k) \xi_\downarrow(x, t_{k-1}) \xi_\uparrow(x, t_{k-1}) \\
& \quad + \left(\frac{\tau_h}{U} \right)^{\frac{1}{2}} \left(\frac{iU\Delta t}{2\hbar} \right) \sum_{\sigma} \bar{\xi}_\sigma(x, t_k) \xi_\sigma(x, t_{k-1}) + \left(\frac{\tau_h}{U} \right) \left(\frac{U\Delta t}{\hbar} \right)^2 \bar{\xi}_\uparrow(x, t_k) \bar{\xi}_\downarrow(x, t_k) \xi_\downarrow(x, t_{k-1}) \xi_\uparrow(x, t_{k-1}) \\
& \quad \left. - \left(\frac{\tau_h}{U} \right)^{\frac{1}{2}} \left(\frac{U\Delta t}{2\hbar} \right)^2 \sum_{\sigma} \bar{\xi}_\sigma(x, t_k) \xi_\sigma(x, t_{k-1}) - \left(\frac{\tau_h}{U} \right)^{\frac{1}{2}} \left(\frac{\tau_h \Delta t}{\hbar} \right)^2 \sum_{\sigma} \bar{\xi}_\sigma(x, t_k) \xi_\sigma(x, t_{k-1}) \right\} \\
& \exp \left\{ \left(\left(\frac{\tau_h}{U} \right)^{\frac{1}{2}} \sum_{\sigma} (\bar{\xi}_\sigma(x, t_1) (-\xi_\sigma(x, t_M)) - \bar{\xi}_\sigma(x, t_M) \xi_\sigma(x, t_1)) \right. \right. \\
& \quad - \left(\frac{\tau_h}{U} \right) \left(\frac{iU\Delta t}{\hbar} \right) \bar{\xi}_\uparrow(x, t_1) \bar{\xi}_\downarrow(x, t_1) (-\xi_\downarrow(x, t_M)) (-\xi_\uparrow(x, t_M)) \\
& \quad + \left(\frac{\tau_h}{U} \right)^{\frac{1}{2}} \left(\frac{iU\Delta t}{2\hbar} \right) \sum_{\sigma} \bar{\xi}_\sigma(x, t_1) (-\xi_\sigma(x, t_M)) + \left(\frac{\tau_h}{U} \right) \left(\frac{U\Delta t}{\hbar} \right)^2 \bar{\xi}_\uparrow(x, t_1) \bar{\xi}_\downarrow(x, t_1) (-\xi_\downarrow(x, t_M)) (-\xi_\uparrow(x, t_M)) \\
& \quad \left. - \left(\frac{\tau_h}{U} \right)^{\frac{1}{2}} \left(\frac{U\Delta t}{2\hbar} \right)^2 \sum_{\sigma} \bar{\xi}_\sigma(x, t_1) (-\xi_\sigma(x, t_M)) - \left(\frac{\tau_h}{U} \right)^{\frac{1}{2}} \left(\frac{\tau_h \Delta t}{\hbar} \right)^2 \sum_{\sigma} \bar{\xi}_\sigma(x, t_1) (-\xi_\sigma(x, t_M)) \right\} \\
& \exp \left\{ \left(\frac{\tau_h}{U} \right) \left(\frac{\tau_h \Delta t}{\hbar} \right)^2 \sum_{k, k'=2}^M \sum_{\sigma_1, \sigma_2} \sum_{y=x+a, x-a} \bar{\xi}_{\sigma_1}(x, t_k) \xi_{\sigma_2}(x, t_{k'-1}) \bar{\xi}_{\sigma_2}(y, t_{k'}) \xi_{\sigma_1}(y, t_{k-1}) \right\} \\
& \exp \left\{ \left(\frac{\tau_h}{U} \right) \left(\frac{\tau_h \Delta t}{\hbar} \right)^2 \sum_{k=2}^M \sum_{\sigma_1, \sigma_2} \sum_{y=x+a, x-a} \left(\bar{\xi}_{\sigma_1}(x, t_k) (-\xi_{\sigma_2}(x, t_M)) \bar{\xi}_{\sigma_2}(y, t_1) \xi_{\sigma_1}(y, t_{k-1}) \right. \right. \\
& \quad \left. \left. + \bar{\xi}_{\sigma_1}(y, t_k) (-\xi_{\sigma_2}(y, t_M)) \bar{\xi}_{\sigma_2}(x, t_1) \xi_{\sigma_1}(x, t_{k-1}) \right) \right\} \\
& \exp \left\{ \left(\frac{\tau_h}{U} \right) \left(\frac{\tau_h \Delta t}{\hbar} \right)^2 \sum_{\sigma_1, \sigma_2} \sum_{y=x+a, x-a} \bar{\xi}_{\sigma_1}(x, t_1) (-\xi_{\sigma_2}(x, t_M)) \bar{\xi}_{\sigma_2}(y, t_1) (-\xi_{\sigma_1}(y, t_M)) \right\}.
\end{aligned} \tag{51}$$

With everything in place, we are now ready to proceed with the bosonization step. The

partition function, expressed in terms of the field $Q(x)$ after bosonization, is given by:

$$\begin{aligned}
& \int_{U(2M)} dQ(x) \text{Det}^{-1}(Q(x)) \\
& \exp \left\{ \sum_{k=1}^M \left(\left(\frac{\tau_h}{U} \right)^{\frac{1}{2}} \sum_{\sigma} (Q_{\sigma\sigma}(x; t_k, t_{k-1}) - Q_{\sigma\sigma}(x; t_{k-1}, t_{k-1})) \right. \right. \\
& \quad - \left. \left(\frac{\tau_h}{U} \right) \left(\frac{iU\Delta t}{\hbar} \right) Q_{\uparrow\uparrow}(x; t_k, t_{k-1}) Q_{\downarrow\downarrow}(x; t_k, t_{k-1}) \right. \\
& \quad + \left. \left(\frac{\tau_h}{U} \right)^{\frac{1}{2}} \left(\frac{iU\Delta t}{2\hbar} \right) \sum_{\sigma} Q_{\sigma\sigma}(x; t_k, t_{k-1}) + \left(\frac{\tau_h}{U} \right) \left(\frac{U\Delta t}{\hbar} \right)^2 Q_{\uparrow\uparrow}(x; t_k, t_{k-1}) Q_{\downarrow\downarrow}(x; t_k, t_{k-1}) \right. \\
& \quad \left. \left. - \left(\frac{\tau_h}{U} \right)^{\frac{1}{2}} \left(\frac{U\Delta t}{2\hbar} \right)^2 \sum_{\sigma} Q_{\sigma\sigma}(x; t_k, t_{k-1}) - \left(\frac{\tau_h}{U} \right)^{\frac{1}{2}} \left(\frac{\tau_h\Delta t}{\hbar} \right)^2 \sum_{\sigma} Q_{\sigma\sigma}(x; t_k, t_{k-1}) \right) \right\} \\
& \exp \left\{ \left(\frac{\tau_h}{U} \right)^{\frac{1}{2}} \sum_{\sigma} 2Q_{\sigma\sigma}(x; t_M, t_M) \right\} \\
& \exp \left\{ \left(\frac{\tau_h}{U} \right) \left(\frac{\tau_h\Delta t}{\hbar} \right)^2 \sum_{k,k'=1}^M \sum_{\sigma_1, \sigma_2} \sum_{y=x+a, x-a} Q_{\sigma_1\sigma_2}(x; t_k, t_{k'-1}) Q_{\sigma_2\sigma_1}(y; t'_k, t_{k-1}) \right\} \\
& \equiv \int_{U(2M)} dQ(x) \exp \left(\frac{iS_{\text{eff}}[Q(x)]}{\hbar} \right),
\end{aligned} \tag{52}$$

where we adopt the notation $t_0 \equiv t_M$.

A word on the equation. The factor 2 in the term $\sum_{\sigma} 2Q_{\sigma\sigma}(x; t_M, t_M)$ in the third-to-last line of equation (52) can be explained by the definition of the $Q(x)$ field in equation (48).

Once again, our objective is to take the continuum limit $\Delta t \rightarrow 0$. However, the procedure for doing so in equation (52), especially concerning the determinant term, is unclear.

Therefore, we will shift our focus to analyzing the equations of motion.

Equations of motion

Utilizing the left and right invariance of the Haar measure, the equations governing the components of the matrix $Q(x)$ are given by¹⁵ :

$$\begin{aligned}
& \left[\partial_t Q_{\sigma_1\sigma_2}(x; t, t') + \partial_{t'} Q_{\sigma_1\sigma_2}(x; t, t') \right] \Big|_{t=t'} \\
& = \left(\frac{\tau_h}{\hbar} \right)^2 \left(\frac{\tau_h}{U} \right)^{\frac{1}{2}} \sum_{\sigma} \sum_{y=x+a, x-a} \int dt'' \left\{ Q_{\sigma_1\sigma}(x; t, t'') Q_{\sigma\sigma_2}(y; t'', t) - Q_{\sigma_1\sigma}(y; t, t'') Q_{\sigma\sigma_2}(x; t'', t) \right\}.
\end{aligned} \tag{53}$$

Our aim is to derive spin-wave solutions in the low-energy limit. With this objective in

¹⁵By applying the three-step procedure outlined in Section 3.2 with some modifications, we derive the equations of motion in the continuum limit. Detailed intermediate steps are provided in Appendix D.

mind, we define the following variables:

$$\begin{aligned} S^1(x, t) &\sim \frac{\hbar}{2}(Q_{\uparrow\downarrow}(x; t, t) + Q_{\downarrow\uparrow}(x; t, t)), \\ S^2(x, t) &\sim \frac{\hbar}{2i}(Q_{\uparrow\downarrow}(x; t, t) - Q_{\downarrow\uparrow}(x; t, t)), \\ S^3(x, t) &\sim \frac{\hbar}{2}(Q_{\uparrow\uparrow}(x; t, t) - Q_{\downarrow\downarrow}(x; t, t)). \end{aligned} \quad (54)$$

Note. The definition in equation (54) is motivated by the expression for the spin operator:

$$\hat{S}^j(x, t) = \frac{\hbar}{2} \sum_{\sigma, \sigma'} \hat{c}_{\sigma}^{\dagger}(x, t) \boldsymbol{\tau}_{\sigma\sigma'}^j \hat{c}_{\sigma'}(x, t), \quad (55)$$

where $j = 1, 2, 3$, and $\boldsymbol{\tau}^j$ denote the standard Pauli matrices.

Let us now begin the analysis of the equations of motion. First, we note that the lattice we are working with is bipartite.

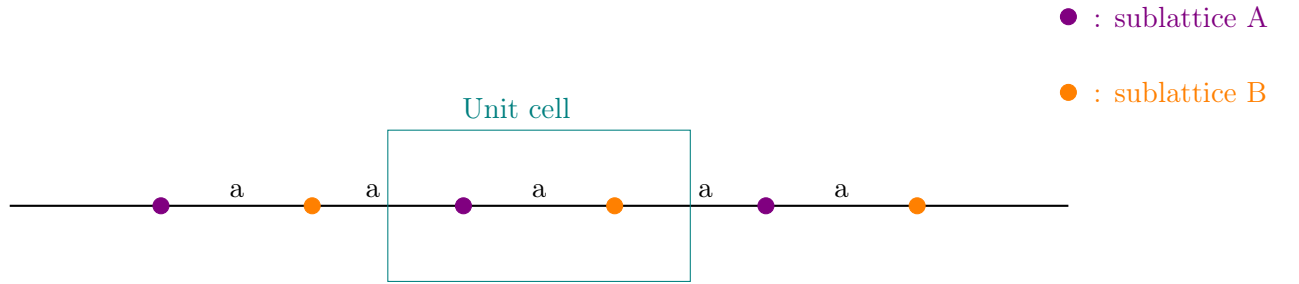


Figure 16: Bipartite lattice illustrating the unit cell.

We propose the following ansatz for the solution of the equations of motion given in (53):

$$Q_{\sigma_1\sigma_2}(x; t, t') = (Q_{\sigma_1\sigma_2})_0(x; t, t') + \delta Q_{\sigma_1\sigma_2}(x; t, t'), \quad (56)$$

where only the non-zero components of the $(Q)_0$ field are shown below:

$$\begin{aligned} (Q_{\uparrow\uparrow})_0(2x; t, t') &= m_1 \delta(t - t') = (Q_{\downarrow\downarrow})_0(2x - a; t, t'), \\ (Q_{\uparrow\uparrow})_0(2x - a; t, t') &= m_2 \delta(t - t') = (Q_{\downarrow\downarrow})_0(2x; t, t'), \end{aligned} \quad (57)$$

where m_1, m_2 have dimensions of time. We also apply a similar decomposition to S^j :

$$\begin{aligned} S^3(x, t) &= (S^3)_0(x, t) + \delta S^3(x, t), \quad \text{with} \\ (S^3)_0(x, t) &= \frac{\hbar}{2}((Q_{\uparrow\uparrow})_0(x; t, t) - (Q_{\downarrow\downarrow})_0(x; t, t)), \quad \text{and} \\ \delta S^3(x, t) &= \frac{\hbar}{2}(\delta Q_{\uparrow\uparrow}(x; t, t) - \delta Q_{\downarrow\downarrow}(x; t, t)). \end{aligned} \quad (58)$$

The variables S^1 and S^2 are decomposed in a similar manner. The proposed solution for the $(Q)_0$ field resembles the classical Néel-state solution of a Heisenberg antiferromagnet (polarized along the $j = 3$ axis).¹⁶

¹⁶To observe this resemblance quickly, refer to the $(S^j)_0$ variables in conjunction with the chosen solution for the $(Q)_0$ field in equation (57).

Next, we substitute the proposed ansatz (56) into equation (53), focusing on terms up to linear order in the fluctuations δQ . It is also convenient to transition to the following time coordinates:

$$(t, t') \rightarrow (\bar{t}, \delta t), \text{ with} \quad (59)$$

$$\bar{t} = \frac{t + t'}{2}, \delta t = t - t'.$$

We aim to analyze fluctuations in directions perpendicular to the specified polarization direction of the Néel-state, specifically along $j = 1, 2$. The governing equation for $\delta S^+ = \delta S^1 + i\delta S^2$ is:

$$\begin{aligned} \partial_{\bar{t}} \delta S^+ (2x; \bar{t}) &= \left(\frac{\tau_h}{\hbar}\right)^2 \left(\frac{\tau_h}{U}\right)^{\frac{1}{2}} (m_1 - m_2) \left\{ \delta S^+ (2x + a; \bar{t}) + \delta S^+ (2x - a; \bar{t}) + 2\delta S^+ (2x; \bar{t}) \right\}, \\ \partial_{\bar{t}} \delta S^+ (2x - a; \bar{t}) &= \left(\frac{\tau_h}{\hbar}\right)^2 \left(\frac{\tau_h}{U}\right)^{\frac{1}{2}} (m_2 - m_1) \left\{ \delta S^+ (2x; \bar{t}) + \delta S^+ (2x - 2a; \bar{t}) + 2\delta S^+ (2x - a; \bar{t}) \right\}. \end{aligned} \quad (60)$$

An analogous equation can be derived for $\delta S^- = \delta S^1 - i\delta S^2$. To obtain spin wave solutions for equation (60), we introduce the following ansatz, using the discrete translational invariance of the bipartite lattice:

$$\begin{pmatrix} \delta S^+ (2x - a; \bar{t}) \\ \delta S^+ (2x; \bar{t}) \end{pmatrix} = \begin{pmatrix} u \\ v \end{pmatrix} e^{i\tilde{k}(2x) - i\omega t}, \quad (61)$$

where $u, v \in \mathbb{C}$.

By substituting the ansatz (61) into the equation for δS^+ (60), we derive the following dispersion relation:

$$\omega^2 = -(m_1 - m_2)^2 \left(\frac{\tau_h}{U}\right) \left(\frac{4\tau_h^4}{\hbar^4}\right) \sin^2(\tilde{k}a). \quad (62)$$

Examining the dispersion relation presented in equation (62), we can draw several conclusions:

1. For the ansatz in equation (61) to correspond to a valid spin-wave solution, the frequency ω must be a real number. This condition implies that $m_1 - m_2$ must take values in $i\mathbb{R}$.
2. In the long-wavelength limit, we observe a linear dispersion relation, $\omega \propto \tilde{k}$, which is consistent with the known result in equation (32).
3. A significant limitation of this analysis is that the “velocity” associated with the dispersion relation remains undetermined. This uncertainty necessitates the specification of the value of $m_1 - m_2$, ensuring it resides in $i\mathbb{R}$. Consequently, we have not fully reproduced the result in equation (32) through our current approach.

At this juncture, we found ourselves at a standstill. We have attempted two different strategies to bosonize the Hubbard model and derive spin-wave solutions as low-energy excitations. While the second approach showed some potential improvements over the first, it remains incomplete. Furthermore, we have yet to fully grasp how to handle the continuum limit at the action level. Consequently, we are preparing to shift our focus and examine an alternative motivation for the bosonization of the Hubbard model in the following section.

3.4 Attempt III: Reformulation of the Partition Function Using a $U(1)$ field $e^{i\phi(x,t_k)}$

We make a third attempt to bosonize the strongly interacting Hubbard model using our formalism. This time, rather than bosonizing all the Grassmann fields, we focus on bosonizing a specific subset and integrating out the remaining fields. The goal is to reformulate the theory in terms of a $U(1)$ bosonic field. We begin by outlining the motivation behind this approach.

3.4.1 Motivation

The motivation for bosonizing the Hubbard model into a $U(1)$ bosonic field theory is summarized in the flowchart below.

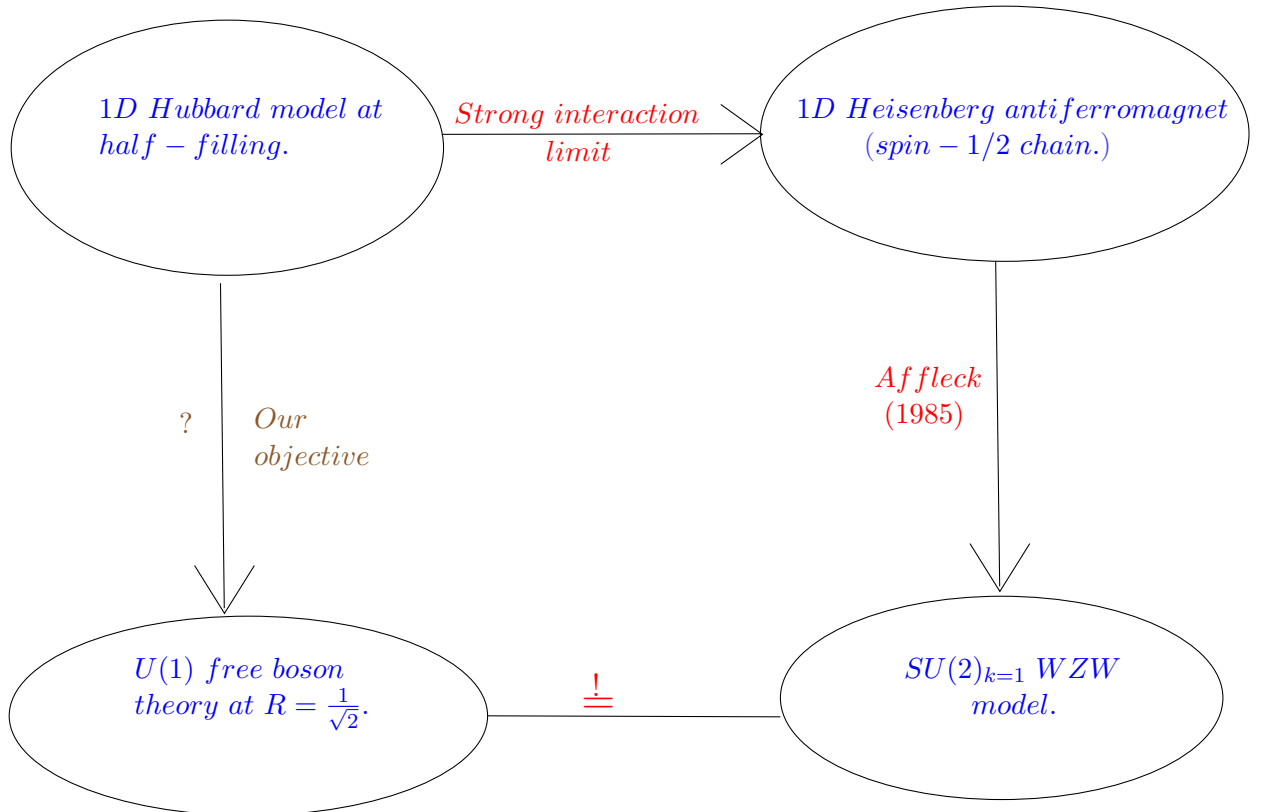


Figure 17: Flowchart illustrating the rationale for bosonizing the Hubbard model with a $U(1)$ field.

1. We previously noted that in the strong interaction limit, and at $\nu = \frac{1}{2}$, the **1D Hubbard model** maps to the **1D spin- $\frac{1}{2}$ quantum Heisenberg antiferromagnet**.
2. In 1985, I. Affleck [26] demonstrated that the **critical behavior** of the **1D spin- $\frac{1}{2}$**

quantum Heisenberg antiferromagnet is described by the $SU(2)_{k=1}$ **Wess-Zumino-Witten (WZW) model**.

The action for the $SU(2)_{k=1}$ WZW model is given by [9, 36]:

$$S = \frac{k}{16\pi} \int_{\Sigma} d^2x \operatorname{Tr} ((\partial_{\mu}g)\partial^{\mu}g^{-1}) + \frac{k}{24\pi} \int_B d^3x \epsilon^{\mu\nu\lambda} \operatorname{Tr} (g^{-1}(\partial_{\mu}g)g^{-1}(\partial_{\nu}g)g^{-1}\partial_{\lambda}g), \quad (63)$$

where the field g is defined by $g : \Sigma \rightarrow SU(2)$, and k denotes the level of the $SU(2)_k$ WZW model, which is equal to one in the present case. The second term in the action (63) is obtained by extending the compactified two-dimensional spacetime Σ to the interior of a ball B [23].¹⁷

The conserved currents of the $SU(2)_{k=1}$ WZW model are denoted as $J(z) = J_a(z)T^a$ and $\bar{J}(\bar{z}) = \bar{J}_a(\bar{z})T^a$, and are given by:

$$\begin{aligned} J(z) &= -\frac{1}{2} (\partial_z g(z, \bar{z})) g^{-1}(z, \bar{z}), \\ \bar{J}(\bar{z}) &= -\frac{1}{2} g^{-1}(z, \bar{z}) (\partial_{\bar{z}} g(z, \bar{z})), \end{aligned} \quad (64)$$

and they satisfy the conservation laws, $\partial_{\bar{z}}J = 0$ and $\partial_z\bar{J} = 0$. Here, $z = x^1 + ix^0$, where x^1 refers to the spatial coordinate and x^0 refers to the time coordinate, and T^a ($a = 1, 2, 3$) are the generators of $SU(2)$. The currents $\{J_a\}_{a=1,2,3}$ satisfy the $SU(2)_{k=1}$ Kac-Moody algebra. For a more detailed explanation, see [9, 36, 23].

3. It is possible to rewrite the $SU(2)_{k=1}$ **Wess-Zumino-Witten (WZW) model** in terms of $U(1)$ **free bosonic field theory** [37].

The action for the $U(1)$ free boson theory (in Euclidean signature) is given by [9, 37]:

$$S = \frac{1}{8\pi} \int_{\Sigma} d^2x \partial_{\mu}\phi\partial^{\mu}\phi. \quad (65)$$

The $U(1)$ bosonic field ϕ is compactified, meaning that ϕ and $\phi + 2\pi R$ are identified, where R is the compactification radius. For solutions of the equation of motion, one finds that $\phi(z, \bar{z}) = \frac{1}{2}(\phi(z) + \phi(\bar{z}))$ separates into two components, exhibiting only holomorphic and anti-holomorphic dependence, respectively.

At $R = \frac{1}{\sqrt{2}}$, the currents $J_3(z) = i\partial_z\phi(z)$ and $J_{\pm} = \exp(\pm i\sqrt{2}\phi(z))$ have the following current-current correlation functions:

$$\begin{aligned} \langle J_3(z) J_3(z') \rangle &= \frac{1}{(z - z')^2}, \\ \langle J_+(z) J_-(z') \rangle &= \frac{1}{(z - z')^2}. \end{aligned} \quad (66)$$

Note. The currents $J_3(z) = i\partial_z\phi(z)$ and $J_{\pm} = \exp(\pm i\sqrt{2}\phi(z))$ are invariant under the

¹⁷The mapping g must be extended to $g : B \rightarrow SU(2)$ for the second term in the action (63) [23].

transformation $\phi \rightarrow \phi + 2\pi R$ at $R = \frac{1}{\sqrt{2}}$.

If we define $J_{\pm} = \frac{1}{\sqrt{2}}(J_1 \pm iJ_2)$, it can be shown that the currents $\{J_a\}_{a=1,2,3}$ satisfy the $SU(2)_{k=1}$ Kac-Moody algebra. For a more detailed explanation, see [9, 36, 37].

Our objective is to rewrite the partition function of the 1D Hubbard model in terms of a $U(1)$ bosonic field, employing our approach.

3.4.2 Implementation of the Reformulation Strategy

Having previously demonstrated the application of the formalism twice, we aim to avoid redundancy and maintain reader engagement. Therefore, we present an outline of the steps in a schematic flowchart (see Figure 18), with detailed calculations included in Appendix E.

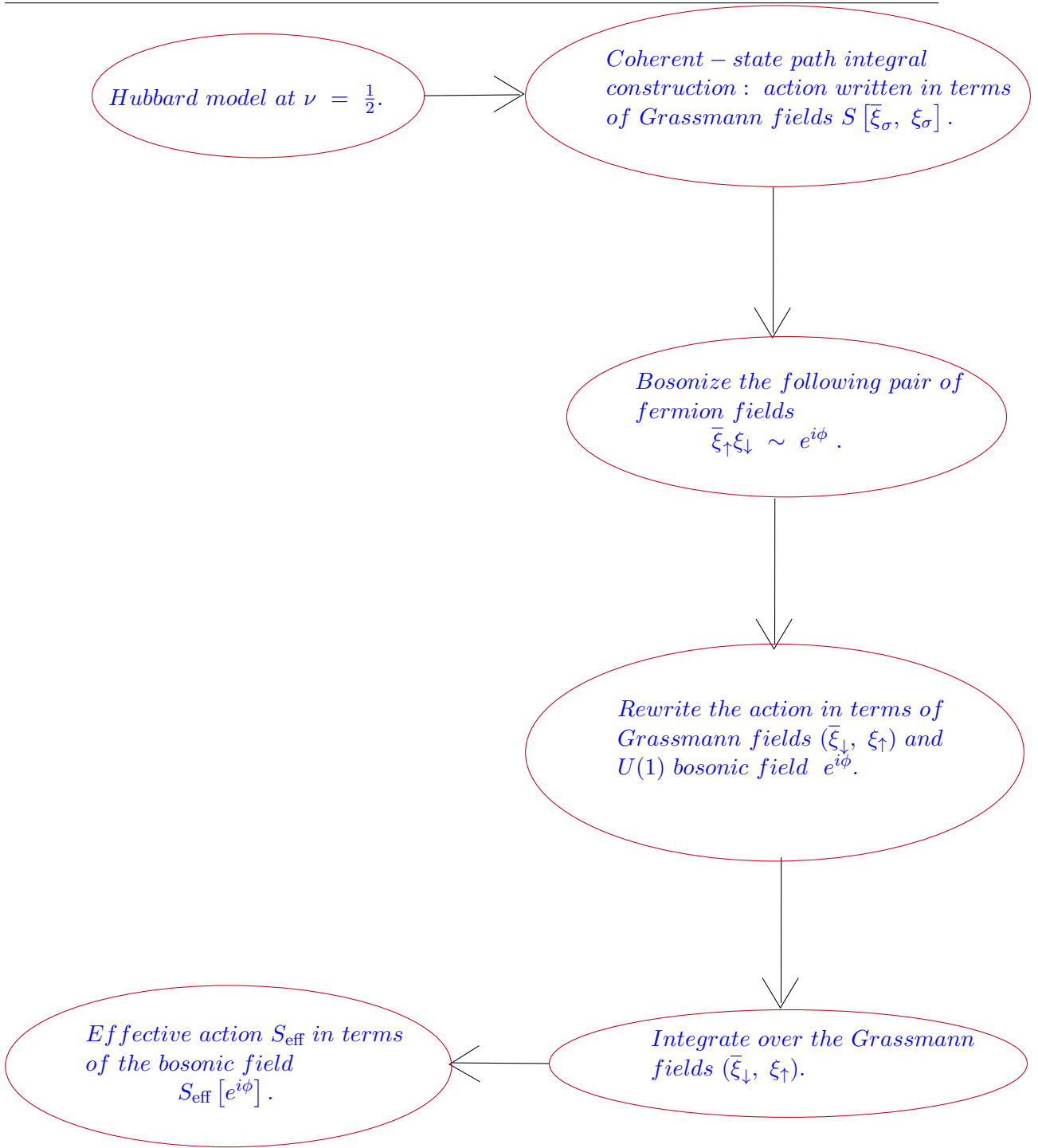


Figure 18: Flowchart outlining the steps involved in the bosonization of the 1D Hubbard model. Detailed calculations can be found in Appendix E.

Following the outlined steps, the partition function can be expressed as:

$$Z = \int_0^{2\pi} \prod_{x,t_k} \frac{d\phi(x,t_k)}{2\pi} \exp \left\{ \frac{iS_{\text{eff}}[e^{i\phi}]}{\hbar} \right\}, \quad (67)$$

where $S_{\text{eff}}[e^{i\phi}]$ is given by:

$$\begin{aligned}
 S_{\text{eff}}[e^{i\phi}] = & -i\hbar \sum_{x,t_k} \left\{ \ln \left(1 + e^{i\phi(x,t_{k-1}) - i\phi(x,t_k)} \right) \right. \\
 & + \left(\left(\frac{\Delta t U}{2\hbar} \right)^2 - 2 \left(\frac{\Delta t \tau_h}{\hbar} \right)^2 \right) \left(1 + e^{i\phi(x,t_k) - i\phi(x,t_{k-1})} \right)^{-1} \\
 & \left. - \left(\frac{\Delta t \tau_h}{\hbar} \right)^2 \left(1 + e^{i\phi(x,t_k) - i\phi(x,t_{k-1})} \right)^{-1} \left(e^{i\phi(x+a,t_{k-1}) - i\phi(x,t_{k-1})} + e^{i\phi(x-a,t_{k-1}) - i\phi(x,t_{k-1})} \right) \right\}.
 \end{aligned} \tag{68}$$

The next step is to determine how to take the continuum limit in time for equation (68). One approach we considered is the stationary phase approximation. However, for this approximation to be applicable, a crucial condition must be satisfied.

To illustrate, let us consider the following integral:

$$\prod_{x,t_k} \frac{d\phi(x,t_k)}{2\pi} \exp \left\{ i\lambda \sum_{x,t_k} e^{i\phi(x,t_k) - i\phi(x,t_{k-1})} \right\}. \tag{69}$$

The stationary phase approximation is valid only in the limit where $\lambda \gg 1$. In this regime, we can assume that fluctuations in the field $\phi(x,t_k)$ are small, allowing us to expand $e^{i\phi(x,t_k) - i\phi(x,t_{k-1})}$ using a Taylor series. However, this condition is not satisfied in equation (68), which precludes the use of this method to establish the continuum limit in time.

3.5 Concluding Remarks

Despite our efforts to apply the bosonization method through three different approaches, the challenge of establishing the continuum limit in time remains unresolved. With no alternative solutions at hand¹⁸, we have opted to pursue the more complex approach of performing renormalization on the system before applying the bosonization formula. We believe this approach may help resolve the difficulties outlined in this chapter and provide a clearer definition of the continuum limit in time. In the next chapter, we will discuss the concept of applying renormalization prior to utilizing the bosonization formula.

¹⁸We recognize the example of Brownian motion and how the continuum limit in time is defined in this context [38, 39, 40]. Brownian motion can be described using a path integral formulation. To properly define the continuum limit in time, one must utilize the property of Brownian motion that the mean squared displacement is proportional to time. For illustration, consider a simple random walk in one spatial dimension [38], as Brownian motion can be viewed as the limit of simple random walks. In this model, a walker starts at an arbitrary origin and takes a fixed length step Δx at each time step Δt . The walker can move either left or right, with each step being independent and uncorrelated. We can examine the normalized probability density function of the position vector after M steps, i.e., at time $M\Delta t$. To demonstrate that this probability density function approaches the fundamental Gaussian solution of the diffusion equation, we must take the limits $M \rightarrow \infty$, $\Delta t \rightarrow 0$, while ensuring that $(\Delta x)^2 \propto \Delta t$ and $T = M\Delta t$. However, it is important to note that this framework does not apply to our current problem, as there is no external input that provides an analogous condition of $(\Delta x)^2 \propto \Delta t$ relevant to our case.

4 Applying Renormalization to Properly Define the Continuum Limit in Time

In the previous chapter, we explored three approaches to bosonizing the system, each of which faced the challenge of defining the continuum limit in time. To address this ongoing issue, we are shifting our approach to renormalization, a key concept in quantum field theory. We want to clarify from the outset that, while we have not yet resolved the continuum limit problem, we will outline how renormalization might offer a potential solution.

We will begin by reviewing some fundamental concepts of renormalization [9]. Suppose we are studying a system described by a general action:

$$S_{\text{bare}}[\{\rho_{\text{bare}}\}], \quad (70)$$

where $\{\rho_{\text{bare}}\}$ denote the “bare” coupling parameters of the system. Assume we are working on a discretized space-time lattice. The renormalization method can be applied to develop a low-energy effective description of the system, and the steps to achieve this are outlined below.

First, we introduce cutoffs in both space and time. This is necessary because, in the low-energy limit, fluctuations at smaller spatial and temporal scales (which correspond to higher energy modes) can generally be neglected. Physical observables remain largely unchanged on scales smaller than these cutoffs. In most condensed matter physics problems, the spatial cutoff is typically chosen to be the lattice constant a . For a system with a mass gap E_{gap} , the corresponding cutoff in time can be defined as follows:

$$t_{\text{cutoff}} \sim \frac{1}{E_{\text{gap}}}. \quad (71)$$

The next stage in the renormalization process involves integrating out the high-energy modes (or, equivalently, the modes associated with short time and length scales). Repeating this integration process generates the renormalization group flow. During this procedure, the coupling parameters $\{\rho_{\text{bare}}\}$ evolve into $\{\rho_{\text{physical}}\}$. Additionally, the original action transforms into an effective action, which is given by:

$$S_{\text{eff}}[\{\rho_{\text{physical}}\}]. \quad (72)$$

Through this process¹⁹, a valid low-energy description of the system is achieved when the renormalized theory is not directly sensitive to variations in the cutoff. In other words, this implies that one can modify the cutoff and adjust the coupling parameters accordingly without altering the low-energy behavior of the system.

Once we have achieved a low-energy description that is independent of the cutoff, we should be able to take the continuum limit in time, ensuring that this low-energy description stays

¹⁹We will not delve into every step of the renormalization process here. Instead, our aim is to review the underlying concept of renormalization.

consistent and well-defined.

Following this brief review of renormalization concepts, we aim to outline how to integrate these concepts with the bosonization formula (7) to analyze the system and derive its low-energy description. To achieve this, we will utilize the Kadanoff block spin transformation method [41, 42] for the renormalization process. First, we will summarize the general idea behind the Kadanoff renormalization scheme, after which we will focus on our specific problem.

4.1 Kadanoff Block Spin Transformation

In this section, we will illustrate the concept of the Kadanoff block spin transformation [42] through an example. Consider a real scalar field defined on a two-dimensional lattice:

$$\phi : \mathbb{Z}^2 \rightarrow \mathbb{R}. \quad (73)$$

The “bare” action for the system is denoted as $S_{\text{bare}}[\phi]$, and the corresponding partition function is given by:

$$Z = \int D\phi e^{-S_{\text{bare}}[\phi]}. \quad (74)$$

Kadanoff’s approach involves grouping the fields associated with individual sites into blocks and defining a new variable for each block. Each site of the original lattice belongs to exactly one block.

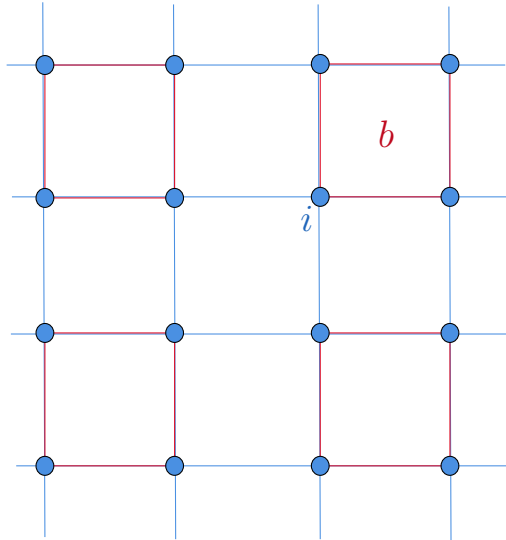


Figure 19: Two-dimensional lattice. To demonstrate Kadanoff’s concept, consider the block labeled b . All four fields linked to the lattice sites within this block (with one site designated as i) are grouped together.

The operational method for connecting the new variable to ϕ_i and subsequently performing renormalization can be summarized in the following steps:

1. As noted earlier, the first step is to introduce a new variable Φ_b for each block (labeled b). The size of this block essentially determines the cutoff for the problem at hand,

indicating that fluctuations of the field Φ_b on scales smaller than this cutoff can be disregarded in the low-energy description of the system.

2. The next step involves inserting the expression

$$1 = \int d\Phi_b \delta(\Phi_b - \text{Av}_b[\phi]) \quad (75)$$

under the functional integral given in equation (74). Here, $\delta(\cdot)$ denotes the Dirac delta function, and $\text{Av}_b[\phi]$ represents an ‘‘averaging’’ procedure applied to the fields ϕ_i , where i refers to the sites within the block b . For the current context, $\text{Av}_b[\phi]$ can be defined as:

$$\text{Av}_b[\phi] = \sum_i \phi_i. \quad (76)$$

3. The final step involves changing the order of integration as shown below:

$$\begin{aligned} Z &= \int D\phi e^{-S_{\text{bare}}[\phi]} = \int D\phi e^{-S_{\text{bare}}[\phi]} \int D\Phi \prod_b \delta(\Phi_b - \text{Av}_b[\phi]) \\ &= \int D\Phi \int D\phi \prod_b \delta(\Phi_b - \text{Av}_b[\phi]) e^{-S_{\text{bare}}[\phi]} = \int D\Phi e^{-S_{\text{eff}}^{(1)}[\Phi]}. \end{aligned} \quad (77)$$

As indicated by the final equation, the initial iteration of the renormalization step transforms the original bare action into an effective action, denoted by $S_{\text{eff}}^{(1)}[\Phi]$. By repeating this process, one obtains the renormalization group flow. As discussed earlier, a low-energy description (or, equivalently, a well-defined theory at large distances) is achieved when the renormalized theory becomes insensitive to variations in the cutoff.

This completes the review of the Kadanoff renormalization scheme, and we will now return to our specific problem.

4.2 Integrating Renormalization Concepts into the Bosonization Approach

We would now like to outline how we intend to incorporate the previously mentioned concept of renormalization into the bosonization framework. We will proceed with the following steps:

1. Start with the fermionic functional integral expression for the partition function in discrete time:

$$Z = \int_{\xi} e^{-S_{\text{bare}}[\bar{\xi}, \xi]}, \quad (78)$$

with the fields $\bar{\xi}, \xi$ representing the ‘‘bare’’ degree of freedom. Here, \int_{ξ} denotes the Berezin integral. Additionally, we are working on a discretized lattice in both space and time.

2. In the next step, we apply the Kadanoff block spin transformation, as discussed in the

previous section. Insert

$$1 = \int_{\xi'} \delta(\bar{\xi}'_b \cdot \xi'_b - \text{Av}_b(\bar{\xi}, \xi)) \quad (79)$$

under the functional integral. Here, we have introduced new fields $(\bar{\xi}'_b, \xi'_b)$ in the equation above using the “averaging” procedure $\text{Av}_b(\bar{\xi}, \xi)$ applied to the “bare” fields. These new fields are defined over a block on the space-time lattice, with the block size determining the cutoff in both space and time. The cutoff has the same significance as before: fluctuations of the fields $(\bar{\xi}'_b, \xi'_b)$ on scales smaller than this cutoff can be neglected in the low-energy description of the system. The dot product in $\bar{\xi} \cdot \xi$ represents the sum over the “color” degrees of freedom, where “color” refers to the sites of the two-dimensional space-time lattice within the chosen block b .

3. Next, we use the bosonization formula (7) to rewrite the expression in (79) as follows:

$$1 = \int_{U(n)} dU_b \text{Det}^{-R}(U_b) \delta(U_b - \text{Av}_b(\bar{\xi}, \xi)). \quad (80)$$

Here n represents the total number of “flavor” degrees of freedom, and R denotes the total number of “color” degrees of freedom.

4. The final step is to change the order of integration, as is also done in the Kadanoff block spin transformation.

$$\begin{aligned} \mathbf{Z} &= \int_{\xi} e^{-S_{\text{bare}}[\bar{\xi}, \xi]} = \int_{\xi} e^{-S_{\text{bare}}[\bar{\xi}, \xi]} \int_{U(n)} DU \prod_b \text{Det}^{-R}(U_b) \delta(U_b - \text{Av}_b(\bar{\xi}, \xi)) \\ &= \int_{U(n)} DU \int_{\xi} \prod_b \text{Det}^{-R}(U_b) \delta(U_b - \text{Av}_b(\bar{\xi}, \xi)) e^{-S_{\text{bare}}[\bar{\xi}, \xi]} = \int_{U(n)} DU e^{-S_{\text{eff}}^{(1)}[U]}. \end{aligned} \quad (81)$$

Here, $S_{\text{eff}}^{(1)}[U]$ denotes the effective action after the first iteration. Repeating this iteration generates the renormalization group flow.

We have outlined the steps necessary to integrate renormalization and bosonization for an accurate low-energy description of the system. However, following these steps can be computationally challenging. While we will mention some key points required to begin the calculations, we must acknowledge that we have not yet advanced beyond this stage in our computations for the system of interest, specifically the 1D Hubbard model.

Firstly, it is necessary to define the “averaging” procedure. One possible way to define $\text{Av}_b(\bar{\xi}, \xi)$ is given below:

$$\frac{1}{2} \text{Tr}(\tau_a \text{Av}_b(\bar{\xi}, \xi)) = \frac{1}{2} \sum_{\sigma, \sigma'} (\tau_a)_{\sigma\sigma'} \sum_{(x,t) \in b} (-1)^x \frac{\bar{\xi}_{\sigma}(x,t) \xi_{\sigma'}(x,t)}{R}. \quad (82)$$

Here, Tr denotes the trace over the “flavor” degrees of freedom, corresponding to the two spin components ($n = 2$). The matrices τ_a represents the standard Pauli matrices ($a = 1, 2, 3$). The pair (x, t) denotes the space-time lattice sites within the block b . An

important aspect of this averaging procedure is the staggering factor $(-1)^x$ in space.²⁰

An additional important point not covered in the section on the Kadanoff block spin transformation, but crucial for computations, is that this transformation offers some flexibility: the Dirac delta function can be replaced by another smooth function. The only requirement is that this function must have a total mass equal to one, as indicated in equation (79). The choice of this function is crucial for computational purposes, as a poor selection can significantly complicate the renormalization process. This concludes our discussion on how to perform the renormalization step, as we have not advanced beyond this point in our computations.

Although we have not completed the renormalization process, let us assume for the sake of discussion that it has been finalized, allowing us to obtain the low-energy effective description of the system. The next step is to take the continuum limit in time, specifically as $\Delta t \rightarrow 0$. Here, Δt represents the time interval between consecutive time slices introduced during the path integral construction of the partition function (78) in discrete time.

In the two-dimensional space-time lattice framework, as we take the continuum limit in time by sending Δt to zero, the block b will progressively cover an increasing number of lattice sites, resulting in more fields being included in the “averaging process”. We expect that once we achieve a low-energy description independent of the cutoff, this description will remain invariant under this process. Consequently, we anticipate a well-defined continuum limit in time, which will address the issues encountered in our analysis.

In summary, we have outlined how to incorporate renormalization into the functional integral bosonization scheme to tackle the technical challenge of taking the continuum limit in time. The implementation of the ideas discussed here will be explored in future work. For now, we conclude the first project of this thesis, with a summary of this project provided in the next chapter.

²⁰This choice of averaging procedure with staggering is motivated by the derivation of the $O(3)$ non-linear sigma model from the 1D Heisenberg antiferromagnet [43, 44, 45, 46].

5 Conclusion from the First Project

This chapter concludes the first project of this thesis by summarizing the key findings and suggesting potential directions for future research. The focus of this project has been on strongly interacting fermion systems, motivated by the lack of analytical methods available to describe such systems effectively. One widely used tool in quantum field theory is the Hubbard-Stratonovich (HS) transformation, which has proven valuable in many applications but is limited to weakly interacting systems. Consequently, the primary goal of this project was to develop an analytical method for studying strongly interacting systems.

The method introduced in this thesis builds on the bosonization formula presented in [1], which has seen limited exploration in the literature. By utilizing this formula within the functional integral framework, we reformulated the theory, originally described in terms of fermion fields, into one based on a unitary matrix in “flavor” space. This reformulation aims to provide a more accurate description of strongly interacting systems.

To validate our method, we applied it to the one-dimensional Hubbard model at half-filling in the strong interaction limit. This model is well-studied, and we used its established results as benchmarks to test the accuracy of our approach. However, a persistent challenge throughout the project has been defining the continuum limit in time. Despite demonstrating three different approaches to bosonizing the system, this issue remained unresolved. While we have not previously discussed them, we also explored alternative approaches by adjusting how we set up the functional integral in an attempt to address this challenge. Although these attempts did not succeed, they are briefly outlined here for completeness.

The first alternative approach involved a different choice of reference state in the construction of the coherent-state functional integral [47]. While the vacuum state (all states unoccupied) is the “standard choice”, given that we are working with the one-dimensional Hubbard model at half-filling and strong interactions, a more suitable reference might be the Néel-state. Thus, we formulated the functional integral using the Néel-state as the reference. The second attempt utilized the Glauber P-representation for fermionic operators, as introduced by Cahill and Glauber in [48, 49]. The third attempt followed the idea proposed by Affleck in [26], where the fermion field in one-dimensional space is split into left- and right-moving components near the two Fermi points. Despite these different setups, the issue with taking the continuum limit in time persisted in all three cases. As such, we do not present them here, but we mention them for completeness.

Recognizing the difficulty of the problem, we ultimately adopted a more intricate approach, as discussed earlier in the thesis: applying renormalization to the system before using the bosonization formula. Renormalization enables us to derive a low-energy description that does not require taking the continuum limit. After obtaining this low-energy description, as outlined in Chapter 4, we expect that the continuum limit can be more effectively addressed. However, as acknowledged, the full execution of this approach remains a topic for

future work.

In conclusion, we hope that the functional integral bosonization method (along with the incorporation of renormalization) can contribute to our understanding of intriguing physical phenomena, such as the physics of high-temperature superconductors [50]. For example, applying this formalism to models describing doped Mott insulators [51] could yield valuable insights. Overall, we hope that this method may pave the way for further exploration in the realm of strongly interacting electron systems.

APPENDICES

A Linked-cluster expansion

We illustrate the linked-cluster expansion discussed in Chapter 2. Starting with the equation

$$\langle e^{-\lambda O(g)} \rangle_{U(R)} := e^{-S_c}, \quad (83)$$

our goal is to express S_c using the linked-cluster expansion method. In this context, λ is a small parameter ($\lambda \ll 1$). The term $\langle e^{-\lambda O(g)} \rangle_{U(R)}$ represents the integration of $e^{-\lambda O(g)}$ with respect to the Haar measure on $U(R)$, where $O(g)$ is a function of $g \in U(R)$. The expression given in (83) can be rewritten as:

$$-S_c = \ln \left(\langle e^{-\lambda O(g)} \rangle_{U(R)} \right). \quad (84)$$

Expanding the expression given in (84) in powers of λ , we obtain the following linked-cluster expansion:

$$S_c = \lambda S_c^1 + \lambda^2 S_c^2 + \dots, \quad (85)$$

where S_c^1 and S_c^2 represent the first and second orders of the linked-cluster expansion, respectively. The ellipsis indicates the higher-order terms that are not detailed here. The expressions for S_c^1 and S_c^2 are provided below:

$$\begin{aligned} S_c^1 &= \langle O(g) \rangle_{U(R)}, \\ S_c^2 &= -\frac{1}{2} \left(\langle O(g)^2 \rangle_{U(R)} - \langle O(g) \rangle_{U(R)}^2 \right). \end{aligned} \quad (86)$$

This concludes the explanation of the linked-cluster expansion that was used in Chapter 2.

B Equations of Motion from Haar Measure Invariance

Within this appendix, we outline how the equations of motion (43) from Section 3.2 are obtained using Haar measure invariance under left and right multiplication. We focus on the derivation related to left invariance here, noting that a similar approach applies to the derivation from right invariance.

Using the left invariance of the Haar measure, we obtain the following equation:

$$\int_{U(4)} dQ(x, t_k) \exp\left(\frac{iS_{\text{eff}}[Q(x, t_k)]}{\hbar}\right) = \int_{U(4)} dQ(x, t_k) \exp\left(\frac{iS_{\text{eff}}[e^{\lambda X} Q(x, t_k)]}{\hbar}\right), \quad (87)$$

where X denotes a generator of the Lie algebra $u(4)$, and λ is a scalar in \mathbb{R} . The above equation implies that

$$\int_{U(4)} dQ(x, t_k) \exp\left(\frac{iS_{\text{eff}}[e^{\lambda X} Q(x, t_k)]}{\hbar}\right) \quad (88)$$

is independent of λ . Another way to express this is:

$$\left. \frac{d}{d\lambda} \right|_{\lambda=0} \int_{U(4)} dQ(x, t_k) \exp\left(\frac{iS_{\text{eff}}[e^{\lambda X} Q(x, t_k)]}{\hbar}\right) = 0. \quad (89)$$

The above equation (89) leads to:

$$\int_{U(4)} dQ(x, t_k) \exp\left(\frac{iS_{\text{eff}}[Q(x, t_k)]}{\hbar}\right) \left. \frac{d}{d\lambda} \right|_{\lambda=0} S_{\text{eff}}[e^{\lambda X} Q(x, t_k)] = 0. \quad (90)$$

Similarly, by applying the right invariance of the Haar measure, one obtains:

$$\int_{U(4)} dQ(x, t_k) \exp\left(\frac{iS_{\text{eff}}[Q(x, t_k)]}{\hbar}\right) \left. \frac{d}{d\lambda} \right|_{\lambda=0} S_{\text{eff}}[Q(x, t_k)e^{\lambda X}] = 0. \quad (91)$$

Thus, we have established that the equation of motion (43), as outlined in Section 3.2, is valid within the integral and is derived from the invariance of the Haar measure.

C Derivation of the Equations of Motion for the Matrix Components of the Field $Q(x, t_k)$ in Section 3.2

In the accompanying appendix, we detail the three-step procedure described in Section 3.2 to derive the equation of motion in the continuum time limit for a specific matrix component of the field $Q(x, t_k)$, specifically $(Q_{++})_{\uparrow\uparrow}(x, t_k)$. The equations of motion for the other matrix components can be obtained following the same steps.

1. The first step is to specify the generator X . To derive the equation of motion for $(Q_{++})_{\uparrow\uparrow}(x, t_k)$, we adopt the following generator:

$$X = \begin{pmatrix} i & 0 & 0 & 0 \\ 0 & 0 & 0 & 0 \\ 0 & 0 & 0 & 0 \\ 0 & 0 & 0 & 0 \end{pmatrix}. \quad (92)$$

Observe that $X = -X^\dagger$, as expected for a generator of the $u(4)$ Lie algebra.

2. The second step involves deriving the equations of motion by exploiting the left and right invariance properties of the Haar measure. The equation

$$L|_{x, t_k} \equiv \left. \frac{d}{d\lambda} \right|_{\lambda=0} S_{\text{eff}}[e^{\lambda X} Q(x, t_k)] = 0, \quad (93)$$

which is derived using the left invariance of the Haar measure, is presented below:

$$\begin{aligned} & -1 + \left(\frac{\tau_h}{U}\right)^{\frac{1}{2}} (Q_{++})_{\uparrow\uparrow}(x, t_k) - \left(\frac{i\tau_h\Delta t}{\hbar}\right) (Q_{++})_{\uparrow\uparrow}(x, t_k) (Q_{++})_{\downarrow\downarrow}(x, t_k) \\ & + \left(\frac{U}{\tau_h}\right)^{\frac{1}{2}} \left(\frac{i\tau_h\Delta t}{2\hbar}\right) (Q_{++})_{\uparrow\uparrow}(x, t_k) + \left(\frac{U}{\tau_h}\right) \left(\frac{\tau_h\Delta t}{\hbar}\right)^2 (Q_{++})_{\uparrow\uparrow}(x, t_k) (Q_{++})_{\downarrow\downarrow}(x, t_k) \\ & - \left(\frac{U}{\tau_h}\right)^{\frac{3}{2}} \left(\frac{\tau_h\Delta t}{2\hbar}\right)^2 (Q_{++})_{\uparrow\uparrow}(x, t_k) - \left(\frac{\tau_h}{U}\right)^{\frac{1}{2}} \left(\frac{\tau_h\Delta t}{\hbar}\right)^2 (Q_{++})_{\uparrow\uparrow}(x, t_k) \\ & + \left(\frac{\tau_h}{U}\right) \left(\frac{\tau_h\Delta t}{\hbar}\right)^2 \sum_{\sigma} \sum_{y=x+a, x-a} \left((Q_{++})_{\uparrow\sigma}(x, t_k) (Q_{++})_{\sigma\uparrow}(y, t_k) - (Q_{+-})_{\uparrow\sigma}(x, t_k) (Q_{-+})_{\sigma\uparrow}(y, t_k) \right) \\ & - \left(\frac{\tau_h}{U}\right) \sum_{\sigma} (Q_{+-})_{\uparrow\sigma}(x, t_k) (Q_{-+})_{\sigma\uparrow}(x, t_{k+1}) \\ & = 0. \end{aligned} \quad (94)$$

The equation

$$R|_{x, t_k} \equiv \left. \frac{d}{d\lambda} \right|_{\lambda=0} S_{\text{eff}}[Q(x, t_k) e^{\lambda X}] = 0, \quad (95)$$

which is derived using the right invariance of the Haar measure, is presented below:

$$\begin{aligned}
& -1 + \left(\frac{\tau_h}{U}\right)^{\frac{1}{2}} (Q_{++})_{\uparrow\uparrow}(x, t_k) - \left(\frac{i\tau_h\Delta t}{\hbar}\right) (Q_{++})_{\uparrow\uparrow}(x, t_k)(Q_{++})_{\downarrow\downarrow}(x, t_k) \\
& + \left(\frac{U}{\tau_h}\right)^{\frac{1}{2}} \left(\frac{i\tau_h\Delta t}{2\hbar}\right) (Q_{++})_{\uparrow\uparrow}(x, t_k) + \left(\frac{U}{\tau_h}\right) \left(\frac{\tau_h\Delta t}{\hbar}\right)^2 (Q_{++})_{\uparrow\uparrow}(x, t_k)(Q_{++})_{\downarrow\downarrow}(x, t_k) \\
& - \left(\frac{U}{\tau_h}\right)^{\frac{3}{2}} \left(\frac{\tau_h\Delta t}{2\hbar}\right)^2 (Q_{++})_{\uparrow\uparrow}(x, t_k) - \left(\frac{\tau_h}{U}\right)^{\frac{1}{2}} \left(\frac{\tau_h\Delta t}{\hbar}\right)^2 (Q_{++})_{\uparrow\uparrow}(x, t_k) \\
& + \left(\frac{\tau_h}{U}\right) \left(\frac{\tau_h\Delta t}{\hbar}\right)^2 \sum_{\sigma} \sum_{y=x+a, x-a} \left((Q_{++})_{\sigma\uparrow}(x, t_k)(Q_{++})_{\uparrow\sigma}(y, t_k) - (Q_{--})_{\sigma\uparrow}(x, t_k)(Q_{+-})_{\uparrow\sigma}(y, t_k) \right) \\
& - \left(\frac{\tau_h}{U}\right) \sum_{\sigma} (Q_{+-})_{\uparrow\sigma}(x, t_{k-1})(Q_{-+})_{\sigma\uparrow}(x, t_k) \\
& = 0.
\end{aligned} \tag{96}$$

3. In the third step, we replace t_k with t_{k+1} in $R|_{x, t_k}$, subtract this from $L|_{x, t_k}$, and then take the continuum limit as $\Delta t \rightarrow 0$. The resulting equation of motion is:

$$\partial_t (Q_{++})_{\uparrow\uparrow}(x, t) = 0. \tag{97}$$

In the continuum limit, t_k is replaced by t , and $\partial_t (Q_{++})_{\uparrow\uparrow}(x, t)$ represents

$$\frac{(Q_{++})_{\uparrow\uparrow}(x, t_{k+1}) - (Q_{++})_{\uparrow\uparrow}(x, t_k)}{\Delta t}. \tag{98}$$

Based on equation (97), we observe that the contribution from the hopping term vanishes in the continuum limit. This completes our detailed calculation of the equations of motion in this limit. As previously mentioned, a similar approach can be used to derive the equations of motion for the other matrix components, where it is also noted that the hopping term does not contribute. For further discussion, readers are invited to refer back to Section 3.2 in the main body of the thesis.

D Derivation of the Equations of Motion for the Matrix Components of the Field $Q(x)$ in Section 3.3

In the following appendix, we present the detailed calculations for the equations of motion (53) for the matrix components of the field $Q(x)$. We will adhere to the three-step method outlined in Section 3.2, though with some modifications. Let's begin with the derivation.

1. The first step follows the procedure outlined in Section 3.2, except that we now select a generator from the Lie algebra $u(2M)$ instead of $u(4)$. In this appendix, we detail the calculations for a specific generator X of the $u(2M)$ algebra. This matrix X is a $2M \times 2M$ matrix, characterized by having a single non-zero matrix element, as specified below:

$$X_{\uparrow\uparrow}(t_v, t_v) = i. \quad (99)$$

As a reminder, in the time discretization step of the coherent-state path integral construction, the time slices are denoted by k , where $k = 1, \dots, M$. In this context, we choose v in equation (99) to be between 1 and M , specifically choosing $v \neq 1$ and $v \neq M$.

2. The second step closely follows the method detailed in Section 3.2. In this step, we derive the equations of motion by exploiting the left and right invariance properties of the Haar measure. The equation

$$L|_x \equiv \frac{d}{d\lambda} \Big|_{\lambda=0} S_{\text{eff}}[e^{\lambda X} Q(x)] = 0, \quad (100)$$

which is derived using the left invariance of the Haar measure, is presented below:

$$\begin{aligned} & -1 + \left(\frac{\tau_h}{U}\right)^{\frac{1}{2}} (Q_{\uparrow\uparrow}(x; t_v, t_{v-1}) - Q_{\uparrow\uparrow}(x; t_v, t_v)) \\ & - \left(\frac{\tau_h}{U}\right) \left(\frac{iU\Delta t}{\hbar}\right) Q_{\uparrow\uparrow}(x; t_v, t_{v-1}) Q_{\downarrow\downarrow}(x; t_v, t_{v-1}) \\ & + \left(\frac{\tau_h}{U}\right)^{\frac{1}{2}} \left(\frac{iU\Delta t}{2\hbar}\right) Q_{\uparrow\uparrow}(x; t_v, t_{v-1}) + \left(\frac{\tau_h}{U}\right) \left(\frac{U\Delta t}{\hbar}\right)^2 Q_{\uparrow\uparrow}(x; t_v, t_{v-1}) Q_{\downarrow\downarrow}(x; t_v, t_{v-1}) \\ & - \left(\frac{\tau_h}{U}\right)^{\frac{1}{2}} \left(\frac{U\Delta t}{2\hbar}\right)^2 Q_{\uparrow\uparrow}(x; t_v, t_{v-1}) - \left(\frac{\tau_h}{U}\right)^{\frac{1}{2}} \left(\frac{\tau_h\Delta t}{\hbar}\right)^2 Q_{\uparrow\uparrow}(x; t_v, t_{v-1}) \\ & + \left(\frac{\tau_h}{U}\right) \left(\frac{\tau_h\Delta t}{\hbar}\right)^2 \sum_{k=1}^M \sum_{\sigma} \sum_{y=x+a, x-a} Q_{\uparrow\sigma}(x; t_v, t_{k-1}) Q_{\sigma\uparrow}(y; t_k, t_{v-1}) \\ & = 0. \end{aligned} \quad (101)$$

The equation

$$R|_x \equiv \frac{d}{d\lambda} \Big|_{\lambda=0} S_{\text{eff}}[Q(x)e^{\lambda X}] = 0, \quad (102)$$

which is derived using the left invariance of the Haar measure, is presented below:

$$\begin{aligned}
& -1 + \left(\frac{\tau_h}{U}\right)^{\frac{1}{2}} (Q_{\uparrow\uparrow}(x; t_{v+1}, t_v) - Q_{\uparrow\uparrow}(x; t_v, t_v)) \\
& - \left(\frac{\tau_h}{U}\right) \left(\frac{iU\Delta t}{\hbar}\right) Q_{\uparrow\uparrow}(x; t_{v+1}, t_v) Q_{\downarrow\downarrow}(x; t_{v+1}, t_v) \\
& + \left(\frac{\tau_h}{U}\right)^{\frac{1}{2}} \left(\frac{iU\Delta t}{2\hbar}\right) Q_{\uparrow\uparrow}(x; t_{v+1}, t_v) + \left(\frac{\tau_h}{U}\right) \left(\frac{U\Delta t}{\hbar}\right)^2 Q_{\uparrow\uparrow}(x; t_{v+1}, t_v) Q_{\downarrow\downarrow}(x; t_{v+1}, t_v) \\
& - \left(\frac{\tau_h}{U}\right)^{\frac{1}{2}} \left(\frac{U\Delta t}{2\hbar}\right)^2 Q_{\uparrow\uparrow}(x; t_{v+1}, t_v) - \left(\frac{\tau_h}{U}\right)^{\frac{1}{2}} \left(\frac{\tau_h\Delta t}{\hbar}\right)^2 Q_{\uparrow\uparrow}(x; t_{v+1}, t_v) \\
& + \left(\frac{\tau_h}{U}\right) \left(\frac{\tau_h\Delta t}{\hbar}\right)^2 \sum_{k=1}^M \sum_{\sigma} \sum_{y=x+a, x-a} Q_{\sigma\uparrow}(x; t_k, t_v) Q_{\uparrow\sigma}(y; t_{v+1}, t_{k-1}) \\
& = 0.
\end{aligned} \tag{103}$$

3. In the third step, we subtract $R|_x$ from $L|_x$, and then take the continuum limit as $\Delta t \rightarrow 0$. This process yields the following equation of motion:

$$\begin{aligned}
& \left[\partial_t Q_{\uparrow\uparrow}(x; t, t') + \partial_{t'} Q_{\uparrow\uparrow}(x; t, t') \right] \Big|_{t=t'} \\
& = \left(\frac{\tau_h}{\hbar}\right)^2 \left(\frac{\tau_h}{U}\right)^{\frac{1}{2}} \sum_{\sigma} \sum_{y=x+a, x-a} \int dt'' \left\{ Q_{\uparrow\sigma}(x; t, t'') Q_{\sigma\uparrow}(y; t'', t) - Q_{\uparrow\sigma}(y; t, t'') Q_{\sigma\uparrow}(x; t'', t) \right\}.
\end{aligned} \tag{104}$$

In the continuum limit, t_v is replaced by t , and t_k is replaced by t'' . The expression

$$\left. \partial_t Q_{\uparrow\uparrow}(x; t, t') \right|_{t=t'} \text{ denotes } \frac{Q_{\uparrow\uparrow}(x; t_{n+1}, t_n) - Q_{\uparrow\uparrow}(x; t_n, t_n)}{\Delta t}, \tag{105}$$

$$\text{while } \left. \partial_{t'} Q_{\uparrow\uparrow}(x; t, t') \right|_{t=t'} \text{ denotes } \frac{Q_{\uparrow\uparrow}(x; t_n, t_n) - Q_{\uparrow\uparrow}(x; t_n, t_{n-1})}{\Delta t}, \tag{106}$$

in the limit $\Delta t \rightarrow 0$. Here, we have derived the equations of motion for $Q_{\uparrow\uparrow}$ as stated in equation (53) in Section 3.3. For the other components, $Q_{\uparrow\downarrow}$, $Q_{\downarrow\uparrow}$, and $Q_{\downarrow\downarrow}$, the same procedure can be applied to derive their respective equations of motion, which are also given in equation (53). To continue the discussion, readers should consult Section 3.3 in the main body of the thesis.

E Detailed Calculations for Attempt-III from Section 3.4

In this appendix, we elaborate on the calculations that were omitted in Section 3.4, where we reformulate the partition function of the 1D Hubbard model using a $U(1)$ bosonic field. The calculations presented here assume a 1D lattice with periodic boundary conditions imposed in the spatial direction.

We begin with the expression for the partition function using the coherent-state path integral formulation, as introduced earlier in equation (46). Therefore, we take equation (46) as our starting point. The first step is to perform the same rescaling as done previously in equation (49). Following that, we apply the following transformation to the fields:

$$\forall x, t_k, \quad \begin{pmatrix} \xi_{\uparrow}(x, t_k) \\ \bar{\xi}_{\uparrow}(x, t_k) \end{pmatrix} \rightarrow \begin{pmatrix} 0 & 1 \\ 1 & 0 \end{pmatrix} \begin{pmatrix} \xi_{\uparrow}(x, t_k) \\ \bar{\xi}_{\uparrow}(x, t_k) \end{pmatrix}. \quad (107)$$

This means swapping the fields $\xi_{\uparrow}(x, t_k)$ and $\bar{\xi}_{\uparrow}(x, t_k)$. This step does not affect the integration measure. In this third attempt at bosonization, we focus on bosonizing only a subset of the Grassmann fields, as indicated below:

$$\forall x, t_k, \quad \bar{\xi}_{\uparrow}(x, t_k) \xi_{\downarrow}(x, t_k) \sim e^{i\phi(x, t_k)}, \quad (108)$$

and integrate over the remaining fields $\xi_{\downarrow}(x, t_k)$ and $\bar{\xi}_{\downarrow}(x, t_k)$. However, as has been encountered previously, there is an obstacle: not all terms in the partition function can be directly expressed in terms of the $U(1)$ bosonic field. To address this, we use a method we have applied before, performing a local $U(1)$ phase rotation:

$$\forall x, t_k, \quad \begin{aligned} \bar{\xi}_{\uparrow}(x, t_k) &\rightarrow \bar{\xi}_{\uparrow}(x, t_k) e^{-i\alpha(x, t_k)}, \\ \xi_{\downarrow}(x, t_k) &\rightarrow e^{i\alpha(x, t_k)} \xi_{\downarrow}(x, t_k). \end{aligned} \quad (109)$$

We then integrate over all possible local $U(1)$ phase rotations. Additionally, we perform another local $U(1)$ phase rotation:

$$\forall x, t_k, \quad \begin{aligned} \bar{\xi}_{\downarrow}(x, t_k) &\rightarrow \bar{\xi}_{\downarrow}(x, t_k) e^{-i\beta(x, t_k)}, \\ \xi_{\uparrow}(x, t_k) &\rightarrow e^{i\beta(x, t_k)} \xi_{\uparrow}(x, t_k). \end{aligned} \quad (110)$$

Again, we integrate over all possible local $U(1)$ phase rotations. The next step is to carry out a linked-cluster expansion, taking into account terms up to $(\Delta t)^2$ and $\frac{T_0}{U}$, while disregarding terms of higher order. We do not detail all the steps here, as this has been addressed in previous bosonization attempts, and we aim to avoid redundancy.

Following the linked-cluster expansion, we then carry out the bosonization step outlined in (108) and integrate over the remaining Grassmann fields. The resulting expression for the partition function, after completing these steps, is:

$$Z = \int_0^{2\pi} \prod_{x, t_k} \frac{d\phi(x, t_k)}{2\pi} e^{-i\phi(x, t_k)} \text{Det}(O). \quad (111)$$

Here, $O = O_0 + O_1$, where O_0 and O_1 are defined as follows:

$$\begin{aligned}
 (O_0)_{x,x';t_k,t_{k'}} &= \frac{\tau\hbar}{U} \delta_{x,x'} \delta_{t_k,t_{k'}} \left[e^{i\phi(x,t_{k-1})} + e^{i\phi(x,t_k)} \right], \\
 (O_1)_{x,x';t_k,t_{k'}} &= \frac{\tau\hbar}{U} \delta_{x,x'} \delta_{t_k,t_{k'}} \left[\left(\frac{U\Delta t}{2\hbar} \right)^2 e^{i\phi(x,t_{k-1})} \right. \\
 &\quad \left. - \left(\frac{\tau\hbar\Delta t}{\hbar} \right)^2 \left(2e^{i\phi(x,t_{k-1})} + e^{i\phi(x+a,t_{k-1})} + e^{i\phi(x-a,t_{k-1})} \right) \right],
 \end{aligned} \tag{112}$$

where a represents the lattice constant in space. We have adopted the notation $t_M \equiv t_0$.

The next step is to express $\text{Det}(O)$ as follows:

$$\begin{aligned}
 \text{Det}(O) &= \exp[\text{Tr} \ln(O)] \\
 &= \exp[\text{Tr} \ln(O_0 + O_1)] \\
 &= \text{Det}(O_0) \exp[\text{Tr} \ln(1 + (O_0)^{-1}O_1)] \\
 &\approx \text{Det}(O_0) \exp[\text{Tr}((O_0)^{-1}O_1)],
 \end{aligned} \tag{113}$$

where we have approximated the expansion of $\text{Tr} \ln(\dots)$ in the last equality, retaining only terms up to $(\Delta t)^2$ and discarding higher-order terms. After completing these steps, we arrive at the expression for the partition function in terms of a $U(1)$ bosonic field, as given in equation (67) in the main text. This concludes the discussion of the calculations that were omitted in Section 3.4, and the reader can now refer back to Section 3.4 in the main body of the thesis.

PROJECT 2

INVESTIGATION INTO STRONG DISORDER IN FERMIONIC
SYSTEMS

6 Introduction to the Second Project

6.1 Motivation

An enduring challenge in condensed matter physics is understanding how interactions and disorder influence a system's properties. The interplay between these factors produces a variety of phenomena, including the quantum Hall effect, metal-insulator transitions, and superconductor-insulator transitions. The first half of this thesis explores systems with strong interactions and negligible disorder. In contrast, the second half examines systems dominated by strong disorder, either neglecting electron interactions or treating them through mean-field approximations.

In condensed matter physics, disorder refers to lattice imperfections, such as vacancies, dislocations, or interstitial atoms. These disruptions break the lattice symmetry, making it difficult to use momentum space and complicating the study of disordered systems. Nonetheless, disorder is essential to consider, as it can significantly alter a system's physical properties and even induce new phases. One notable phenomenon where disorder plays a crucial role is the Anderson transition, which will be the subject of the following discussion.²¹

In 1958, Philip Anderson [54] published a pivotal paper in which he introduced the concept of localization of mobile electrons in disordered materials. This phenomenon, known as Anderson localization, describes how disorder causes the wavefunction to become exponentially localized in position space. Building on this work, the concept of the Anderson transition was subsequently developed. The Anderson transition [52] is a quantum phase transition observed in disordered systems. As disorder increases (depending on spatial dimensionality), the system transitions from a metallic state, where the wavefunction is extended or delocalized, to an insulating state, where the wavefunction becomes localized in position space.

In 1979, the “gang of four” researchers proposed a one-parameter scaling hypothesis [55] for the Anderson transition, suggesting that a single relevant parameter is sufficient to describe the universal behavior at criticality. Subsequently, the nonlinear sigma model by Wegner [56] and Efetov [57] was proposed as an effective field theory to explain the critical behavior of Anderson transitions. This model validated the one-parameter scaling hypothesis for Anderson transitions near two-dimensional space. However, the accurate description of Anderson transitions in higher dimensions remained unclear. Although some argue [58] that Wegner and Efetov's nonlinear sigma model can also account for the critical behavior in higher dimensions, there are skeptics [59] who believe this might not provide the complete picture.

Most studies on Anderson transitions have focused on the weak disorder regime, leaving the strong disorder regime relatively underexplored. However, recent investigations into strong

²¹The following discussion draws on insights from [6, 52, 53, 5, 4].

disorder have provided new insights. We mention two studies below [4, 5, 6] that challenge the conventional perspective and offer a new description of Anderson transitions, which forms the basis for our study.

The first study, although in a somewhat different context, was published in 2019 [4]. While examining the scaling behavior near the transition between plateaus of the integer quantum Hall (IQH) effect in two dimensions, a novel scenario of spontaneous symmetry breaking (SSB) was proposed. The second study, from 2023 [5, 6], observed this novel SSB scenario again while investigating the Anderson transition in the Wegner N-orbital model, revealing a new phase beyond the two previously recognized phases in Anderson transitions. Here, we provide a concise overview of the novel SSB mechanism detailed in these studies.

First, let us revisit the classical perspective on Anderson localization through the lens of spontaneous symmetry breaking (SSB). Traditionally, Anderson localization involves two distinct phases: metallic and insulating. In the insulating phase, the symmetry group of the non-linear sigma model remains intact. Conversely, in the metallic phase (in three-dimensional space), spontaneous symmetry breaking occurs. This symmetry breaking occurs because, under renormalization, the stiffness of the non-linear field, which is a scale-dependent parameter, flows to infinity [4].

Now, the novel SSB scenario proposed in [6, 5, 4] is partial symmetry breaking (PSB). In this scenario, the symmetry is partially broken. Specifically, under renormalization, the field stiffness flows to infinity for some of the field degrees of freedom, while for the remaining degrees of freedom, the stiffness flows to a finite value. This indicates the presence of a non-trivial renormalization-group fixed point. As detailed in [6], in this scenario, the field extends along some “light-like” directions of the target space, which corresponds to the restoration of symmetry for a subgroup of the symmetry group. Conversely, the field becomes confined in the transverse “space-like” directions, signifying symmetry breaking for the group elements that act transversally. This novel concept of partial symmetry breaking (PSB) has been a key inspiration for the second project of this thesis.

The systems studied in these works fall under symmetry class A in the Altland-Zirnbauer classification [3]. Anticipating that the PSB scenario might occur for a variety of Anderson transitions at strong disorder [6], this thesis shifts focus to systems within a different symmetry class, specifically symmetry class D^{22} , to explore whether this scenario also applies to these systems.

Before concluding this introduction, it is essential to emphasize another key point. Since we are working in the strong disorder regime, the conventional Hubbard-Stratonovich transformation is not employed, as it is more suited for weak disorder scenarios. Instead, we utilize the superbosonization method [1, 2], which is briefly reviewed in the following section.

²²The following chapter will outline important details regarding this class of systems.

6.2 Superbosonization Formula

The superbosonization technique was introduced in [1, 2]. We previously encountered a segment of this formula in the first part of this thesis (see Section 1.2), where we applied bosonization to functions involving only anti-commuting Grassmann variables. In this section, we present the complete superbosonization formula following [1]. However, we will state the formula without delving into its proof. For a detailed derivation and proof, the reader is referred to [1].

Consider a set of complex variables $z_{r,a}$ and their complex conjugates $\tilde{z}_{a,r} := \bar{z}_{r,a}$, where indices are in the range $r = 1, \dots, R$ and $a = 1, \dots, \tilde{A}$. Alongside these, we have two sets of anti-commuting variables: $\xi_{r,b}$ and $\tilde{\xi}_{b,r}$, with index range $r = 1, \dots, R$ and $b = 1, \dots, \tilde{B}$. Here, r represents the “color” degrees of freedom, while a and b indicate the number of bosonic and fermionic replicas, respectively.

The complex variables $z_{r,a}$ can be organized into an $R \times \tilde{A}$ rectangular matrix, denoted as z , with each matrix element corresponding to $z_{r,a}$. Similarly, the variables $\tilde{z}_{a,r}$ can be structured into an $\tilde{A} \times R$ rectangular matrix, denoted as \tilde{z} , with elements $\tilde{z}_{a,r}$. In the same manner, the sets of anti-commuting variables $\xi_{r,b}$ and $\tilde{\xi}_{b,r}$ can be arranged into rectangular matrices ξ and $\tilde{\xi}$ with dimensions $R \times \tilde{B}$ and $\tilde{B} \times R$, respectively.

Suppose we want to integrate a function $f(z, \tilde{z}; \xi, \tilde{\xi})$:

$$\int f = \int D(z, \xi) f(z, \tilde{z}; \xi, \tilde{\xi}), \quad (114)$$

where the integration measure is given by:

$$D(z, \xi) := \prod_{r,a,b} \frac{d\tilde{z}_{a,r} dz_{r,a}}{\pi} \frac{\partial^2}{\partial \tilde{\xi}_{b,r} \partial \xi_{r,b}}. \quad (115)$$

Let f in the integral (114) be an analytic and $O(R)$ -invariant function²³ of the variables $z, \tilde{z}, \xi, \tilde{\xi}$:

$$f(z, \tilde{z}; \xi, \tilde{\xi}) = f(gz, \tilde{z}g^{-1}; g\xi, \tilde{\xi}g^{-1}), \quad g \in O(R). \quad (116)$$

It is further assumed that f extends to a holomorphic function invariant under $O(R, \mathbb{C})$ when z and \tilde{z} are treated as independent complex matrices. The symmetry relation (116) for this extended function remains valid for all $g \in O(R, \mathbb{C})$, the complexified version of $O(R)$.

The superbosonization formula enables us to derive a reduction formula for the integral $\int f$ of functions that satisfy the conditions specified above. To introduce the superbosonization formula, the following components are required:

1. First, we use a result from classical invariant theory [28]. The algebra of

$O(R, \mathbb{C})$ -invariant polynomial functions in $z, \tilde{z}, \xi, \tilde{\xi}$ is generated by invariants that

²³The superbosonization formula is defined for the three groups $U(R)$, $O(R)$, and $USp(R)$ [1]. However, in this second part of the thesis, we will focus exclusively on the $O(R)$ case.

arise at the quadratic level. We now proceed to construct all quadratic invariants under the $O(R)$ symmetry group, using the variables $z, \tilde{z}, \xi, \tilde{\xi}$:

$$\begin{aligned}
 (\tilde{z} \cdot z)_{aa'} &= \sum_r \tilde{z}_{a,r} z_{r,a'}, & (\tilde{z} \cdot \tilde{z}^T)_{aa'} &= \sum_r \tilde{z}_{a,r} \tilde{z}_{r,a'}^T = \sum_r \tilde{z}_{a,r} \tilde{z}_{a',r}, \\
 (z^T \cdot z)_{aa'} &= \sum_r z_{a,r}^T z_{r,a'} = \sum_r z_{r,a} z_{r,a'}, & (z^T \cdot \tilde{z}^T)_{aa'} &= \sum_r z_{a,r}^T \tilde{z}_{r,a'}^T = \sum_r z_{r,a} \tilde{z}_{a',r}, \\
 (\tilde{z} \cdot \xi)_{ab'} &= \sum_r \tilde{z}_{a,r} \xi_{r,b'}, & (\tilde{z} \cdot \tilde{\xi}^T)_{ab'} &= \sum_r \tilde{z}_{a,r} \tilde{\xi}_{r,b'}^T = \sum_r \tilde{z}_{a,r} \tilde{\xi}_{b',r}, \\
 (z^T \cdot \xi)_{ab'} &= \sum_r z_{a,r}^T \xi_{r,b'} = \sum_r z_{r,a} \xi_{r,b'}, & (z^T \cdot \tilde{\xi}^T)_{ab'} &= \sum_r z_{a,r}^T \tilde{\xi}_{r,b'}^T = \sum_r z_{r,a} \tilde{\xi}_{b',r}, \\
 (\tilde{\xi} \cdot z)_{ba'} &= \sum_r \tilde{\xi}_{b,r} z_{r,a'}, & (\tilde{\xi} \cdot \tilde{z}^T)_{ba'} &= \sum_r \tilde{\xi}_{b,r} \tilde{z}_{r,a'}^T = \sum_r \tilde{\xi}_{b,r} \tilde{z}_{a',r}, \\
 (\xi^T \cdot z)_{ba'} &= \sum_r \xi_{b,r}^T z_{r,a'} = \sum_r \xi_{r,b} z_{r,a'}, & (\xi^T \cdot \tilde{z}^T)_{ba'} &= \sum_r \xi_{b,r}^T \tilde{z}_{r,a'}^T = \sum_r \xi_{r,b} \tilde{z}_{a',r}, \\
 (\tilde{\xi} \cdot \xi)_{bb'} &= \sum_r \tilde{\xi}_{b,r} \xi_{r,b'}, & (\tilde{\xi} \cdot \tilde{\xi}^T)_{bb'} &= \sum_r \tilde{\xi}_{b,r} \tilde{\xi}_{r,b'}^T = \sum_r \tilde{\xi}_{b,r} \tilde{\xi}_{b',r}, \\
 (\xi^T \cdot \xi)_{bb'} &= \sum_r \xi_{b,r}^T \xi_{r,b'} = \sum_r \xi_{r,b} \xi_{r,b'}, & (\xi^T \cdot \tilde{\xi}^T)_{bb'} &= \sum_r \xi_{b,r}^T \tilde{\xi}_{r,b'}^T = \sum_r \xi_{r,b} \tilde{\xi}_{b',r},
 \end{aligned} \tag{117}$$

where T denotes transpose. All these quadratic invariants can be organized into a supermatrix, as demonstrated below:

$$\begin{pmatrix}
 \tilde{z} \cdot z & \tilde{z} \cdot \tilde{z}^T & \tilde{z} \cdot \xi & \tilde{z} \cdot \tilde{\xi}^T \\
 z^T \cdot z & z^T \cdot \tilde{z}^T & z^T \cdot \xi & z^T \cdot \tilde{\xi}^T \\
 \tilde{\xi} \cdot z & \tilde{\xi} \cdot \tilde{z}^T & \tilde{\xi} \cdot \xi & \tilde{\xi} \cdot \tilde{\xi}^T \\
 \xi^T \cdot z & \xi^T \cdot \tilde{z}^T & \xi^T \cdot \xi & \xi^T \cdot \tilde{\xi}^T
 \end{pmatrix}. \tag{118}$$

2. Next, consider a supermatrix Q with the following structure:

$$Q = \begin{pmatrix} Q_{BB} & Q_{BF} \\ Q_{FB} & Q_{FF} \end{pmatrix}, \tag{119}$$

where the blocks Q_{BB} and Q_{FF} are square matrices of size $2\tilde{A} \times 2\tilde{A}$ and $2\tilde{B} \times 2\tilde{B}$, respectively, with commuting variables as entries. Meanwhile, Q_{BF} and Q_{FB} are rectangular matrices of size $2\tilde{A} \times 2\tilde{B}$ and $2\tilde{B} \times 2\tilde{A}$, respectively, with anti-commuting entries. Then, impose on Q the symmetry relation:

$$Q = \tilde{\gamma} Q^{sT} \tilde{\gamma}^{-1}, \tag{120}$$

where $\tilde{\gamma}$ is given by:

$$\begin{pmatrix}
 0 & 1_{\tilde{A}} & 0 & 0 \\
 1_{\tilde{A}} & 0 & 0 & 0 \\
 0 & 0 & 0 & -1_{\tilde{B}} \\
 0 & 0 & 1_{\tilde{B}} & 0
 \end{pmatrix}, \tag{121}$$

with $1_{\tilde{A}}$ and $1_{\tilde{B}}$ denoting the identity matrix of dimensions $\tilde{A} \times \tilde{A}$ and $\tilde{B} \times \tilde{B}$,

respectively. Q^{sT} denotes the supertranspose of the supermatrix Q , which is defined as follows:

$$Q^{sT} = \begin{pmatrix} Q_{BB}^T & Q_{FB}^T \\ -Q_{BF}^T & Q_{FF}^T \end{pmatrix}. \quad (122)$$

We are now prepared to present the $O(R)$ -superbosonization formula. This formula provides a method for rewriting the integral in equation (114) as an integral over the supermatrix Q , which has been defined previously. Specifically, the integral can be expressed as follows:

$$\int f = \int d\mu(Q) \text{SDet}^{\frac{R}{2}}(Q) F(Q). \quad (123)$$

Here, $F(Q)$ represents a function of the supermatrix Q . Under the substitution

$$Q \rightarrow \begin{pmatrix} \tilde{z} \cdot z & \tilde{z} \cdot \tilde{z}^T & \tilde{z} \cdot \xi & \tilde{z} \cdot \tilde{\xi}^T \\ z^T \cdot z & z^T \cdot \tilde{z}^T & z^T \cdot \xi & z^T \cdot \tilde{\xi}^T \\ \tilde{\xi} \cdot z & \tilde{\xi} \cdot \tilde{z}^T & \tilde{\xi} \cdot \xi & \tilde{\xi} \cdot \tilde{\xi}^T \\ \xi^T \cdot z & \xi^T \cdot \tilde{z}^T & \xi^T \cdot \xi & \xi^T \cdot \tilde{\xi}^T \end{pmatrix}, \quad (124)$$

the function $F(Q)$ becomes equal to the given function $f(z, \tilde{z}; \xi, \tilde{\xi})$. It is important to note that the choice of the function F is not unique.

$\text{SDet}(Q)$ denotes the superdeterminant of the supermatrix Q and is defined as:

$$\text{SDet}(Q) = \frac{\text{Det}(Q_{BB})}{\text{Det}(Q_{FF} - Q_{FB}Q_{BB}^{-1}Q_{BF})}. \quad (125)$$

The measure in equation (123) is given by:

$$d\mu(Q) = DQ \text{SDet}^{-\frac{1}{2}}(Q). \quad (126)$$

where DQ denotes the flat measure. It is crucial to emphasize that the $O(R)$ -superbosonization formula holds true only if the condition $R \geq 2\tilde{A}$ is met.

This concludes the presentation of the $O(R)$ -superbosonization formula. For a detailed discussion and proof, we recommend consulting [1]. For a simpler discussion, please refer to [60].

6.3 Outline of the Second Project

We are now set to explore the realm of strongly disordered systems. The following outline provides a brief roadmap for the second half of this thesis.

In Chapter 7, we discuss the supersymmetric field theory framework for studying disordered class D systems. We analyze the strong disorder limit of a general system, not restricted to any specific model, using the superbosonization method and explore its implications.

In Chapter 8, we focus specifically on the study of monitored free fermions within symmetry class D that exhibit measurement-induced phase transitions. We discuss a method based on the supersymmetry technique, which differs from the more common replica trick used in the literature, to analyze the system. We propose a reformulation of the theory, utilizing concepts from universality and scaling, which provides a novel perspective for system analysis. Finally, we suggest possible avenues for future research based on the concepts discussed here.

7 Supersymmetric Field Theory Approach to Strongly Disordered Class D Systems

In this chapter, we introduce the supersymmetric field theory framework for analyzing disordered class D systems and investigate their behavior under strong disorder. Rather than relying on the traditional Hubbard-Stratonovich transformation, which is suitable for weak disorder, we adopt the superbosonization technique to effectively address the challenges posed by strong disorder. Before delving into the main analysis, we provide an overview of class D systems, following the classification in [3].

7.1 Symmetry Class D

Class D is one of the ten symmetry classes in the Altland-Zirnbauer classification [3] for non-interacting fermions. Systems in this symmetry class describe superconductors that break time-reversal symmetry and lack spin-rotation invariance. For these systems, the Bardeen–Cooper–Schrieffer (BCS) Hamiltonian, in the Hartree-Fock-Bogoliubov mean-field approximation, is given by:

$$\hat{H} = \sum_{i,j} h_{ij} c_i^\dagger c_j + \frac{1}{2} \Delta_{ij} c_i^\dagger c_j^\dagger + \frac{1}{2} \overline{\Delta}_{ij} c_j c_i, \quad (127)$$

where (i, j) refers to the physical space $\mathbb{C}^{2N} = \mathbb{C}^N \otimes \mathbb{C}^2$ (which includes both orbitals and spin).

The second-quantized Hamiltonian (\hat{H}) can be expressed in an equivalent first-quantized form (H) through the Bogoliubov-deGennes formalism:

$$\hat{H} = \frac{1}{2} \sum_{i,j} \begin{pmatrix} c_i^\dagger & c_i \end{pmatrix} \begin{pmatrix} h_{ij} & \Delta_{ij} \\ -\overline{\Delta}_{ij} & (-h^T)_{ij} \end{pmatrix} \begin{pmatrix} c_j \\ c_j^\dagger \end{pmatrix} + \text{const.}, \quad (128)$$

where the first-quantized Hamiltonian $H = \begin{pmatrix} h & \Delta \\ -\overline{\Delta} & -h^T \end{pmatrix}$ is a $4N \times 4N$ matrix defined in the enlarged physical space $\mathbb{C}^{4N} = \mathbb{C}_{\text{BdG}}^2 \otimes \mathbb{C}^{2N}$. Here, $\mathbb{C}_{\text{BdG}}^2$ represents the additional “particle-hole” degree of freedom.

The Hermiticity of \hat{H} , along with the canonical anti-commutation relations for fermions, impose a specific “symmetry” on the Hamiltonian:

$$h = h^\dagger, \Delta = -\Delta^T. \quad (129)$$

Note. “Symmetry” is placed in quotes because it is not exactly a symmetry but rather a structure imposed on the Hamiltonian by the canonical anti-commutation relations for fermions.

These two conditions can be combined into a single equation:

$$H^\dagger = H = -\Sigma_1 H^T \Sigma_1, \quad (130)$$

where $\Sigma_1 = \sigma_1 \otimes 1_{2N}$. Here, $\sigma_1 = \begin{pmatrix} 0 & 1 \\ 1 & 0 \end{pmatrix}$ is the standard Pauli matrix in $\mathbb{C}_{\text{BdG}}^2$ space, and 1_{2N} is the identity matrix in \mathbb{C}^{2N} space.

Using the above equation (130), it is evident that $X_H = iH$ belongs to $so(4N, \mathbb{R})$ Lie algebra:

$$-X_H^\dagger = X_H = -\Sigma_1 X_H^T \Sigma_1. \quad (131)$$

This identification of X_H with the $so(4N, \mathbb{R})$ Lie algebra becomes clearer when applying a change of basis given by $X_H \rightarrow \widetilde{X}_H = U_0 X_H U_0^{-1}$, where

$$U_0 = \frac{1}{\sqrt{2}} \begin{pmatrix} 1 & 1 \\ i & -i \end{pmatrix} \otimes 1_{2N}. \quad (132)$$

After this transformation, one obtains:

$$\widetilde{X}_H = \overline{\widetilde{X}_H} = -\widetilde{X}_H^T, \quad (133)$$

which is the standard defining equation for the $so(4N, \mathbb{R})$ Lie algebra.

We will now conclude our overview of Class D systems, noting that the key aspect to focus on is the constraint on the Hamiltonian specified in equation (130), which will be crucial for the analysis in the following section.

Remark. *This class of systems, in two spatial dimensions, exhibits the thermal quantum Hall effect [61].*

7.2 Supersymmetric Field Theory

We begin with the exposition of the supersymmetric field theory formalism [62] applied to disordered class D systems. To illustrate the method, we examine the generating function, which is given by the average ratio of spectral determinants²⁴:

$$\mathbf{Z}(\lambda_0, \lambda_1) = \mathbb{E} \left(\frac{\text{Det}(\lambda_1 - H)}{\text{Det}(\lambda_0 - H)} \right), \quad (134)$$

where λ_0, λ_1 are complex numbers, H denotes the Hamiltonian belonging to symmetry class D, and \mathbb{E} represents the disorder average.²⁵ We will provide more details about how to perform the disorder average later in this section. For now, we first express the above formula as a supersymmetric functional integral, i.e., an integral over both bosonic and fermionic variables.

Since a Gaussian integral over complex (bosonic) variables yields an inverse determinant term, and a Gaussian Berezin integral over complex Grassmann (fermionic) variables results

²⁴The generating function can be used to calculate the trace of the resolvent operator, from which the density of states can be derived [62].

²⁵For the generating function to be well-defined, we also require that λ_0 is not in the spectrum of H .

in a determinant term, the generating function in equation (134) can be reformulated as an integral over both complex (bosonic) variables and complex Grassmann (fermionic) variables. Specifically, this can be written as:

$$\begin{aligned}
 Z(\lambda_0, \lambda_1) &= Z(\Lambda) = \mathbb{E} \left(\frac{\text{Det}(\lambda_1 - H)}{\text{Det}(\lambda_0 - H)} \right) \\
 &= \mathbb{E} \left(\int_{\Psi} \exp \left\{ -i \sum_{\mu, \nu} \sum_{i_c, j_c} (-1)^\mu \tilde{\Psi}_{\mu; i_c} (\Lambda_{\nu\mu} \delta_{i_c j_c} - \delta_{\nu\mu} H_{i_c j_c}) \Psi_{j_c; \nu} \right\} \right) \\
 &= \mathbb{E} \left(\int_{\Psi} \exp \left\{ -i \text{STr}_{\mathbb{C}^{1|1}} (\tilde{\Psi} \Psi \Lambda - \tilde{\Psi} H \Psi) \right\} \right).
 \end{aligned} \tag{135}$$

Here, (μ, ν) denotes the space $\mathbb{C}^{1|1}$, which is a \mathbb{Z}_2 -graded sum $W_B \oplus W_F$, where $W_B = \mathbb{C}$ represents the bosonic space, and $W_F = \mathbb{C}$ represents the fermionic space.

The variables $\Psi_{i_c; \mu=0} = z_{i_c}$ are complex bosonic variables, and $\tilde{\Psi}_{\mu=0; i_c} = \bar{z}_{i_c}$ denote their complex conjugates. The variables $\Psi_{i_c; \mu=1} = \xi_{i_c}$ and $\tilde{\Psi}_{\mu=1; i_c} = \tilde{\xi}_{i_c}$ are independent complex Grassmann (fermionic) variables. Here, the index i_c denotes the composite index $i_c = (\tau, i)$, where $\tau = p, h$ represents the ‘‘particle-hole (p - h)’’ space $\mathbb{C}_{\text{BdG}}^2$, and i refers to the physical space \mathbb{C}^{2N} .

The matrix $\Lambda = \text{diag}(\lambda_0, \lambda_1)$ is a diagonal matrix in the $\mathbb{C}^{1|1}$ space. The matrix $\delta_{i_c j_c}$ denotes the Kronecker delta in the space $\mathbb{C}_{\text{BdG}}^2 \otimes \mathbb{C}^{2N}$, while $\delta_{\nu\mu}$ represents the Kronecker delta in the space $\mathbb{C}^{1|1}$.

The integration measure for the integral in the preceding equation (135) is given by:

$$\int_{\Psi} := \int \prod_{i_c} \frac{d\bar{z}_{i_c} dz_{i_c}}{\pi} \frac{\partial^2}{\partial \tilde{\xi}_{i_c} \partial \xi_{i_c}}. \tag{136}$$

We require the imaginary part of λ_0 to be negative, $\text{Im}(\lambda_0) < 0$, to ensure the convergence of the bosonic integral.

Lastly, the supertrace denoted as $\text{STr}_{\mathbb{C}^{1|1}}$ over the $\mathbb{C}^{1|1}$ space is defined by the expression:

$$\text{STr}_{\mathbb{C}^{1|1}}(O) = \sum_{\mu} (-1)^\mu O_{\mu\mu}, \tag{137}$$

where O represents an arbitrary matrix within this space.

To advance our analysis, we aim to utilize the fact that H is Hermitian and satisfies the ‘‘symmetry’’ condition outlined in equation (130). We will incorporate this information into the expression given in equation (135). To achieve this, we apply the idea presented in [62].

Let us begin by examining the following expression:

$$\begin{aligned}
 \text{STr}_{\mathbb{C}^{1|1} \otimes \mathbb{C}_{\text{flavor}}^2} (\tilde{\Psi} H \Psi) &= \sum_{\mu} \sum_f \sum_{i_c, j_c} (-1)^\mu \tilde{\Psi}_{\mu, f; i_c} H_{i_c j_c} \Psi_{j_c; \mu, f}, \\
 &= \sum_{i_c, j_c} \sum_{\mu} \sum_f H_{i_c j_c} \Psi_{j_c; \mu, f} \tilde{\Psi}_{\mu, f; i_c}, \\
 &= \text{Tr}_{\mathbb{C}_{\text{color}}^{4N}} (H \Psi \tilde{\Psi}).
 \end{aligned} \tag{138}$$

In this equation, we introduce an additional two-dimensional ‘‘flavor’’ space, denoted as $\mathbb{C}_{\text{flavor}}^2$, with $f = 1_f, 2_f$ indexing this space. We will justify shortly why this space must have a minimum dimension of two. The first equality defines the supertrace over the $\mathbb{C}^{1|1} \otimes \mathbb{C}_{\text{flavor}}^2$ space. In the second equality of equation (138), we utilize the property that the Grassmann variables ($\mu = 1$) anticommute. Additionally, it is noted that $\mathbb{C}_{\text{color}}^{4N} = \mathbb{C}_{\text{BdG}}^2 \otimes \mathbb{C}^{2N}$.

To avoid confusion, it is essential to clarify that, despite using the same notation for the fields in equations (135) and (138), we do not initially assume any specific relationships between these fields. Moreover, the fields Ψ and $\tilde{\Psi}$ in equation (138) are treated as independent variables, in contrast to equation (135), where $\tilde{\Psi}_{\mu=0; i_c}$ represents the complex conjugate of $\Psi_{i_c; \mu=0}$. As the analysis progresses, we will elucidate the relationships between the fields described in equations (135) and (138).

To proceed, we will analyze the two terms below, which pertain to the bosonic and fermionic spaces separately:

$$\text{Tr}_{\mathbb{C}_{\text{color}}^{4N}} (H \Psi \tilde{\Psi}) = \text{Tr}_{\mathbb{C}_{\text{color}}^{4N}} (H z \tilde{z}) + \text{Tr}_{\mathbb{C}_{\text{color}}^{4N}} (H \xi \tilde{\xi}), \tag{139}$$

where $\text{Tr}_{\mathbb{C}_{\text{color}}^{4N}} (H z \tilde{z})$ is defined as:

$$\text{Tr}_{\mathbb{C}_{\text{color}}^{4N}} (H z \tilde{z}) = \sum_{i_c, j_c} \sum_f H_{i_c j_c} z_{j_c; f} \tilde{z}_{f; i_c}, \tag{140}$$

and a similar definition follows for the fermionic term.

Bosonic sector

Examining the term $\text{Tr}_{\mathbb{C}_{\text{color}}^{4N}} (H z \tilde{z})$, and considering the ‘‘symmetry’’ of H given by (130), we aim for $X = z \tilde{z}$ to adhere to the same structure:

$$X = -\Sigma_1 X^T \Sigma_1. \tag{141}$$

We implement the above structure on X in the following manner.

$$\begin{array}{ccc}
 \mathbb{C}_{\text{color}}^{4N} & \begin{array}{c} \xrightarrow{\tilde{z}} \\ \xleftarrow{z} \end{array} & \mathbb{C}_{\text{flavor}}^2
 \end{array} \tag{142}$$

Here, $\tilde{z} : \mathbb{C}_{\text{color}}^{4N} \rightarrow \mathbb{C}_{\text{flavor}}^2$ and $z : \mathbb{C}_{\text{flavor}}^2 \rightarrow \mathbb{C}_{\text{color}}^{4N}$. Then, $X = z \tilde{z} \in \text{End}(\mathbb{C}_{\text{color}}^{4N})$ obeys (141) if

we define z to be:

$$z = \Sigma_1 \tilde{z}^T (i\sigma_2). \quad (143)$$

Here, $\sigma_2 = \begin{pmatrix} 0 & -i \\ i & 0 \end{pmatrix}$ is the standard Pauli matrix in $\mathbb{C}_{\text{flavor}}^2$ space. We observe that the “flavor” space must have a minimum dimension of two for $X = z \otimes \tilde{z}$ to comply with the conditions outlined in equation (141).

CHECK. $-\Sigma_1 X^T \Sigma_1 = -\Sigma_1 (z\tilde{z})^T \Sigma_1 = -\Sigma_1 \tilde{z}^T z^T \Sigma_1 = -(\Sigma_1 \tilde{z}^T i\sigma_2)(-i\sigma_2 z^T \Sigma_1) = -(z)(-\tilde{z}) = z\tilde{z} = X.$

Another feature of H is that it is Hermitian. Considering the term $\text{Tr}_{\mathbb{C}_{\text{color}}^{4N}}(HX)$, we require that X also be Hermitian, i.e., $X = X^\dagger$. This is implemented by $z = \tilde{z}^\dagger \sigma_3$.

CHECK. $X^\dagger = (z\tilde{z})^\dagger = \tilde{z}^\dagger z^\dagger = z\sigma_3\sigma_3\tilde{z} = z\tilde{z} = X.$

To summarize, for X to be Hermitian and satisfy equation (141), z must fulfill the following conditions:

$$\begin{aligned} z &= \Sigma_1 \tilde{z}^T (i\sigma_2), \\ z &= \tilde{z}^\dagger \sigma_3. \end{aligned} \quad (144)$$

Fermionic sector

The discussion presented here closely parallels that of the bosonic sector. Examining the term $\text{Tr}_{\mathbb{C}_{\text{color}}^{4N}}(H\xi\tilde{\xi})$, and considering the “symmetry” of H given by (130), we want $Y = \xi\tilde{\xi}$ to obey the same structure:

$$Y = -\Sigma_1 Y^T \Sigma_1. \quad (145)$$

The above structure on Y is implemented in the following manner.

$$\mathbb{C}_{\text{color}}^{4N} \begin{array}{c} \xrightarrow{\tilde{\xi}} \\ \xleftarrow{\xi} \end{array} \mathbb{C}_{\text{flavor}}^2 \quad (146)$$

Here, $\tilde{\xi} : \mathbb{C}_{\text{color}}^{4N} \rightarrow \mathbb{C}_{\text{flavor}}^2$ and $\xi : \mathbb{C}_{\text{flavor}}^2 \rightarrow \mathbb{C}_{\text{color}}^{4N}$. Then, $Y = \xi\tilde{\xi} \in \text{End}(\mathbb{C}_{\text{color}}^{4N})$ obeys (145) if we define ξ to be:

$$\xi = \Sigma_1 \tilde{\xi}^T \sigma_1, \quad (147)$$

where $\sigma_1 = \begin{pmatrix} 0 & 1 \\ 1 & 0 \end{pmatrix}$ is the standard Pauli matrix in $\mathbb{C}_{\text{flavor}}^2$ space.

CHECK.

$$-\Sigma_1 Y^T \Sigma_1 = -\Sigma_1 (\xi\tilde{\xi})^T \Sigma_1 = -\Sigma_1 (-\tilde{\xi}^T \xi^T) \Sigma_1 = (\Sigma_1 \tilde{\xi}^T \sigma_1)(\sigma_1 \xi^T \Sigma_1) = \xi\tilde{\xi} = Y.$$

Using the discussion above, we can now incorporate the fact that H belongs to symmetry class D and satisfies the constraints specified in equation (130) into the expression for the generating function given in (135). We will first present the resulting expression and then explain how to verify its equivalence to the expression in equation (135). The reformulated expression for the generating function is as follows:

$$Z(\Lambda) = \mathbb{E} \left(\int_{\Psi} \exp \left\{ -i \sum_{\mu, \nu} \sum_{f, f'} \sum_{i_c, j_c} \frac{(-1)^\mu}{2} \tilde{\Psi}_{\mu, f; i_c} (\Lambda_{\nu \mu, f' f} \delta_{i_c j_c} - \delta_{\nu \mu, f' f} H_{i_c j_c}) \Psi_{j_c; \nu, f'} \right\} \right), \quad (148)$$

with the following definitions:

$$\begin{aligned} \tilde{z}_{1_f; \tau, i} &:= \bar{z}_{\tau, i}, & z_{\tau, i; 1_f} &:= z_{\tau, i}, \\ \tilde{\xi}_{1_f; \tau, i} &:= \tilde{\xi}_{\tau, i}, & \xi_{\tau, i; 1_f} &:= \xi_{\tau, i}, \end{aligned} \quad (149)$$

and incorporating the relations provided in equations (144) and (147). The matrix $\Lambda = \text{diag}(\lambda_0, -\lambda_0, \lambda_1, -\lambda_1)$ in equation (148) represents a diagonal matrix in the $\mathbb{C}^{1|1} \otimes \mathbb{C}_{\text{flavor}}^2$ space, and $\delta_{\nu \mu, f' f}$ denotes the Kronecker delta in this same space. The integration measure in equation (148) remains the same as in equation (136).

Based on the definitions provided in equation (149) and the relations obtained in equations (144) and (147), we can express the relations between the fields in equations (135) and (138) as follows:

$$\begin{aligned} \tilde{z}_{1_f; \tau, i} &= \bar{z}_{\tau, i}, & z_{\tau, i; 1_f} &= z_{\tau, i}, \\ \tilde{z}_{2_f; \tau, i} &= -z_{-\tau, i}, & z_{\tau, i; 2_f} &= \bar{z}_{-\tau, i}, \\ \tilde{\xi}_{1_f; \tau, i} &= \tilde{\xi}_{\tau, i}, & \xi_{\tau, i; 1_f} &= \xi_{\tau, i}, \\ \tilde{\xi}_{2_f; \tau, i} &= \xi_{-\tau, i}, & \xi_{\tau, i; 2_f} &= \tilde{\xi}_{-\tau, i}, \end{aligned} \quad (150)$$

where the notation $-\tau$ denotes $-p \equiv h$ and $-h \equiv p$.

Using the relations specified in equation (150), it is straightforward to demonstrate that the generating functions described in equations (135) and (148) are equivalent. From this point onward, we will work with the expression in equation (148). Let us now outline the Hamiltonian governing the system under investigation.

7.2.1 Model: Hamiltonian

The Hamiltonian for the model we aim to study consists of two components:

$$H = H_{\text{det}} + H_{\text{dis}}, \quad (151)$$

where H_{det} represents the deterministic component of the model, and H_{dis} denotes the disorder component. We will discuss several important points regarding this Hamiltonian.

First, to ensure that the Hamiltonian falls within symmetry class D, it must satisfy the

conditions specified in equation (130). Additionally, the component H_{det} is diagonal in momentum space, while H_{dis} is diagonal in position space. We do not specify the exact form of H_{det} here, as we aim to keep it general. In this chapter, we will focus on the overarching formalism.

For the disorder component, H_{dis} , we assume the following structure:

$$H_{\text{dis}} = \begin{pmatrix} h_{\text{dis}} & \Delta_{\text{dis}} \\ -\overline{\Delta_{\text{dis}}} & -h_{\text{dis}}^T \end{pmatrix}, \quad (152)$$

where:

$$\begin{aligned} (h_{\text{dis}})_{ij}(x, y) &= (h_{\text{dis}})_{ij}\delta(x, y), \\ (\Delta_{\text{dis}})_{ij}(x, y) &= (\Delta_{\text{dis}})_{ij}\delta(x, y). \end{aligned} \quad (153)$$

Here, (i, j) refers to indices in the physical space \mathbb{C}^{2N} , and $\delta(x, y)$ denotes the Dirac-delta function in D -dimensional space. Additionally, we have:

$$\begin{aligned} \overline{(h_{\text{dis}})_{ij}} &= (h_{\text{dis}})_{ji}, \\ (\Delta_{\text{dis}})_{ij} &= -(\Delta_{\text{dis}})_{ji}, \end{aligned} \quad (154)$$

which ensures that H_{dis} complies with the ‘‘symmetry’’ condition specified in equation (130).

7.2.2 Disorder Averaging

Having described the Hamiltonian for the model, we now turn our attention to the process of taking the disorder average \mathbb{E} . In this context, disorder is modeled such that all matrix elements of H_{dis} are assumed to be Gaussian-distributed random variables with zero mean and the following variance:

$$\begin{aligned} \mathbb{E} \left((h_{\text{dis}})_{ij} (h_{\text{dis}})_{kl} \right) &= U \delta_{il} \delta_{jk}, \\ \mathbb{E} \left((\Delta_{\text{dis}})_{ij} \overline{(\Delta_{\text{dis}})_{kl}} \right) &= \frac{U}{2} (\delta_{ik} \delta_{jl} - \delta_{il} \delta_{jk}), \end{aligned} \quad (155)$$

where U denotes the strength of the disorder.

Next, we perform the disorder average \mathbb{E} on equation (148) with respect to the Gaussian probability distribution defined in equation (155). After carrying out this average, we obtain:

$$\begin{aligned} Z(\Lambda) &= \int_{\Psi} \exp \left\{ -i \sum_x \sum_{\mu, \nu} \sum_{f, f'} \sum_{i_c} \frac{(-1)^\mu}{2} \tilde{\Psi}_{\mu, f; i_c}(x) \Psi_{i_c; \nu, f'}(x) \Lambda_{\nu \mu, f' f} \right\} \\ &\quad \exp \left\{ -i \sum_{x, y} \sum_{\mu} \sum_f \sum_{i_c, j_c} \frac{(-1)^\mu}{2} \tilde{\Psi}_{\mu, f; i_c}(x) (H_{\text{det}})_{i_c j_c}(x, y) \Psi_{j_c; \mu, f}(y) \right\} \\ &\quad \exp \left\{ -U \sum_x \sum_{\mu, \nu} \sum_{f, f'} \sum_{i_c, j_c} (-1)^\mu \tilde{\Psi}_{\mu, f; i_c}(x) \Psi_{i_c; \nu, f'}(x) \tilde{\Psi}_{\nu, f'; j_c}(x) \Psi_{j_c; \mu, f}(x) \right\}. \end{aligned} \quad (156)$$

7.2.3 Superbosonization

At this stage, it is essential to reiterate the primary objective of this chapter: to study the system in the strong disorder regime. As outlined in the introduction (see Section 6.2), we apply the $O(4N)$ -superbosonization method to investigate the system under these conditions. Consequently, the next step is to reformulate the generating function in equation (156) in terms of the field:

$$(Q_{\mu\nu})_{ff'}(x) = \frac{1}{4N} \sum_{i_c} \tilde{\Psi}_{\mu,f;i_c}(x) \Psi_{i_c;\nu,f'}(x), \quad (157)$$

using the superbosonization technique.

Before proceeding with the superbosonization, we will discuss some aspects of the field $Q(x)$. The field $Q(x)$ is a 4×4 matrix in the space $\mathbb{C}^{1|1} \otimes \mathbb{C}_{\text{flavor}}^2$, exhibiting the following block structure:

$$Q(x) = \begin{bmatrix} Q_{BB}(x) & Q_{BF}(x) \\ Q_{FB}(x) & Q_{FF}(x) \end{bmatrix}, \quad (158)$$

where each block is a 2×2 matrix. Below, we will examine the $Q_{FF}(x)$ and $Q_{BB}(x)$ blocks in more detail.

Fermion-Fermion (FF) sector

The components of the FF block of the $Q(x)$ matrix, expressed in terms of ‘‘color singlets’’, are as follows:

$$(Q_{FF})_{ff'}(x) = \frac{1}{4N} \sum_{i_c} \tilde{\xi}_{f;i_c}(x) \xi_{i_c;f'}(x). \quad (159)$$

This block satisfies the following conditions:

$$(Q_{FF})^{-1\dagger} = Q_{FF} = -\sigma_1(Q_{FF})^T \sigma_1. \quad (160)$$

The first equality reflects the condition of unitarity, while the second equality can be confirmed by applying relation (147).

CHECK. $-\sigma_1(Q_{FF})^T \sigma_1 = -\frac{1}{4N} \sigma_1(\tilde{\xi}\xi)^T \sigma_1 = \frac{1}{4N} (\sigma_1 \xi^T \Sigma_1)(\Sigma_1 \tilde{\xi}^T \sigma_1) = \frac{1}{4N} \tilde{\xi}\xi = Q_{FF}$.

A possible representation for Q_{FF} is given by $Q_{FF} = \sigma_3 e^{i\theta}$, where θ is a real parameter.

Symmetry group of FF sector

Next, we aim to identify the group that leaves the relations in equation (160) invariant under the adjoint action $Q_{FF} \rightarrow g_F Q_{FF} g_F^{-1}$. The group in question is $g_F \in O(2, \mathbb{R})$. To confirm this, we substitute Q_{FF} with $g_F Q_{FF} g_F^{-1}$ in (160) and derive the conditions that g_F

must satisfy. The resulting conditions are:

$$\begin{aligned} g_F^{-1} &= g_F^\dagger, \\ g_F &= \sigma_1 g_F^{-1T} \sigma_1. \end{aligned} \tag{161}$$

These relations constrain g_F to belong to $O(2, \mathbb{R})$.

Boson-Boson (BB) sector

The components of the BB block of the $Q(x)$ matrix, expressed in terms of ‘‘color-singlets’’, are as follows:

$$(Q_{BB})_{ff'}(x) = \frac{1}{4N} \sum_{i_c} \tilde{z}_{f;i_c}(x) z_{i_c;f'}(x). \tag{162}$$

This block satisfies the following conditions:

$$\sigma_3 Q_{BB}^\dagger \sigma_3 = Q_{BB} = -\sigma_2 Q_{BB}^T \sigma_2. \tag{163}$$

The above relations can be verified using equation (144).

CHECK. $\sigma_3 Q_{BB}^\dagger \sigma_3 = \frac{1}{4N} \sigma_3 (\tilde{z}z)^\dagger \sigma_3 = \frac{1}{4N} (\sigma_3 z^\dagger) (\tilde{z}^\dagger \sigma_3) = \frac{1}{4N} \tilde{z}z = Q_{BB}.$
 $-\sigma_2 Q_{BB}^T \sigma_2 = -\frac{1}{4N} \sigma_2 (\tilde{z}z)^T \sigma_2 = \frac{1}{4N} (i\sigma_2 z^T \Sigma_1) (\Sigma_1 \tilde{z}^T i\sigma_2) = \frac{1}{4N} \tilde{z}z = Q_{BB}.$

Using equation (163), we conclude that iQ_{BB} is an element of the Lie algebra $su(1, 1)$. A possible representation of Q_{BB} is given by:

$$Q_{BB} = \begin{pmatrix} r & b \\ -\bar{b} & -r \end{pmatrix}, \tag{164}$$

where $r > 0$, and $r^2 \geq |b|^2$. This can be verified by applying the definition of Q_{BB} (162) along with the following properties:

1. The condition $\|u\| > 0$ for any non-zero vector u implies $r > 0$.
2. The inequality $r^2 \geq |b|^2$ follows from the Cauchy-Schwarz inequality:
 $|\langle u, v \rangle| \leq \|u\| \|v\|$ for any two vectors u, v .

The parameterization of Q_{BB} involves three real parameters: r , $\text{Re}(b)$, and $\text{Im}(b)$ (where $b = \text{Re}(b) + i\text{Im}(b)$).

Symmetry group of BB sector

Next, we will address a question similar to the one explored in the FF sector above. Specifically, under what conditions does $Q_{BB} \rightarrow g_B Q_{BB} g_B^{-1}$ preserve the relations in equation (163)? The answer is $g_B \in SU(1, 1) \cong SL(2, \mathbb{R}) \cong Sp(2, \mathbb{R})$. To see this, we

substitute Q_{BB} with $g_B Q_{BB} g_B^{-1}$ in equation (163) and obtain the following relations on g_B :

$$\begin{aligned} g_B &= \sigma_3 g_F^{-1\dagger} \sigma_3, \\ g_B &= \sigma_2 g_F^{-1T} \sigma_2. \end{aligned} \quad (165)$$

These relations constrain g_B to be an element of $SU(1,1)$. It is important to note that the symmetry group in the BB sector is a non-compact group.

Having explored the field $Q(x)$, we are now ready to proceed with the superbosonization step. However, there is a challenge in expressing the generating function in equation (156) in terms of the field $Q(x)$. Specifically, not all terms in the partition function can be directly expressed using the $Q(x)$ field, particularly the contribution from H_{\det} (highlighted in blue in equation (156)). For these terms, one possible resolution is to employ a trick (which we also encountered in the first half of the thesis). This trick involves performing a local $O(4N)$ -transformation as follows:

$$\begin{aligned} \tilde{\Psi}_{\mu,f;i_c}(x) &\rightarrow \sum_{i'_c} \tilde{\Psi}_{\mu,f;i'_c}(x) g^{-1}(x)_{i'_c i_c}, \\ \Psi_{j_c;\mu,f}(x) &\rightarrow \sum_{j'_c} g(x)_{j_c j'_c} \Psi_{j'_c;\mu,f}(x), \end{aligned} \quad (166)$$

where $g(x) \in O(4N)$. We then integrate over all possible local $O(4N)$ transformations. After applying these transformations, we refer to the contribution from the deterministic component of the Hamiltonian to the generating function as e^{-S_c} .²⁶ The terms in S_c can be expressed in terms of the field $Q(x)$.

We are now ready to perform superbosonization. After this procedure, the generating function, expressed in terms of the field $Q(x)$, is given by:

$$\begin{aligned} Z(\Lambda) &= \int \prod_x DQ(x) \text{SDet}^{\frac{4N-1}{2}}(Q(x)), \\ &\quad \exp \left\{ -i(2N) \widetilde{\text{STr}}_{\mathbb{C}^{1|1} \otimes \mathbb{C}_{\text{flavor}}^2}(Q\Lambda) \right\} \\ &\quad \exp \left\{ -16N^2 U \widetilde{\text{STr}}_{\mathbb{C}^{1|1} \otimes \mathbb{C}_{\text{flavor}}^2}(Q^2) \right\} \\ &\quad \exp \left\{ -S_c[Q] \right\} \\ &:= \int \prod_x DQ(x) \exp\{-S_{\text{eff}}[Q(x)]\}. \end{aligned} \quad (167)$$

Here, $\widetilde{\text{STr}}_{\mathbb{C}^{1|1} \otimes \mathbb{C}_{\text{flavor}}^2}$ also includes a trace over the position space. For example, the expanded form of the supertrace in one of the terms is given below:

$$\widetilde{\text{STr}}_{\mathbb{C}^{1|1} \otimes \mathbb{C}_{\text{flavor}}^2}(Q^2) = \sum_x \sum_{\mu,\nu} \sum_{f,f'} (-1)^\mu (Q_{\mu\nu})_{ff'}(x) (Q_{\nu\mu})_{f'f}(x). \quad (168)$$

²⁶In this chapter, we adopt a general form for H_{\det} and thus do not conduct explicit calculations.

The field $Q(x)$ satisfies the following condition:

$$Q = -\gamma Q^{sT} \gamma^{-1} \quad (169)$$

where $\gamma = \begin{pmatrix} i\sigma_2 & 0 \\ 0 & \sigma_1 \end{pmatrix}$.

Note. One might observe that the condition on the field Q in equation (169) differs from the condition in equation (120) (for $\tilde{A} = 1 = \tilde{B}$) presented in the superbosonization formula from the introduction chapter 6.2. Nevertheless, it is not difficult to understand how one equation transforms into the other. To see this, start with equation (169) and apply the following transformation to Q :

$$Q \rightarrow Q' = Q\Gamma_3, \quad (170)$$

where $\Gamma_3 = \begin{pmatrix} \sigma_3 & 0 \\ 0 & -\sigma_3 \end{pmatrix}$. This transformation does not alter the integration measure.

Consequently, it is straightforward to see that Q' satisfies equation (120) with $\tilde{A} = 1 = \tilde{B}$:

$$Q' = \tilde{\gamma} (Q')^{sT} \tilde{\gamma}^{-1}. \quad (171)$$

CHECK. $Q' = Q\Gamma_3 = (-\gamma Q^{sT} \gamma^{-1})\Gamma_3 = -\gamma (Q'\Gamma_3)^{sT} \gamma^{-1} \Gamma_3 = -(\gamma\Gamma_3)(Q')^{sT} (\gamma^{-1}\Gamma_3) = -(-\tilde{\gamma})(Q')^{sT} (\tilde{\gamma}^{-1}) = \tilde{\gamma} (Q')^{sT} \tilde{\gamma}^{-1}$.

To summarize our work thus far, we have reformulated the generating function using the superbosonization method, expressing it in terms of the field $Q(x)$. We are now prepared to explore the system within the strong disorder regime.

7.3 Understanding the Strong Disorder Limit

Upon examining equation (167), we find that the strong-disorder limit (where U is large) imposes the following constraint:

$$\text{STr}_{\mathbb{C}^1|1 \otimes \mathbb{C}_{\text{flavor}}^2} (Q_0^2) = \text{Tr}_{\mathbb{C}_{\text{flavor}}^2} (Q_{BB,0}^2) - \text{Tr}_{\mathbb{C}_{\text{flavor}}^2} (Q_{FF,0}^2) + 2\text{Tr}_{\mathbb{C}_{\text{flavor}}^2} (Q_{BF,0} Q_{FB,0}) \approx 0, \quad (172)$$

where the exact equality holds in the limit as U approaches infinity. The notation Q_0 signifies that we are in the strong-disorder limit. From this point forward, we will use Tr to denote $\text{Tr}_{\mathbb{C}_{\text{flavor}}^2}$.

Assuming we eliminate the Grassmann variables (specifically, the last term $\text{Tr}(Q_{BF,0} Q_{FB,0})$ in expression (172)) by performing the Berezin integral, we obtain:

$$\text{Tr}(Q_{BB,0}^2) - \text{Tr}(Q_{FF,0}^2) \approx 0. \quad (173)$$

Next, we recall that the superbosonization step for the fermion-fermion sector (see Section 1.2) can be interpreted as replacing the Berezin integral with the evaluation of residues at the poles of a complex contour integral, according to the residue theorem. We apply this

concept in conjunction with Cauchy's idea that the value of the contour integral remains unchanged when the contour is rescaled, provided that the rescaling occurs in a region where the function is holomorphic. This approach allows us to further simplify the constraint in expression (172).

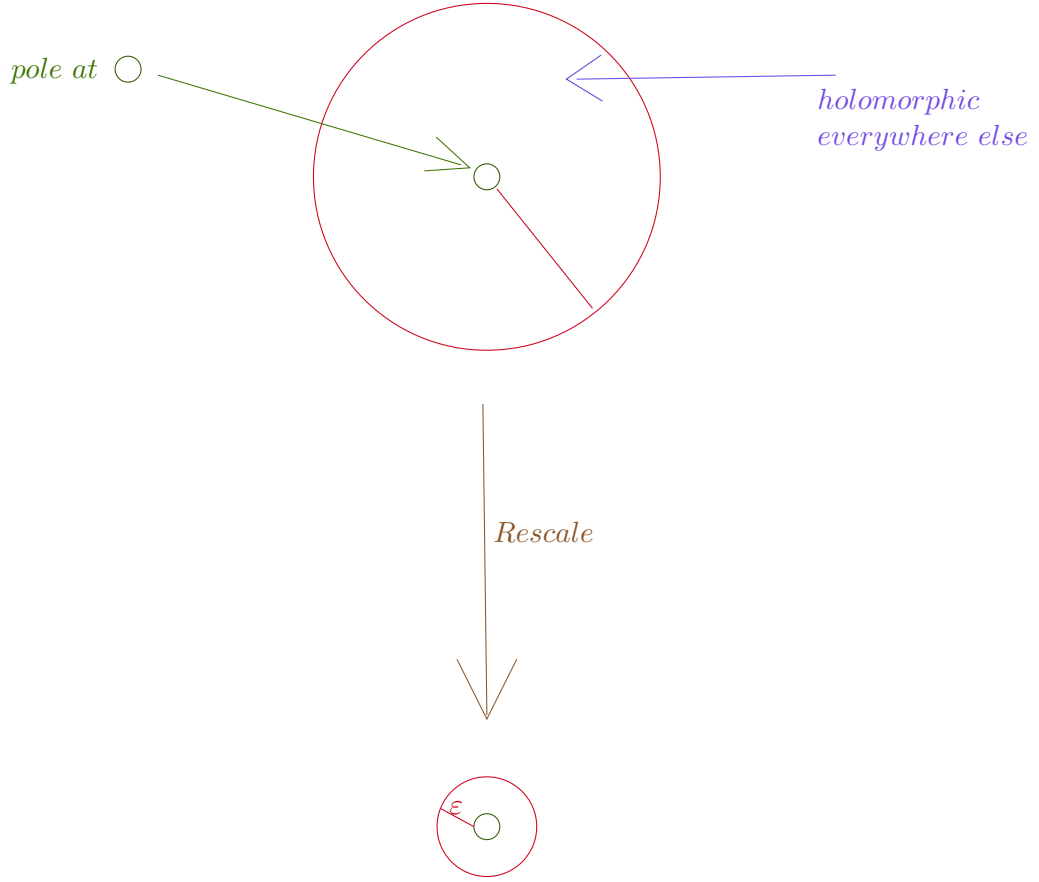


Figure 20: Cauchy's idea: the value of the contour integral remains unchanged when the contour is rescaled, provided that the rescaling occurs in a region where the function is holomorphic.

We rescale the radius of the contour integral to ε , where ε is infinitesimally small. This results in:

$$\text{Tr}(Q_{FF,0}^2) \approx 0. \quad (174)$$

Combining all the elements, the constraint now takes the form:

$$\begin{aligned} \text{Tr}(Q_{BB,0}^2) &\approx 0, \\ \implies r^2 - |b|^2 &\approx 0, \end{aligned} \quad (175)$$

where we have used the parametrization of Q_{BB} specified in equation (164). For the solution $Q_{BB,0}$, we can parametrize b as $b = re^{i\phi}$.

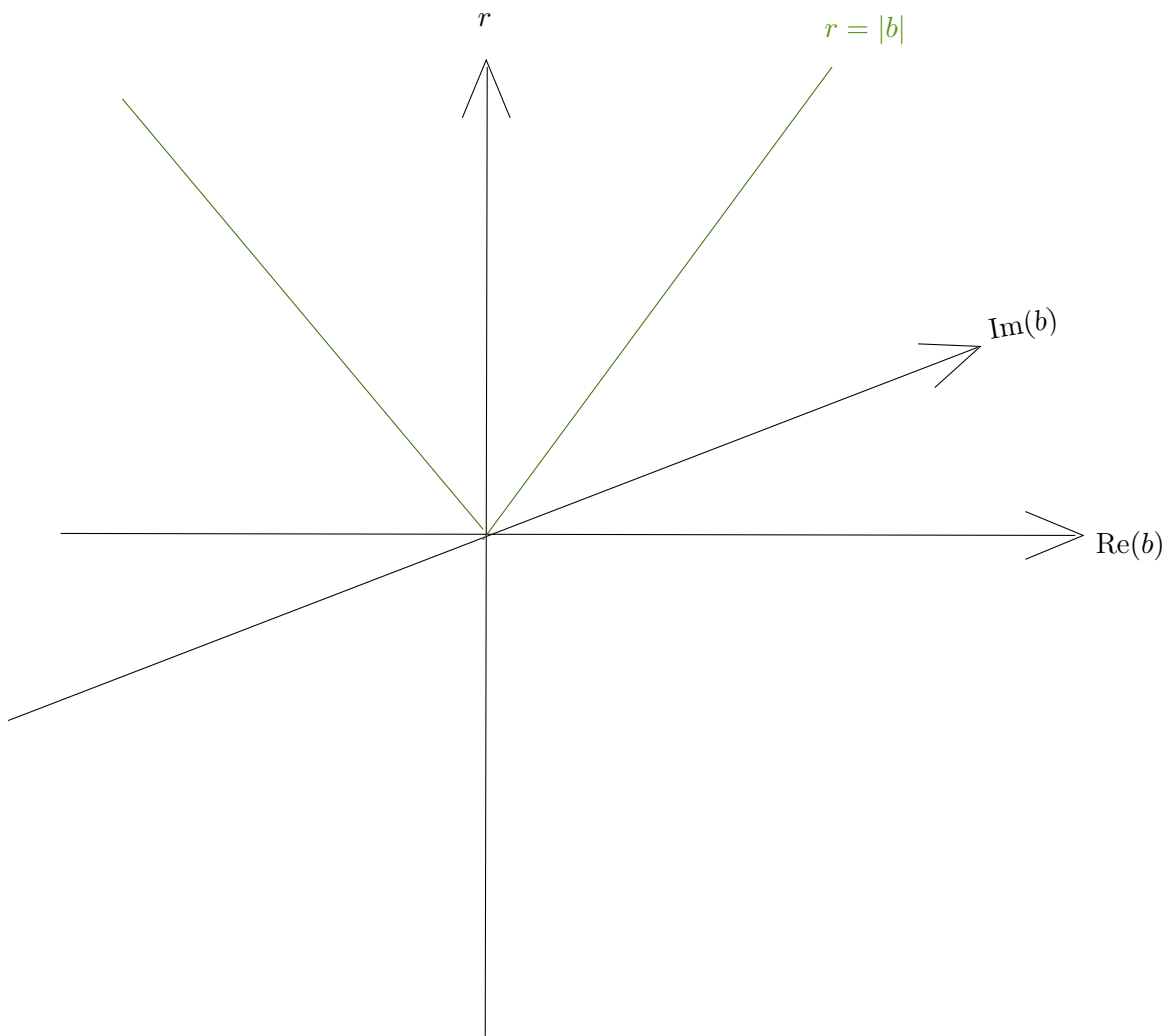


Figure 21: The solution space of the bosonic sector is parametrized by three parameters: r , $\text{Im}(b)$, and $\text{Re}(b)$, with the constraint $r \geq |b|$. The “light-cone”, defined by the surface $r = |b|$, is highlighted in green.

By plotting the graph using the three parameters r , $\text{Im}(b)$, and $\text{Re}(b)$ that parametrize Q_{BB} , and based on equation (175), we observe that in the strong-disorder limit, the primary contributions to the field integral arise from the region near the “light-cone”. The “light-cone” is represented by the surface defined by $r = |b|$, which is highlighted in green in the figure above.

To further our understanding, let us explore additional insights into the solution space within the strong-disorder limit.²⁷ First, it is important to note that the matrix $Q_{BB,0}$ is nilpotent, implying $Q_{BB,0}^2 = 0$. The symmetry group $g_B \in SU(1, 1)$, associated with the boson-boson sector, acts on $iQ_{BB,0}$ through the adjoint action of the Lie group on its Lie algebra:

$$\begin{aligned} iQ_{BB,0} &\rightarrow g_B (iQ_{BB,0}) g_B^{-1} \\ &= g_B (h_B iQ_{BB,0} h_B^{-1}) g_B^{-1}. \end{aligned} \tag{176}$$

The adjoint action generates the orbit of $iQ_{BB,0}$, with $h_B \in U(1)$ representing the isotropy group of $iQ_{BB,0}$. This orbit can be identified with the homogeneous space

²⁷From this point onward, we will closely follow the analysis presented in [4].

$SU(1, 1)/U(1) \cong H^2$ (hyperboloid).

The $SU(1, 1)$ -invariant metric tensor on this homogenous space $SU(1, 1)/U(1)$ is proportional to²⁸:

$$-\text{Tr}(\text{d}Q_{BB,0})^2 \propto r^2 (\text{d}\phi)^2 + 0 \cdot (\text{d}r)^2. \quad (177)$$

We note that this metric is degenerate, specifically vanishing along the r direction. It separates into “stiff” degrees of freedom along ϕ and “stiffness-free” degrees of freedom along r .

In the strong disorder limit, we observe that the dominant contributions to the field integral come from the nilpotent orbit on which the invariant metric degenerates. This observation is promising, as a similar finding in a different class of systems (symmetry class A) served as the foundation for the novel spontaneous symmetry breaking phenomenon proposed in [4, 5, 6]. However, to ascertain whether this phenomenon can also manifest in class D systems, it is essential to move beyond the general formalism and apply these concepts to a specific system, thoroughly examining its phases. In the next chapter, we will specifically focus on the study of measurement-induced phase transitions in free fermions belonging to class D.

²⁸The numerical constant that precedes the expression for the metric tensor has not been specified.

8 Application: Measurement-Induced Phase Transitions in Free Fermions of Class D

8.1 Introduction

Building upon the general framework of supersymmetry applied to class D systems discussed in the previous chapter, we now turn our attention to the study of a specific model. Specifically, we focus on a current and active research area concerning measurement-induced entanglement phase transitions in free fermion systems, which has attracted significant attention in recent literature. Several significant contributions in this area have been made, including [63, 64, 65, 66, 67, 68, 69, 70, 71]. The objective of this work is to introduce a novel perspective to this problem. Before delving into the analysis, we will briefly introduce the problem of measurement-induced entanglement phase transitions in free fermion systems, drawing from [70, 64], and subsequently proceed with the analysis.

Measurement-induced phase transitions arise from the interplay between two fundamental quantum mechanical processes: unitary time evolution and measurement. To illustrate this, consider a lattice of free fermions evolving according to a quadratic hopping Hamiltonian. In addition to this unitary evolution, the system is subjected to continuous monitoring through repeated measurements at short time intervals, denoted by $\{t_k\}$, at all lattice sites $\{j\}$. These measurements involve local fermion bilinears, and the random measurement outcomes, denoted by $\{m_{k,j}\}$, influence the system's evolution, defining a quantum trajectory $\{t_k, j, m_{k,j}\}$.

The measurement process can be described using the formalism of generalized measurements [64]. Without delving into the full details of this formalism, we emphasize a key point: each quantum trajectory is assigned a statistical weight determined by the Born-rule probability associated with the measurement outcomes. To study the universal properties of the system, one can consider a statistical ensemble of quantum trajectories and perform an average over all such trajectories in the ensemble.

Alternatively, as outlined in [70] and as we adopt here, the system can be modeled using a non-Hermitian “Hamiltonian” that describes non-interacting fermions. This “Hamiltonian” has two components: a quadratic hopping term responsible for unitary dynamics and a non-Hermitian term representing the effects of the measurements. The non-Hermitian term is parameterized by random variables to reflect the stochastic nature of the measurement outcomes. For simplicity, one can also assume that the quadratic hopping term is random in space and time, an assumption we adopt in our analysis as well.

Averaging over quantum trajectories, as mentioned earlier, corresponds to averaging over the random variables in the Hamiltonian using a probability distribution [63, 64]. It is important to incorporate the Born-rule into this averaging process, as detailed in [70, 64, 69]. Later in this chapter, we will also demonstrate, following [70], how the statistics of the random variables describing the measurement process in the “Hamiltonian” are influenced by

the Born rule.

A key quantitative measure for analyzing different phases of a system subjected to measurements is entanglement entropy. The scaling behavior of entanglement entropy with system size reveals distinct phases. In free fermion systems, the volume-law phase, where entanglement entropy scales proportionally with the system’s volume, is typically destroyed even by very weak measurements [72]. It was argued in [72] that the area-law phase, where entanglement entropy scales proportionally with the area, always persists in the presence of measurements. However, several studies [63, 67, 65, 66, 68] suggest that within certain ranges of measurement rates, entanglement entropy may exhibit power-law or logarithmic scaling, which is referred to as a “critical phase” in the literature. The observation of this “critical phase” motivated us to further investigate these systems, applying the methods and ideas discussed in the previous chapter to gain deeper insights into this phase and explore the potential for novel spontaneous symmetry breaking phenomena.²⁹

In the literature, the study of measurement-induced phase transitions often relies on the replica trick, a method also employed in [70], which we follow closely to set up the model describing the system. In this work, however, we propose replacing the replica trick³⁰ with supersymmetry techniques to analyze the system.

Before beginning the analysis, it is important to recognize that free fermion systems can be classified according to the symmetry properties of their Hamiltonians, as outlined in the Altland-Zirnbauer classification of non-interacting fermions [3]. In the context of measurement-induced phase transitions, the literature has explored at least two distinct categories: symmetry class A and symmetry class D. Here, we specifically focus on systems within symmetry class D.

We will now proceed with the analysis by first describing the model that will be the central focus of our investigation.

8.2 Model: Hamiltonian

Consider a one-dimensional chain of Majorana fermions undergoing continuous monitoring, i.e., subject to repeated measurements in the regime where the measurements are both highly frequent and weak. Following the framework established by [70], we model the dynamics of this system using the following time-dependent “Hamiltonian”³¹:

$$\begin{aligned} \hat{H}_{\tau_h, M}(t) &= \sum_{j, l=1}^L \sum_{r, r'=1}^{2N} \left(\tau_h(t)_{jl}^{rr'} + iM(t)_{jl}^{rr'} \right) i\hat{\gamma}_{j,r} \hat{\gamma}_{l,r'} \\ &= \hat{H}_{\tau_h}(t) + \hat{H}_M(t). \end{aligned} \tag{178}$$

²⁹We are grateful to Prof. Alexander Altland for bringing the topic of measurement-induced phase transitions to our attention and suggesting it as a potential application of the formalism presented in Chapter 7.

³⁰Given the general criticisms of the replica trick (for example, [73]), we adopt an alternative method in this work.

³¹In this chapter of the thesis, operators are denoted with a “hat”, unlike the notation used in earlier chapters.

Here, $\hat{\gamma}_{j,r}$ represents standard Majorana fermion operators that satisfy the following anti-commutation relations:

$$\{\hat{\gamma}_{j,r}, \hat{\gamma}_{l,r'}\} = 2\delta_{jl}\delta_{rr'}\mathbb{I}, \quad (179)$$

where \mathbb{I} is the identity operator, and $\hat{\gamma}_{j,r}^\dagger = \hat{\gamma}_{j,r}$, implying that each Majorana fermion is its own Hermitian conjugate. The indices j, l denote the site positions, with $j, l = 1, \dots, L$. Additionally, the Majorana fermions are indexed by r , which ranges from 1 to $2N$, indicating that we are considering $2N$ Majorana modes at each lattice site.

Now, let us describe the two terms in the Hamiltonian (178):

1. Hermitian Part Contributing to Unitary Dynamics: The term

$$\hat{H}_{\tau_h}(t) = \sum_{j,l=1}^L \sum_{r,r'=1}^{2N} \tau_h(t)_{jl}^{rr'} i\hat{\gamma}_{j,r}\hat{\gamma}_{l,r'}, \quad (180)$$

in the ‘‘Hamiltonian’’ (178) represents the Hermitian component, which governs the unitary evolution of the system. The Hermiticity of this term, combined with the anti-commutation relations of the Majorana fermions, impose certain ‘‘symmetry’’ constraints on the coefficients $\tau_h(t)_{jl}^{rr'}$:

$$\begin{aligned} \tau_h(t)_{jl}^{rr'} &= \overline{\tau_h(t)_{jl}^{rr'}}, \\ \tau_h(t)_{jl}^{rr'} &= -\tau_h(t)_{lj}^{r'r}. \end{aligned} \quad (181)$$

Additionally, we assume that the only non-zero elements of $\tau_h(t)_{jl}^{rr'}$ arise from nearest-neighbor interactions on the lattice, meaning they contribute only when $l = j + 1$ or $l = j - 1$, and for any r and r' . By defining $J(t)_j^{rr'} := 2\tau_h(t)_{j,j+1}^{rr'}$, the Hamiltonian $\hat{H}_{\tau_h}(t)$ can be rewritten as $\hat{H}_J(t)$, which takes the following form³²³³:

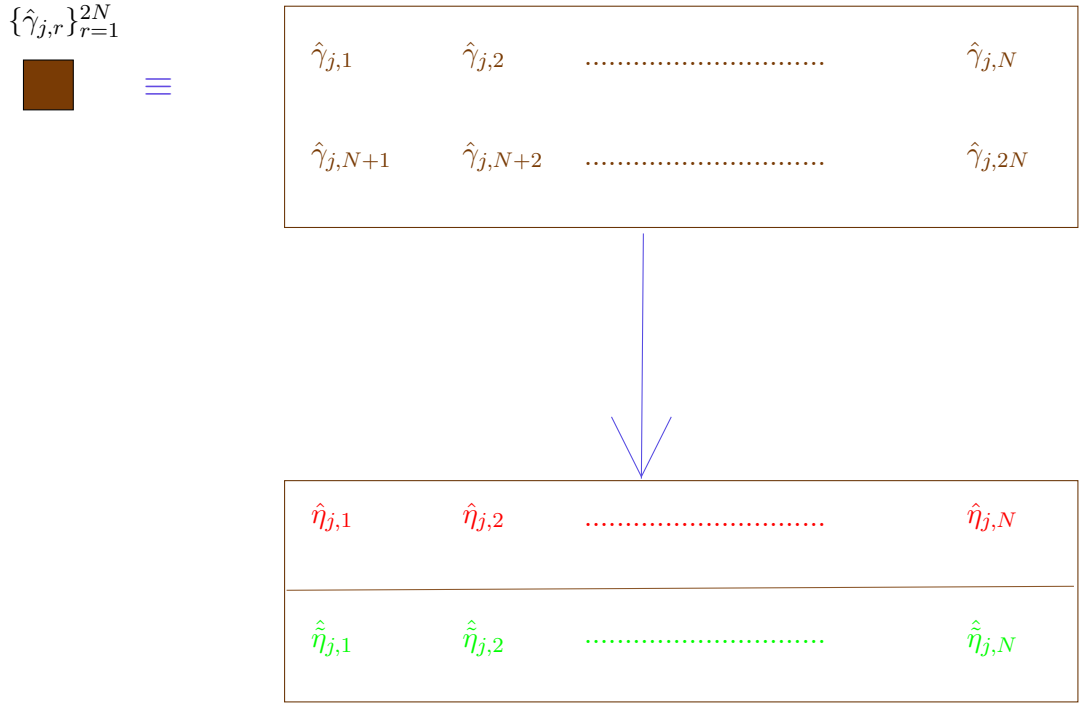
$$\hat{H}_J(t) = \sum_{j=1}^L \sum_{r,r'=1}^{2N} J(t)_j^{rr'} i\hat{\gamma}_{j,r}\hat{\gamma}_{j+1,r'}. \quad (182)$$

There exists an alternative representation of $\hat{H}_J(t)$ in terms of complex fermions rather than Majorana fermions. For the purposes of our analysis, we choose to work with complex fermions. To construct complex fermions from Majorana fermions, we use a well-established procedure. Specifically, for each lattice site j , where there are $2N$ Majorana fermions, we divide these $2N$ Majorana fermions into two sets as follows:

$$\begin{aligned} \hat{\eta}_{j,r} &:= \hat{\gamma}_{j,r}, & r = 1, \dots, N, \\ \hat{\tilde{\eta}}_{j,r} &:= \hat{\gamma}_{j,r+N}, & r = 1, \dots, N. \end{aligned} \quad (183)$$

³²Here, we omit explicit details of the boundary conditions. For simplicity, we assume periodic boundary conditions.

³³This is the form in which it is presented in [70].


 Figure 22: Division of $2N$ Majorana fermions into two sets.

Using the two sets of Majorana fermions defined above, the complex fermion operators can be constructed as follows:

$$\begin{aligned} \hat{c}_{j,r} &:= \frac{\hat{\eta}_{j,r} + i\hat{\eta}_{j,r}}{2}, \quad r = 1, \dots, N, \\ \hat{c}_{j,r}^\dagger &:= \frac{\hat{\eta}_{j,r} - i\hat{\eta}_{j,r}}{2}, \quad r = 1, \dots, N. \end{aligned} \quad (184)$$

By applying (179) and (183), it can be confirmed that the complex fermion operators constructed above obey the standard canonical anti-commutation relations:

$$\begin{aligned} \{\hat{c}_{j,r}, \hat{c}_{l,r'}^\dagger\} &= \delta_{jl}\delta_{rr'}\mathbb{I}, \\ \{\hat{c}_{j,r}, \hat{c}_{l,r'}\} &= 0, \\ \{\hat{c}_{j,r}^\dagger, \hat{c}_{l,r'}^\dagger\} &= 0. \end{aligned} \quad (185)$$

For simplicity, we assume

$$J(t)_j^{r,N+r'} = 0 = J(t)_j^{N+r,r'} \quad \text{for } r, r' = 1, \dots, N. \quad (186)$$

The Hamiltonian $\hat{H}_J(t)$ in equation (182) can be expressed using the complex fermions defined in equation (184) as follows:

$$\hat{H}_J(t) = \frac{1}{2} \sum_{j=1}^L \sum_{r,r'=1}^N \begin{pmatrix} \hat{c}_{j,r}^\dagger & \hat{c}_{j,r} \end{pmatrix} \begin{pmatrix} A_J(t)_{j,j+1}^{rr'} & B_J(t)_{j,j+1}^{rr'} \\ C_J(t)_{j,j+1}^{rr'} & A_J(t)_{j,j+1}^{rr'} \end{pmatrix} \begin{pmatrix} \hat{c}_{j+1,r'} \\ \hat{c}_{j+1,r'}^\dagger \end{pmatrix}. \quad (187)$$

The matrix elements of the matrix $\tilde{J}(t) = \begin{pmatrix} \tilde{J}(t)_{pp} & \tilde{J}(t)_{ph} \\ \tilde{J}(t)_{hp} & \tilde{J}(t)_{hh} \end{pmatrix} = \begin{pmatrix} A_J(t) & B_J(t) \\ C_J(t) & A_J(t) \end{pmatrix}$ are

given by:

$$\begin{aligned}
 A_J(t)_{j,j+1}^{rr'} &= 2iJ(t)_j^{rr'} + 2iJ(t)_j^{N+r,N+r'}, \\
 B_J(t)_{j,j+1}^{rr'} &= 2iJ(t)_j^{rr'} - 2iJ(t)_j^{N+r,N+r'}, \\
 C_J(t)_{j,j+1}^{rr'} &= 2iJ(t)_j^{rr'} - 2iJ(t)_j^{N+r,N+r'}.
 \end{aligned} \tag{188}$$

The indices $\eta = \{p, h\}$ represent the ‘‘particle-hole’’ space, adhering to the Bogoliubov-de Gennes notation.

2. **Non-Hermitian Part Leading to Nonunitary Dynamics:** The ‘‘Hamiltonian’’ in equation (178) has a non-Hermitian extension given by:

$$\hat{H}_M(t) = - \sum_{j,l=1}^L \sum_{r,r'=1}^{2N} M(t)_{jl}^{rr'} \hat{\gamma}_{j,r} \hat{\gamma}_{l,r'}, \tag{189}$$

which models the measurement protocol in the system. We will outline some features of $\hat{H}_M(t)$. First, we assume that $M(t)_{jl}^{rr'}$ is real:

$$M(t)_{jl}^{rr'} = \overline{M(t)_{jl}^{rr'}}. \tag{190}$$

The anticommutation relations of the Majorana fermions impose the following constraints on $M(t)_{jl}^{rr'}$:³⁴

$$M(t)_{jl}^{rr'} = -M(t)_{lj}^{r'r}. \tag{191}$$

It is clear that $\hat{H}_M(t)$ is not Hermitian, i.e. $\hat{H}_M(t)^\dagger \neq \hat{H}_M(t)$. We assume that the only non-zero terms in $M(t)_{jl}^{rr'}$ are the diagonal terms in space, specifically when $l = j$, for any r and r' , under the condition that $r \neq r'$.³⁵ Under this assumption, the expression for $\hat{H}_M(t)$ becomes:

$$\hat{H}_M(t) = - \sum_{j=1}^L \sum_{r,r'=1}^{2N} M(t)_j^{rr'} \hat{\gamma}_{j,r} \hat{\gamma}_{j,r'}. \tag{192}$$

In the equation above, and henceforth, we denote $M(t)_{jj}^{rr'} \equiv M(t)_j^{rr'}$.

There exists an alternative representation of $\hat{H}_M(t)$ using complex fermions instead of Majorana fermions. Based on the definitions given in (184), $\hat{H}_M(t)$ can be expressed as follows:

$$\hat{H}_M(t) = \frac{1}{2} \sum_{j=1}^L \sum_{r,r'=1}^N \begin{pmatrix} \hat{c}_{j,r}^\dagger & \hat{c}_{j,r} \end{pmatrix} \begin{pmatrix} A_{M,j}(t)^{rr'} & B_{M,j}(t)^{rr'} \\ C_{M,j}(t)^{rr'} & -A_{M,j}^T(t)^{rr'} \end{pmatrix} \begin{pmatrix} \hat{c}_{j,r'} \\ \hat{c}_{j,r'}^\dagger \end{pmatrix}, \tag{193}$$

where T represents the transpose in the \mathbb{C}^N space, and the matrix elements of the

³⁴For $j = l$ and $r = r'$, the term in $\hat{H}_M(t)$ is $M(t)_{jj}^{rr} \cdot \mathbb{I}$, using $\hat{\gamma}_{j,r}^2 = \mathbb{I}$. For simplicity, we can assume $M(t)_{jj}^{rr} = 0$.

³⁵This choice differs from that in [70], where the non-zero contributions to $M(t)_{jl}^{rr'}$ arise from adjacent sites, specifically for $l = j + 1$ or $l = j - 1$.

matrix $\widetilde{M}_j(t) = \begin{pmatrix} \widetilde{M}_j(t)_{pp} & \widetilde{M}_j(t)_{ph} \\ \widetilde{M}_j(t)_{hp} & \widetilde{M}_j(t)_{hh} \end{pmatrix} = \begin{pmatrix} A_{M,j}(t) & B_{M,j}(t) \\ C_{M,j}(t) & -A_{M,j}^T(t) \end{pmatrix}$ are as follows:

$$\begin{aligned} A_{M,j}(t)^{rr'} &= -2M(t)_j^{rr'} - 2M(t)_j^{N+r,N+r'} - 2iM(t)_j^{N+r,r'} + 2iM(t)_j^{r,N+r'}, \\ B_{M,j}(t)^{rr'} &= -2M(t)_j^{rr'} + 2M(t)_j^{N+r,N+r'} - 2iM(t)_j^{N+r,r'} - 2iM(t)_j^{r,N+r'}, \\ C_{M,j}(t)^{rr'} &= -2M(t)_j^{rr'} + 2M(t)_j^{N+r,N+r'} + 2iM(t)_j^{N+r,r'} + 2iM(t)_j^{r,N+r'}. \end{aligned} \quad (194)$$

It is straightforward to observe that:

$$\begin{aligned} B_{M,j}^T(t) &= -B_{M,j}(t), \\ C_{M,j}^T(t) &= -C_{M,j}(t). \end{aligned} \quad (195)$$

This indicates that $\widetilde{M}_j(t)$ belongs to $so(2N, \mathbb{C})$ Lie algebra. Additionally, the block components of the matrix $\widetilde{M}_j(t)$ satisfy the following conditions:

$$\begin{aligned} A_{M,j}(t)^\dagger &= -A_{M,j}(t), \\ B_{M,j}(t)^\dagger &= -C_{M,j}(t). \end{aligned} \quad (196)$$

From equations (195) and (196), it can be concluded that $\widetilde{M}_j(t)$ belongs to $so(2N, \mathbb{R})$ Lie algebra (class D). As a preview, we would like to highlight that this characteristic of the matrix $\widetilde{M}_j(t)$ will be significant in our analysis, as will be demonstrated later in this chapter.

From this point onward, we will refer to $\hat{H}_{\tau_h, M}(t)$ as $\hat{H}_{J, M}(t)$. To complete our description of the system's modeling, it is important to mention one additional detail. The quantities $J(t)_j^{rr'}$ and $M(t)_j^{rr'}$ are treated as random variables, and we must define probability distributions for both in order to carry out an average over these variables. Further information regarding the choice of probability distributions for these random variables will be provided later in this chapter.

8.3 Supersymmetry-Based Analysis of the Model

Having outlined the model, we will now begin our analysis by exploring how the state represented by the density matrix $\hat{\rho}_{J, M}(t)$ evolves along a quantum trajectory determined by the couplings $J = \{J(t')_j^{rr'} \mid t' \in [0, t], j = 1, \dots, L, r, r' = 1, \dots, N\}$ and the measurement outcomes $M = \{M(t')_j^{rr'} \mid t' \in [0, t], j = 1, \dots, L, r, r' = 1, \dots, N\}$, beginning from the initial state $\hat{\rho}(0)$. The density matrix $\hat{\rho}_{J, M}(t)$ represents the unnormalized density matrix. To obtain the physical density matrix $\hat{\rho}_{J, M}(t)$, we need to normalize $\hat{\rho}_{J, M}(t)$, such that $\hat{\rho}_{J, M}(t) = \frac{\hat{\rho}_{J, M}(t)}{\text{Tr} \hat{\rho}_{J, M}(t)}$. The expression for $\hat{\rho}_{J, M}(t)$ is given by:

$$\hat{\rho}_{J, M}(t) = \hat{K}_{J, M}(t) \hat{\rho}(0) \hat{K}_{J, M}(t)^\dagger, \quad (197)$$

where $\hat{K}_{J, M}(t)$ is a non-unitary “time-evolution” operator due to the non-Hermitian nature of the “Hamiltonian” $\hat{H}_{J, M}(t)$. The expression for $\hat{K}_{J, M}(t)$ is:

$$\hat{K}_{J, M}(t) = \mathcal{T} \exp \left(-i \int_0^t dt' \hat{H}_{J, M}(t') \right), \quad (198)$$

where \mathcal{T} denotes time-ordering.³⁶

To continue, let us revisit the discussion introduced at the beginning of this chapter. The main objective of examining monitored free fermion systems is to explore the entanglement within the system and to characterize the various phases of the system based on its entanglement properties. With this in mind, we aim to compute the system's entropy as a measure of entanglement. Following [70], we use the n th Rényi entropy, denoted by S_n to quantify the entanglement. For simplicity, we start with $n = 2$ to illustrate our method. The expression for second Rényi entropy is given by:

$$\mathbb{E}[e^{-S_2(t)}] = \mathbb{E}[\text{Tr} \hat{\rho}_{J,M}(t)^2]. \quad (199)$$

Here, $\mathbb{E}[(.)]$ represents the average of the quantity $(.)$ with respect to the probability distributions of the couplings J and the measurement outcomes M , treating these variables as random. The specific probability distributions will be discussed in more detail later in this chapter. For the moment, it is important to emphasize a key aspect of the averaging process related to measurement outcomes, as highlighted in [70, 64, 69].

In particular, the normalization factor $\text{Tr} \hat{\rho}_{J,M}(t)$ must be incorporated into the averaging procedure. This factor is crucial as it represents the probability of observing a given measurement record M according to Born's rule. Therefore, the expression for $\mathbb{E}[(.)]$ is given by:

$$\mathbb{E}[(.)] = \mathbb{E}_{J,M}[(.) \text{Tr} \hat{\rho}_{J,M}(t)], \quad (200)$$

where $\mathbb{E}_{J,M}$ indicates averaging over the probability distributions for J and M . The normalization factor $\text{Tr} \hat{\rho}_{J,M}(t)$ ensures that the quantum trajectories are sampled in accordance with Born's rule.

Using equation (200) and $\hat{\rho}_{J,M}(t) = \frac{\hat{\rho}_{J,M}(t)}{\text{Tr} \hat{\rho}_{J,M}(t)}$, we can rewrite the expression for second Rényi entropy as:

$$\mathbb{E}[e^{-S_2(t)}] = \mathbb{E}_{J,M} \left[\frac{\text{Tr} \hat{\rho}_{J,M}(t)^2}{\text{Tr} \hat{\rho}_{J,M}(t)} \right]. \quad (201)$$

Having written the second Rényi entropy in the aforementioned manner, we will proceed to work with it from here. Up to this point, we have been closely following the discussion in [70]. However, from here, we diverge significantly from the method used in [70]. Instead of applying the replica trick as done in [70] to compute the Rényi entropy, we will utilize the supersymmetry technique. The following discussion is a prelude to the supersymmetry technique that will be used in our analysis.

³⁶ \hbar is set to 1.

8.3.1 Prelude

To apply the supersymmetry technique, let us first review some key results that will be useful in our analysis.

Let us consider a quadratic Hamiltonian that describes a system of fermions, expressed within the framework of second quantization as follows:

$$\hat{H}_F = \sum_{u,v=1}^N c_u^\dagger H_{uv} c_v, \quad (202)$$

where c_u^\dagger and c_v represent the fermionic creation and annihilation operators associated with the single-particle states labeled by u and v , respectively.

Next, we will calculate the trace of $e^{-\beta\hat{H}_F}$ over the fermionic Fock space, where β represents a scalar quantity. It can be verified that the trace is given by:

$$\text{Tr} (e^{-\beta\hat{H}_F}) \Big|_{\text{Fermion}} = \text{Det} (1 + e^{-\beta H}). \quad (203)$$

Comment. *To verify the expression in the equation above, one can diagonalize the Hamiltonian H and express \hat{H}_F in this diagonal basis. This simplifies the computation of the trace of $e^{-\beta\hat{H}_F}$ over the fermionic Fock space, allowing us to confirm that it is equal to $\text{Det}(1 + e^{-\beta H})$.*

Now, let us replace the fermionic creation and annihilation operators in equation (202) with the bosonic operators, denoted as b^\dagger for creation and b for annihilation:

$$\hat{H}_B = \sum_{u,v=1}^N b_u^\dagger H_{uv} b_v. \quad (204)$$

We will compute the supertrace (as opposed to the trace—this difference will be clarified shortly) of $e^{-\beta\hat{H}_B}$ over the bosonic Fock space, as demonstrated below:

$$\text{STr} (e^{-\beta\hat{H}_B}) \Big|_{\text{Boson}} := \text{Tr} ((-1)^{\hat{n}_B} e^{-\beta\hat{H}_B}) \Big|_{\text{Boson}}, \quad (205)$$

where \hat{n}_B is the total number operator for bosons. It can be shown that the supertrace is given by:

$$\text{STr} (e^{-\beta\hat{H}_B}) \Big|_{\text{Boson}} = \text{Det}^{-1} (1 + e^{-\beta H}). \quad (206)$$

Comment. *To confirm the result in the equation above, one can follow a similar procedure: diagonalize the Hamiltonian H and express \hat{H}_B in this diagonal basis. This makes it easier to compute the supertrace of $e^{-\beta\hat{H}_B}$ over the bosonic Fock space, and it can be confirmed that it equals $\text{Det}^{-1} (1 + e^{-\beta H})$.*

The main takeaway from the above discussion, which serves as a guiding principle for applying supersymmetry, is that the trace of $e^{-\beta\hat{H}_F}$ over the fermionic Fock space can be

expressed as the supertrace of $e^{-\beta\hat{H}_B}$ over the bosonic Fock space, as demonstrated below:

$$\text{STr}(e^{-\beta\hat{H}_B}) \Big|_{\text{Boson}} = \text{Det}^{-1}(1 + e^{-\beta H}) = \left(\text{Tr}(e^{-\beta\hat{H}_F}) \Big|_{\text{Fermion}} \right)^{-1}. \quad (207)$$

Note. We can now elucidate the rationale for selecting the supertrace over the trace on the bosonic side. When we perform the trace, we arrive at the following expression:

$$\text{Tr}(e^{-\beta\hat{H}_B}) \Big|_{\text{Boson}} = \text{Det}^{-1}(1 - e^{-\beta H}), \quad (208)$$

which reveals the presence of the $-$ sign in the final result. To facilitate a comparison with the calculations conducted on the fermionic side, we compute the supertrace on the bosonic side.

The preceding discussion focused on Hamiltonians classified under symmetry class A in the Altland-Zirnbauer classification [3] for non-interacting fermions. However, our interest lies in quadratic Hamiltonians that are categorized as belonging to class D, expressed in the following form:

$$\hat{H}_F = \frac{1}{2} \sum_{u,v=1}^N \begin{pmatrix} \hat{c}_u^\dagger & \hat{c}_u \end{pmatrix} H_{uv} \begin{pmatrix} \hat{c}_v \\ \hat{c}_v^\dagger \end{pmatrix}, \quad (209)$$

where

$$H = \begin{pmatrix} A & B \\ C & -A^T \end{pmatrix} \quad (210)$$

is a $2N \times 2N$ matrix with the properties $B = -B^T$ and $C = -C^T$. This structure indicates that H satisfies the relation $H = -\Sigma_1 H^T \Sigma_1$, where $\Sigma_1 = \sigma_1 \otimes 1_N$, placing it within the $so(2N, \mathbb{C})$ Lie algebra. Furthermore, the Hamiltonian \hat{H}_F is Hermitian, which enforces the condition $H = H^\dagger$. Consequently, it follows that iH belongs to $so(2N, \mathbb{R})$ Lie algebra. One can confirm that the trace of $e^{-\beta\hat{H}_F}$ over the fermionic Fock space is given by:

$$\text{Tr}(e^{-\beta\hat{H}_F}) \Big|_{\text{Fermion}} = \text{Det}^{\frac{1}{2}}(1 + e^{-\beta H}). \quad (211)$$

Comment. To verify (211), we utilize the fact that iH belongs to $so(2N, \mathbb{R})$ Lie algebra, allowing it to be transformed into a diagonal form as follows:

$$H \rightarrow gHg^{-1} = \begin{pmatrix} \lambda & 0 \\ 0 & -\lambda \end{pmatrix}, \quad (212)$$

where $\lambda = \text{diag}(\lambda_1, \lambda_2, \dots, \lambda_N)$ is a $N \times N$ diagonal matrix with $\lambda_r \in \mathbb{R} \forall r$, and g satisfies:

$$(g^{-1})^\dagger = g = \Sigma_1 (g^{-1})^T \Sigma_1. \quad (213)$$

By expressing \hat{H}_F in this diagonal basis (essentially performing a Bogoliubov transformation for fermions), we simplify the computation of the trace of $e^{-\beta\hat{H}_F}$ over the fermionic Fock space, confirming that it equals $\text{Det}^{\frac{1}{2}}(1 + e^{-\beta H})$.

The next step involves substituting fermionic creation and annihilation operators with bosonic ones, similar to what we did previously. However, this process presents some challenges for class D systems, unlike the class A systems we examined earlier. Specifically, we need to address two main issues:

1. The first issue arises because the off-diagonal blocks B and C of the matrix H are antisymmetric. Since bosonic operators follow canonical commutation relations, in contrast to the fermionic operators that adhere to canonical anticommutation relations, the contributions from these off-diagonal blocks become zero. This is expressed mathematically as:

$$\begin{aligned} \sum_{u,v=1}^N b_u^\dagger B_{uv} b_v^\dagger &= 0, \\ \sum_{u,v=1}^N b_u C_{uv} b_v &= 0. \end{aligned} \tag{214}$$

Therefore, we cannot simply replace the fermionic operators with bosonic ones.

2. The second issue is that class D Hamiltonians are not particle-conserving; they do not commute with the particle number operator. Thus, to derive results analogous to those for class A Hamiltonians, we must clarify the interpretation of supertrace in the bosonic context for this situation.

We begin by addressing the second problem, recalling the oscillator representation for bosons [74].

Consider an element from the symplectic Lie group in $2N$ dimensions, represented as $g_S = \exp \begin{pmatrix} A' & B' \\ C' & -A'^T \end{pmatrix}$, where each block in $\begin{pmatrix} A' & B' \\ C' & -A'^T \end{pmatrix}$ is a $N \times N$ matrix, and both B' and C' are symmetric, meaning $B' = B'^T$ and $C' = C'^T$. Now, consider the transformation:

$$g_S \rightarrow \hat{\rho}_B(g_S) = \exp \left[\frac{1}{2} \sum_{u,v=1}^N \begin{pmatrix} \hat{b}_u^\dagger & -\hat{b}_u \end{pmatrix} \begin{pmatrix} A'_{uv} & B'_{uv} \\ C'_{uv} & (-A'^T)_{uv} \end{pmatrix} \begin{pmatrix} \hat{b}_v \\ \hat{b}_v^\dagger \end{pmatrix} \right]. \tag{215}$$

This defines a representation that satisfies the following property:

$$\hat{\rho}_B(g_S h_S) = \hat{\rho}_B(g_S) \hat{\rho}_B(h_S), \tag{216}$$

where g_S and h_S are elements of the symplectic Lie group. It can be confirmed that the trace of $\hat{\rho}_B(g_S)$ over the bosonic space is given by:

$$\text{Tr} \hat{\rho}_B(g_S) \Big|_{\text{Boson}} = (\pm i)^N \text{Det}^{-\frac{1}{2}}(1 - g_S). \tag{217}$$

Comment. To verify (217), the concept of the Bogoliubov transformation for bosons can be employed to diagonalize the matrix $\begin{pmatrix} A' & B' \\ C' & -A'^T \end{pmatrix}$. This allows for the expression of $\hat{\rho}_B(g_S)$ in the diagonal basis. By computing the trace of $\hat{\rho}_B(g_S)$ over the bosonic Fock space, it can

be confirmed that the result is equal to $(\pm i)^N \text{Det}^{-\frac{1}{2}}(1-g_S)$.

As observed earlier in the case of class A Hamiltonians, we aim to define a supertrace such that the $-$ in the expression (217) is replaced with a $+$. To achieve this, we utilize the property of the representation $\hat{\rho}_B$ outlined in equation (216).

Let us consider

$$\hat{\rho}_B(-1) = \exp \left[\frac{1}{2} \sum_{u,v=1}^N \begin{pmatrix} \hat{b}_u^\dagger & -\hat{b}_u \end{pmatrix} \begin{pmatrix} +i\pi\delta_{uv} & 0 \\ 0 & -i\pi\delta_{uv} \end{pmatrix} \begin{pmatrix} \hat{b}_v \\ \hat{b}_v^\dagger \end{pmatrix} \right], \quad (218)$$

where δ_{uv} denotes the Kronecker delta. It can be verified that

$$\hat{\rho}_B(-1) = (-1)^{\hat{n}_B} (\pm i)^N, \quad (219)$$

with \hat{n}_B representing the total number operator for bosons.

By applying the property from (216), we find that:

$$\text{Tr} \hat{\rho}_B(-1) \hat{\rho}_B(g_S) \Big|_{\text{Boson}} = \text{Tr} \hat{\rho}_B(-g_S) \Big|_{\text{Boson}} = (\pm i)^N \text{Det}^{-\frac{1}{2}}(1+g_S). \quad (220)$$

Using the above equation and (219), we are now ready to define the supertrace over the bosonic Fock space as follows:

$$\text{STr} \hat{\rho}_B(g_S) \Big|_{\text{Boson}} := \text{Tr} (-1)^{\hat{n}_B} \hat{\rho}_B(g_S) \Big|_{\text{Boson}} = \text{Det}^{-\frac{1}{2}}(1+g_S). \quad (221)$$

After addressing the understanding of the supertrace, we will now turn our attention to the first issue outlined earlier: the antisymmetric off-diagonal blocks B and C of the matrix H , which complicate the substitution of fermionic operators with bosonic ones. To overcome this challenge, we will proceed as follows.

Consider two copies of the fermionic system, denoted by $\alpha = 1_f, 2_f$, both described by the same Hamiltonian \hat{H}_F given in equation (209). The Hamiltonian $\hat{\tilde{H}}_F$ for the combined system is defined as follows:

$$\hat{\tilde{H}}_F = \frac{1}{2} \sum_{u,v=1}^N \sum_{\alpha=1_f,2_f} \begin{pmatrix} \hat{c}_{u,\alpha}^\dagger & \hat{c}_{u,\alpha} \end{pmatrix} H_{uv} \begin{pmatrix} \hat{c}_{v,\alpha} \\ \hat{c}_{v,\alpha}^\dagger \end{pmatrix}. \quad (222)$$

This expression can be rewritten in a more compact form:

$$\hat{\tilde{H}}_F = \frac{1}{2} \sum_{u,v=1}^N \begin{pmatrix} \hat{\mathbf{c}}_u^\dagger & \hat{\mathbf{c}}_u \end{pmatrix} \begin{pmatrix} A_{uv} \otimes 1_2 & B_{uv} \otimes 1_2 \\ C_{uv} \otimes 1_2 & -(A^T)_{uv} \otimes 1_2 \end{pmatrix} \begin{pmatrix} \hat{\mathbf{c}}_v \\ \hat{\mathbf{c}}_v^\dagger \end{pmatrix}, \quad (223)$$

where 1_2 represents the 2×2 identity matrix, and

$$\begin{aligned} \begin{pmatrix} \hat{\mathbf{c}}_{\mathbf{u}}^\dagger & \hat{\mathbf{c}}_{\mathbf{u}} \end{pmatrix} &\equiv \begin{pmatrix} \hat{c}_{u,1_f}^\dagger & \hat{c}_{u,2_f}^\dagger & \hat{c}_{u,1_f} & \hat{c}_{u,2_f} \end{pmatrix}, \\ \begin{pmatrix} \hat{\mathbf{c}}_{\mathbf{v}} \\ \hat{\mathbf{c}}_{\mathbf{v}}^\dagger \end{pmatrix} &\equiv \begin{pmatrix} \hat{c}_{v,1_f} \\ \hat{c}_{v,2_f} \\ \hat{c}_{v,1_f}^\dagger \\ \hat{c}_{v,2_f}^\dagger \end{pmatrix}. \end{aligned} \quad (224)$$

It can be verified that

$$\widetilde{\text{Tr}}(e^{-\beta \hat{H}_F}) \Big|_{\text{Fermion}} = \left(\text{Det}^{\frac{1}{2}}(1 + e^{-\beta H}) \right)^2 = \text{Det}(1 + e^{-\beta H}), \quad (225)$$

where $\widetilde{\text{Tr}}$ denotes the trace over the enlarged space, which arises from considering the two fermionic copies labeled 1_f and 2_f .

We are now set to substitute the fermionic creation and annihilation operators with their bosonic counterparts in equation (223). Besides replacing the operators, an additional substitution must be made in (223), as illustrated below:

$$\begin{pmatrix} A_{uv} \otimes 1_2 & B_{uv} \otimes 1_2 \\ C_{uv} \otimes 1_2 & -(A^T)_{uv} \otimes 1_2 \end{pmatrix} \rightarrow \begin{pmatrix} A_{uv} \otimes 1_2 & B_{uv} \otimes \varepsilon \\ C_{uv} \otimes \varepsilon^{-1} & -(A^T)_{uv} \otimes 1_2 \end{pmatrix}, \quad (226)$$

where $\varepsilon = \begin{pmatrix} 0 & 1 \\ -1 & 0 \end{pmatrix}$. The expression for the Hamiltonian in the bosonic case is as follows:

$$\hat{H}_B = \frac{1}{2} \sum_{u,v=1}^N \begin{pmatrix} \hat{\mathbf{b}}_{\mathbf{u}}^\dagger & -\hat{\mathbf{b}}_{\mathbf{u}} \end{pmatrix} \begin{pmatrix} A_{uv} \otimes 1_2 & B_{uv} \otimes \varepsilon \\ C_{uv} \otimes \varepsilon^{-1} & -(A^T)_{uv} \otimes 1_2 \end{pmatrix} \begin{pmatrix} \hat{\mathbf{b}}_{\mathbf{v}} \\ \hat{\mathbf{b}}_{\mathbf{v}}^\dagger \end{pmatrix}. \quad (227)$$

where

$$\begin{aligned} \begin{pmatrix} \hat{\mathbf{b}}_{\mathbf{u}}^\dagger & -\hat{\mathbf{b}}_{\mathbf{u}} \end{pmatrix} &\equiv \begin{pmatrix} \hat{b}_{u,1_b}^\dagger & \hat{b}_{u,2_b}^\dagger & -\hat{b}_{u,1_b} & -\hat{b}_{u,2_b} \end{pmatrix}, \\ \begin{pmatrix} \hat{\mathbf{b}}_{\mathbf{v}} \\ \hat{\mathbf{b}}_{\mathbf{v}}^\dagger \end{pmatrix} &\equiv \begin{pmatrix} \hat{b}_{v,1_b} \\ \hat{b}_{v,2_b} \\ \hat{b}_{v,1_b}^\dagger \\ \hat{b}_{v,2_b}^\dagger \end{pmatrix}. \end{aligned} \quad (228)$$

Here, for the bosonic side, we also consider two copies of bosons denoted by $\alpha = 1_b, 2_b$. It is important to note that the off-diagonal blocks in the matrix from equation (227) are symmetric:

$$\begin{aligned} [(B \otimes \varepsilon)^T]_{uv,\alpha\alpha'} &= (B^T)_{uv}(\varepsilon^T)_{\alpha\alpha'} = (-B_{uv})(-\varepsilon_{\alpha\alpha'}) = [(B \otimes \varepsilon)]_{uv,\alpha\alpha'}, \\ [(C \otimes \varepsilon^{-1})^T]_{uv,\alpha\alpha'} &= (C^T)_{uv}((\varepsilon^{-1})^T)_{\alpha\alpha'} = (-C_{uv})(-\varepsilon_{\alpha\alpha'}^{-1}) = [(C \otimes \varepsilon^{-1})]_{uv,\alpha\alpha'}, \end{aligned} \quad (229)$$

which is the outcome we aimed for. Thus, we have resolved the issue of the contributions from the off-diagonal blocks vanishing in the bosonic scenario. The expression for \hat{H}_B can

be rewritten as follows:

$$\begin{aligned} \hat{H}_B = & \frac{1}{2} \sum_{u,v=1}^N \begin{pmatrix} \hat{b}_{u,1_b}^\dagger & -\hat{b}_{u,2_b} \end{pmatrix} \begin{pmatrix} A_{uv} & B_{uv} \\ C_{uv} & -(A^T)_{uv} \end{pmatrix} \begin{pmatrix} \hat{b}_{v,1_b} \\ \hat{b}_{v,2_b}^\dagger \end{pmatrix} \\ & + \frac{1}{2} \sum_{u,v=1}^N \begin{pmatrix} \hat{b}_{u,2_b}^\dagger & \hat{b}_{u,1_b} \end{pmatrix} \begin{pmatrix} A_{uv} & B_{uv} \\ C_{uv} & -(A^T)_{uv} \end{pmatrix} \begin{pmatrix} \hat{b}_{v,2_b} \\ -\hat{b}_{v,1_b}^\dagger \end{pmatrix}. \end{aligned} \quad (230)$$

We will utilize this form in our analysis later within this chapter. It's worth noting that \hat{H}_B is not Hermitian, but this does not influence the forthcoming result we will present. The following relation can be verified:

$$\widetilde{\text{STr}}(e^{-\beta\hat{H}_B}) \Big|_{\text{Boson}} = \text{Det}^{-\frac{1}{2}} \left[1 + \exp \left\{ -\beta \begin{pmatrix} A \otimes 1_2 & B \otimes \varepsilon \\ C \otimes \varepsilon^{-1} & -A^T \otimes 1_2 \end{pmatrix} \right\} \right] = \text{Det}^{-1} (1 + e^{-\beta H}), \quad (231)$$

where $\widetilde{\text{STr}}$ denotes the supertrace over the enlarged space, which arises from considering two copies of bosons designated by 1_b and 2_b .

Comment. *The first equality in (231) can be confirmed by referring to the result in (221).*

To establish the second equality, we can perform a Taylor expansion of

$$\exp \left\{ -\beta \begin{pmatrix} A \otimes 1_2 & B \otimes \varepsilon \\ C \otimes \varepsilon^{-1} & -A^T \otimes 1_2 \end{pmatrix} \right\}, \text{ and apply the following determinant property:}$$

$$\text{Det} \begin{pmatrix} P & Q \\ R & S \end{pmatrix} = \text{Det}(S) \text{Det}(P - QS^{-1}R). \quad (232)$$

By following these steps, the second equality can be demonstrated.

After all these efforts, we have arrived at the key takeaway from this discussion, which acts as a guiding principle for using the supersymmetry technique in our analysis of class D systems:

$$\begin{aligned} \widetilde{\text{STr}}(e^{-\beta\hat{H}_B}) \Big|_{\text{Boson}} & := \widetilde{\text{Tr}}((-1)^{\hat{n}_B} e^{-\beta\hat{H}_B}) \Big|_{\text{Boson}} = \text{Det}^{-1} (1 + e^{-\beta H}) \\ & = \left(\widetilde{\text{Tr}}(e^{-\beta\hat{H}_F}) \Big|_{\text{Fermion}} \right)^{-1}. \end{aligned} \quad (233)$$

In words, the inverse of the trace of $e^{-\beta\hat{H}_F}$ calculated in the fermionic Fock space is equivalent to the supertrace of $e^{-\beta\hat{H}_B}$ evaluated in the bosonic Fock space.

Note. *It is crucial to emphasize that caution is required when dealing with expressions involving bosons, as opposed to fermions. Specifically, one must ensure that the expressions involving bosons are convergent and well-defined, which may impose additional constraints. This consideration will be significant in our analysis later on.*

We have now reached the conclusion of this prelude. Even if the reader has overlooked the mathematical details in between, it is important to remember equation (233) from this discussion. We will use this equation in the next section to express the trace of the density

matrix over fermions governed by a quadratic Hamiltonian as the supertrace of the density matrix defined over bosons.

8.3.2 Supersymmetry Approach to the Second Rényi Entropy

We are now prepared to express the second Rényi entropy using the concepts discussed in the previous section. Before proceeding, however, it is important to recall the measurement process. Since measurements are taken at very short time intervals, it is more appropriate to work in a discrete-time formulation.

With this in mind, we can now write the expression for $\text{Tr } \hat{\varrho}_{J,M}(t)$ in discrete time. To do so, we will use the following identity [70, 75]:

$$\begin{aligned}
 \text{Tr}(\hat{O}_1 \hat{O}_2) &= \sum_{m,n} \langle n | \hat{O}_1 | m \rangle \langle m | \hat{O}_2 | n \rangle \\
 &= \sum_{m,n} (\langle n | \otimes \langle m |) (\hat{O}_1 \otimes \hat{O}_2) (|m\rangle \otimes |n\rangle) \\
 &= \sum_{m,n} (\langle n | \otimes \langle m |) (\hat{O}_1 \otimes \hat{O}_2) \hat{S}(|n\rangle \otimes |m\rangle) \\
 &= \widetilde{\text{Tr}} \left((\hat{O}_1 \otimes \hat{O}_2) \hat{S} \right).
 \end{aligned} \tag{234}$$

Let us clarify the above equation. First, $\{|n\rangle\}$ represents a complete set of states in Fock space. The operator \hat{S} refers to the swap operator, which acts as follows:

$$\hat{S}(|n\rangle \otimes |m\rangle) := |m\rangle \otimes |n\rangle. \tag{235}$$

Essentially, in equation (234), we have rewritten the trace over the original space as a trace over an enlarged space, formed by taking two copies of the original space. The trace in this enlarged space is denoted by $\widetilde{\text{Tr}}$.

We are now prepared to express $\text{Tr } \hat{\varrho}_{J,M}(t)$ in discrete time. To do this, we discretize time t into n intervals, denoted as t_k , where k ranges from 1 to n . The time interval between two successive time slices is given by $\Delta t = t_k - t_{k-1}$. The resulting expression is:

$$\begin{aligned}
 \text{Tr } \hat{\varrho}_{J,M}(t) &= \text{Tr}(\hat{K}_{J,M}(t) \hat{\rho}(0) \hat{K}_{J,M}(t)^\dagger) \\
 &= \widetilde{\text{Tr}} \left((\hat{K}_{J,M}(t) \hat{\rho}(0) \otimes \hat{K}_{J,M}(t)^\dagger) \hat{S} \right) \\
 &= \widetilde{\text{Tr}} \left(e^{-i\Delta t \hat{H}_{J,M,+}(t_n)} \dots e^{-i\Delta t \hat{H}_{J,M,+}(t_2)} e^{-i\Delta t \hat{H}_{J,M,+}(t_1)} \hat{\rho}(0)_+ \right. \\
 &\quad \left. e^{i\Delta t \hat{H}_{J,M,-}(t_1)^\dagger} e^{i\Delta t \hat{H}_{J,M,-}(t_2)^\dagger} \dots e^{i\Delta t \hat{H}_{J,M,-}(t_n)^\dagger} \hat{S}^{+,-} \right).
 \end{aligned} \tag{236}$$

In the second equality, we apply the identity outlined in equation (234). To differentiate between the two copies of fermions in the enlarged space, we introduce indices $c = \{+, -\}$. Furthermore, we introduce a superscript on the swap operator $\hat{S}^{+,-}$ to indicate its action

within this enlarged space. The Hamiltonian represented in the equation above is given by:

$$\begin{aligned}
 \hat{H}_{J,M,c}(t_k) &= \frac{1}{2} \sum_{j=1}^L \sum_{r,r'=1}^N \begin{pmatrix} \hat{c}_{c,j,r}^\dagger & \hat{c}_{c,j,r} \end{pmatrix} \begin{pmatrix} A_J(t_k)_{j,j+1}^{rr'} & B_J(t_k)_{j,j+1}^{rr'} \\ C_J(t_k)_{j,j+1}^{rr'} & A_J(t_k)_{j,j+1}^{rr'} \end{pmatrix} \begin{pmatrix} \hat{c}_{c,j+1,r'} \\ \hat{c}_{c,j+1,r'}^\dagger \end{pmatrix} \\
 &+ \frac{1}{2} \sum_{j=1}^L \sum_{r,r'=1}^N \begin{pmatrix} \hat{c}_{c,j,r}^\dagger & \hat{c}_{c,j,r} \end{pmatrix} \begin{pmatrix} A_{M,j}(t_k)^{rr'} & B_{M,j}(t_k)^{rr'} \\ C_{M,j}(t_k)^{rr'} & -A_{M,j}^T(t_k)^{rr'} \end{pmatrix} \begin{pmatrix} \hat{c}_{c,j,r'} \\ \hat{c}_{c,j,r'}^\dagger \end{pmatrix} \\
 &= \hat{H}_{J,c}(t) + \hat{H}_{M,c}(t),
 \end{aligned} \tag{237}$$

where the matrix elements are specified in equations (188) and (194). The terms labeled with + and – in equation (236) arise from the discretization of the operators $\hat{K}_{J,M}(t)$ and $\hat{K}_{J,M}(t)^\dagger$, respectively.

For our analysis, we assume that $\hat{\rho}(0)_+ \propto \hat{1}$. We can express $\text{Tr} \hat{\rho}_{J,M}(t)$ in a more compact form as follows:

$$\begin{aligned}
 \text{Tr} \hat{\rho}_{J,M}(t) &= \widetilde{\text{Tr}} \left\{ \left(\prod_{k=1}^n e^{-i\Delta t \hat{H}_{J,M,+}(t_k)} e^{i\Delta t \hat{H}_{J,M,-}(t_k)^\dagger} \right) \hat{\rho}(0)_+ \hat{S}^{+,-} \right\} \\
 &\sim \widetilde{\text{Tr}} \left\{ \left(\prod_{k=1}^n \prod_{c=+,-} e^{-i\Delta t \hat{H}_{M,c}(t_k)} e^{-ic\Delta t \hat{H}_{J,c}(t_k)} \right) \hat{\rho}(0)_+ \hat{S}^{+,-} \right\}.
 \end{aligned} \tag{238}$$

Here, we have disregarded terms of order $(\Delta t)^2$ and higher. Furthermore, we have utilized the properties $\hat{H}_{M,c}(t_k)^\dagger = -\hat{H}_{M,c}(t_k)$ and $\hat{H}_{J,c}(t_k)^\dagger = \hat{H}_{J,c}(t_k)$ relevant to our model.

Having rewritten the trace of the density matrix in discrete time, we will now revisit the expression for the second Rényi entropy. To refresh our memory, the expression is given by:

$$\begin{aligned}
 \mathbb{E}[e^{-S_2(t)}] &= \mathbb{E}_{J,M} \left[\frac{\text{Tr} \hat{\rho}_{J,M}(t)^2}{\text{Tr} \hat{\rho}_{J,M}(t)} \right] \\
 &= \mathbb{E}_{J,M} \left[\frac{\text{Tr} \hat{\rho}_{J,M}(t)^2 \text{Tr} \hat{\rho}_{J,M}(t)}{(\text{Tr} \hat{\rho}_{J,M}(t))^2} \right].
 \end{aligned} \tag{239}$$

In the second equality, we have introduced a factor of $1 = \frac{\text{Tr} \hat{\rho}_{J,M}(t)}{\text{Tr} \hat{\rho}_{J,M}(t)}$ to exploit the discussion presented in Section 8.3.1 about creating two copies of fermions. This allows us to reformulate the trace over the fermionic Fock space in the denominator as a supertrace over the bosonic Fock space, as demonstrated in equation (233).

We simplify the analysis by initially focusing on the measurement-only model, where $J = 0$. We will illustrate how to express the second Rényi entropy using the supersymmetry technique specifically for this model, highlighting the essential ideas involved. Henceforth, we will denote $\hat{\rho}_{J=0,M}(t) \equiv \hat{\rho}_M(t)$.³⁷

Equation (239) contains three terms that need to be represented in discrete time. We will examine each of these terms one at a time.

³⁷The analysis presented here can be generalized to include the case where $J \neq 0$.

1. The term $\text{Tr } \hat{\rho}_M(t)^2$ in the numerator

One can express $\text{Tr } \hat{\rho}_M(t)^2$ in the following manner [70, 75]:

$$\begin{aligned}
 \text{Tr } \hat{\rho}_M(t)^2 &= \text{Tr}(\hat{K}_M(t) \hat{\rho}(0) \hat{K}_M(t)^\dagger \hat{K}_M(t) \hat{\rho}(0) \hat{K}_M(t)^\dagger) \\
 &= \sum_{n_1, n_2, m_1, m_2} \left(\langle n_1 | \hat{K}_M(t) \hat{\rho}(0) | n_2 \rangle \langle n_2 | \hat{K}_M(t)^\dagger | m_1 \rangle \right. \\
 &\quad \left. \langle m_1 | \hat{K}_M(t) \hat{\rho}(0) | m_2 \rangle \langle m_2 | \hat{K}_M(t)^\dagger | n_1 \rangle \right) \\
 &= \sum_{n_1, n_2, m_1, m_2} \left((\langle n_1 | \otimes \langle n_2 | \otimes \langle m_1 | \otimes \langle m_2 |) \right. \\
 &\quad (\hat{K}_M(t) \hat{\rho}(0) \otimes \hat{K}_M(t)^\dagger \otimes \hat{K}_M(t) \hat{\rho}(0) \otimes \hat{K}_M(t)^\dagger) \\
 &\quad \left. (|n_2\rangle \otimes |m_1\rangle \otimes |m_2\rangle \otimes |n_1\rangle) \right) \tag{240} \\
 &= \sum_{n_1, n_2, m_1, m_2} \left((\langle n_1 | \otimes \langle n_2 | \otimes \langle m_1 | \otimes \langle m_2 |) \right. \\
 &\quad (\hat{K}_M(t) \hat{\rho}(0) \otimes \hat{K}_M(t)^\dagger \otimes \hat{K}_M(t) \hat{\rho}(0) \otimes \hat{K}_M(t)^\dagger) \\
 &\quad \left. \hat{C}_{1 \rightarrow 4}(|n_1\rangle \otimes |n_2\rangle \otimes |m_1\rangle \otimes |m_2\rangle) \right) \\
 &= \widetilde{\text{Tr}} \left((\hat{K}_M(t) \hat{\rho}(0) \otimes \hat{K}_M(t)^\dagger \otimes \hat{K}_M(t) \hat{\rho}(0) \otimes \hat{K}_M(t)^\dagger) \hat{C}_{4 \rightarrow 1} \right),
 \end{aligned}$$

where $\widetilde{\text{Tr}}$ indicates the trace over the enlarged space, and $\hat{C}_{1 \rightarrow 4}$ is a permutation operator defined as follows:

$$\hat{C}_{1 \rightarrow 4}(|n_1\rangle \otimes |n_2\rangle \otimes |m_1\rangle \otimes |m_2\rangle) := |n_2\rangle \otimes |m_1\rangle \otimes |m_2\rangle \otimes |n_1\rangle. \tag{241}$$

Using equations (238) and (240), we can express $\text{Tr } \hat{\rho}_M(t)^2$ in discrete time as:

$$\text{Tr } \hat{\rho}_M(t)^2 \sim \widetilde{\text{Tr}} \left\{ \left(\prod_{k=1}^n \prod_{\mu=1_f, 2_f} \prod_{c=+, -} e^{-i\Delta t \hat{H}_{M, \mu, c}(t_k)} \right) \hat{\rho}(0)_{1_f, +} \hat{\rho}(0)_{2_f, +} \hat{C}_{1 \rightarrow 4}^{(1_f, +), (1_f, -), (2_f, +), (2_f, -)} \right\}. \tag{242}$$

In this expression, we have introduced indices

$(\mu, c) = \{(1_f, +), (1_f, -), (2_f, +), (2_f, -)\}$ to differentiate the four copies of fermions in the enlarged space. Additionally, a superscript has been added to the permutation operator $\hat{C}_{1 \rightarrow 4}^{(1_f, +), (1_f, -), (2_f, +), (2_f, -)}$ to indicate its operation in this enlarged space. The Hamiltonian $\hat{H}_{M, \mu, c}(t_k)$ is expressed as follows:

$$\begin{aligned}
 \hat{H}_{M, \mu, c}(t_k) &= \frac{1}{2} \sum_{j=1}^L \sum_{r, r'=1}^N \left(\hat{c}_{\mu, c, j, r}^\dagger \quad \hat{c}_{\mu, c, j, r} \right) \begin{pmatrix} A_{M, j}(t_k)^{rr'} & B_{M, j}(t_k)^{rr'} \\ C_{M, j}(t_k)^{rr'} & -A_{M, j}^T(t_k)^{rr'} \end{pmatrix} \begin{pmatrix} \hat{c}_{\mu, c, j, r'} \\ \hat{c}_{\mu, c, j, r'}^\dagger \end{pmatrix} \\
 &= \frac{1}{2} \sum_{j=1}^L \sum_{r, r'=1}^N \sum_{\eta, \eta'=p, h} \hat{\Psi}_{\mu, c, j, \eta, r} \widetilde{M}_j(t_k)_{\eta \eta'}^{rr'} \hat{\Psi}_{j, \eta', r'; \mu, c}.
 \end{aligned} \tag{243}$$

The definitions of $\hat{\Psi}_{\mu,c;j,\eta,r}$ and $\hat{\Psi}_{j,\eta',r';\mu,c}$ can be determined by comparing the two forms of $\hat{H}_{M,\mu,c}(t_k)$ presented above, and applying the relation:

$$\begin{pmatrix} \widetilde{M}_j(t)_{pp} & \widetilde{M}_j(t)_{ph} \\ \widetilde{M}_j(t)_{hp} & \widetilde{M}_j(t)_{hh} \end{pmatrix} = \begin{pmatrix} A_{M,j}(t) & B_{M,j}(t) \\ C_{M,j}(t) & -A_{M,j}^T(t) \end{pmatrix}. \quad (244)$$

2. The term $\text{Tr } \hat{\varrho}_M(t)$ in the numerator

We have previously expressed $\text{Tr } \hat{\varrho}_M(t)$ in discrete time in equation (238). Here, we present it again with a slight modification: we introduce an additional index 3_f for the fermionic operators, as shown below:

$$\text{Tr } \hat{\varrho}_M(t) \sim \widetilde{\text{Tr}} \left\{ \left(\prod_{k=1}^n \prod_{c=+,-} e^{-i\Delta t \hat{H}_{M,3_f,c}(t_k)} \right) \hat{\rho}(0)_{3_f,+} \hat{S}^{3_f;+,-} \right\}. \quad (245)$$

In this expression, we have added a superscript to the swap operator $\hat{S}^{3_f;+,-}$ to indicate that it operates within this enlarged space.

3. The term $(\text{Tr } \hat{\varrho}_M(t))^2$ in the denominator

We have reached the point where we will utilize the discussion in Section 8.3.1 to express $(\text{Tr } \hat{\varrho}_M(t))^2$ in the denominator as a trace over bosonic Fock space, applying the result from (233) as demonstrated below³⁸³⁹:

$$(\text{Tr } \hat{\varrho}_M(t))^{-2} \sim \widetilde{\text{Tr}} \left\{ \left(\prod_{k=1}^n \prod_{c=+,-} e^{-i\Delta t \hat{H}_{M,B,c}(t_k)} \right) \hat{\rho}(0)_{B,+} (-1)^{\hat{n}_{B,-}} \hat{S}^{B;+,-} \right\}. \quad (246)$$

Here, $\widetilde{\text{Tr}}$ represents the trace over the enlarged bosonic Fock space created by taking two copies, denoted as $+$ and $-$, while $\hat{S}^{B;+,-}$ denotes the swap operator acting within this space. Using equation (227), the Hamiltonian $\hat{H}_{M,B,c}(t_k)$ in the equation above can be expressed as follows:

$$\hat{H}_{M,B,c}(t_k) = \hat{H}_{M,1B,c}(t_k) + \hat{H}_{M,2B,c}(t_k), \quad (247)$$

³⁸It is worth noting that the ‘‘Hamiltonian’’ needs to be quadratic for the result (233) to be applicable, and that condition is met in this instance.

³⁹To utilize the result, we also assume that the measurement process is independent across different time slices and lattice sites, and that the averaging \mathbb{E}_M employs the same probability distribution for these different time slices and lattice sites, as will be discussed in the following Section 8.3.3.

where $\hat{H}_{M,1B,c}(t_k)$ and $\hat{H}_{M,2B,c}(t_k)$ are defined as:

$$\begin{aligned}
 \hat{H}_{M,1B,c}(t_k) &= \frac{1}{2} \sum_{j=1}^L \sum_{r,r'=1}^N \left(\hat{b}_{1_b,c,j,r}^\dagger \quad -\hat{b}_{2_b,c,j,r} \right) \begin{pmatrix} A_{M,j}(t_k)^{rr'} & B_{M,j}(t_k)^{rr'} \\ C_{M,j}(t_k)^{rr'} & -A_{M,j}^T(t_k)^{rr'} \end{pmatrix} \begin{pmatrix} \hat{b}_{1_b,c,j,r'} \\ \hat{b}_{2_b,c,j,r'}^\dagger \end{pmatrix} \\
 &= \frac{1}{2} \sum_{j=1}^L \sum_{r,r'=1}^N \sum_{\eta,\eta'=p,h} \hat{\Psi}_{1B,c;j,\eta,r} \widetilde{M}_j(t_k)_{\eta\eta'}^{rr'} \hat{\Psi}_{j,\eta',r';1B,c} , \\
 \hat{H}_{M,2B,c}(t_k) &= \frac{1}{2} \sum_{j=1}^L \sum_{r,r'=1}^N \left(\hat{b}_{2_b,c,j,r}^\dagger \quad \hat{b}_{1_b,c,j,r} \right) \begin{pmatrix} A_{M,j}(t_k)^{rr'} & B_{M,j}(t_k)^{rr'} \\ C_{M,j}(t_k)^{rr'} & -A_{M,j}^T(t_k)^{rr'} \end{pmatrix} \begin{pmatrix} \hat{b}_{2_b,c,j,r'} \\ -\hat{b}_{1_b,c,j,r'}^\dagger \end{pmatrix} \\
 &= \frac{1}{2} \sum_{j=1}^L \sum_{r,r'=1}^N \sum_{\eta,\eta'=p,h} \hat{\Psi}_{2B,c;j,\eta,r} \widetilde{M}_j(t_k)_{\eta\eta'}^{rr'} \hat{\Psi}_{j,\eta',r';2B,c} .
 \end{aligned} \tag{248}$$

By combining all three terms, we can now express the second Rényi entropy in a concise form as follows:

$$\begin{aligned}
 \mathbb{E}[e^{-S_2(t)}] &= \mathbb{E}_M \left[\widetilde{\text{Tr}} \left\{ \left(\prod_{k=1}^n e^{-\frac{i}{2} \Delta t \sum_{j=1}^L \sum_{r,r'=1}^N \sum_{\eta,\eta'=p,h} \sum_{\kappa} \hat{\Psi}_{\kappa;j,\eta,r} \widetilde{M}_j(t_k)_{\eta\eta'}^{rr'} \hat{\Psi}_{j,\eta',r';\kappa}} \right) \right. \right. \\
 &\quad \left. \left. \hat{\rho}(0)_{F,+} \hat{\rho}(0)_{B,+} (-1)^{\hat{n}_{B,-}} \hat{C}_{1 \rightarrow 4}^{(1_f,+),(1_f,-),(2_f,+),(2_f,-)} \hat{S}_{3_f;+,-} \hat{S}_{B;+,-} \right\} \right],
 \end{aligned} \tag{249}$$

where the summation over κ encompasses the set

$\{(1_f, +), (1_f, -), (2_f, +), (2_f, -), (3_f, +), (3_f, -), (1_B, +), (1_B, -), (2_B, +), (2_B, -)\}$ and accounts for the contributions from all three terms mentioned above. Additionally, $\hat{\rho}(0)_{F,+}$ is a shorthand for $\hat{\rho}(0)_{1_f,+} \hat{\rho}(0)_{2_f,+} \hat{\rho}(0)_{3_f,+}$, and $\hat{n}_B = \hat{n}_{1_b} + \hat{n}_{2_b}$. Here $\widetilde{\text{Tr}}$ represents the trace over the enlarged space that combines all the fermionic and bosonic species.

Having expressed the second Rényi entropy using the supersymmetry technique in discrete time, the next step is to perform the average over the measurements, denoted by \mathbb{E}_M , which will be addressed in the following section.

8.3.3 Averaging Over Random Measurement Outcomes

Up until now, we have delayed discussing the procedure for performing \mathbb{E}_M , which entails specifying the probability distribution associated with averaging the random measurement outcomes. A review of the literature reveals that the Gaussian probability distribution is the most frequently employed choice, primarily due to its mathematical tractability. This choice is generally acceptable within the context of the replica trick, where the focus is solely on expressions involving fermionic operators. In contrast, our approach uses supersymmetry techniques, which require careful consideration of convergence when dealing with expressions involving bosons. Specifically, in our case, since the measurement process is non-unitary, utilizing a Gaussian probability distribution is inappropriate, as it can result in divergent expressions. To clarify this point, we first examine a simpler example before addressing our main problem.

Example

Consider the following expression:

$$\text{Tr} e^{-E\hat{b}^\dagger\hat{b}} \Big|_{\text{Boson}}, \quad (250)$$

where E is a real-valued random variable ($E \in \mathbb{R}$). Suppose the probability distribution of E is Gaussian, which allows E to take both positive and negative values. However, negative values of E lead to a divergent sum. To demonstrate this, we explicitly compute the trace:

$$\text{Tr} e^{-E\hat{b}^\dagger\hat{b}} \Big|_{\text{Boson}} = 1 + e^{-E} + e^{-2E} + e^{-3E} + \dots \quad (251)$$

For the series to converge, the following condition must be satisfied:

$$e^{-E} < 1. \quad (252)$$

This inequality holds only when $E > 0$. Consequently, for $E < 0$, the series diverges, indicating that a Gaussian distribution is inappropriate in this context due to its support over negative values of E .

To avoid this divergence, the probability distribution for E should exclude negative values. One potential solution is to truncate the negative part of the Gaussian distribution. For example, a chi-squared distribution [76] with parameter χ could be considered. However, even this distribution proves inadequate for our specific case.

To explain why, let us first outline the chi-squared distribution. Consider the following expression:

$$\text{Tr} e^{-\sum_{u,v=1}^N \hat{b}_u^\dagger H_{uv} \hat{b}_v} \Big|_{\text{Boson}}, \quad (253)$$

where H is a Hermitian matrix and is treated as a random variable. Following the reasoning from the previous example, we require $H > 0$ for the above trace to converge. Thus, we adopt a chi-squared distribution with the following probability measure:

$$(\text{const.}) \text{Det}^\chi(H) \exp\left(-\frac{\text{Tr} H}{2\sigma^2}\right) d\mu(H), \quad (254)$$

where (const.) denotes the normalization factor, and σ is a scalar. In this probability measure, $H = H^\dagger > 0$ and the integration measure $d\mu(H)$ is defined over $\text{GL}(N, \mathbb{C})/U(N)$ [1]. This can be understood as follows. One way to realise $H = H^\dagger > 0$ is to express it as $H = gg^\dagger > 0$, where $g \in \text{GL}(N, \mathbb{C})$. However, this is not the full picture. We can perform the transformation $g \rightarrow gh$, where $h \in U(N)$, without altering H , as shown below:

$$(gh)(gh)^\dagger = g(hh^\dagger)g^\dagger = g(1)g^\dagger = gg^\dagger. \quad (255)$$

Thus, the integration domain for H is $\text{GL}(N, \mathbb{C})/U(N)$. While this probability measure may

be appropriate for systems in symmetry class A, it is not suitable for symmetry class D. One characteristic of Hamiltonians in symmetry class D is that they are traceless, implying the absence of the exponential decay factor in the probability measure. This factor is crucial for normalizing the distribution, meaning this probability measure cannot be applied in our case. Nonetheless, the insights from this discussion will guide us as we construct the probability measure suited to our problem.

Following the discussion of the two examples above, we now revisit the main problem. The key assumption here is that the measurement process is uncorrelated between different time slices and lattice sites. Under this assumption, we will outline the averaging process for the measurement random variables at a single chosen lattice site and time slice, with the understanding that the same procedure applies uniformly across all other lattice sites and time slices. Thus, we proceed by performing the averaging on the following expression:

$$\mathbb{E}_M \left(e^{-i\Delta t \sum_{r,r'=1}^N \sum_{\eta,\eta'=p,h} \sum_{\kappa} \hat{\Psi}_{\kappa;j,\eta,r} \widetilde{M}_j(t_k)_{\eta\eta'}^{rr'} \hat{\Psi}_{j,\eta',r';\kappa}} \right). \quad (256)$$

The matrix $i\widetilde{M}_j(t_k)$ belongs to $i \cdot so(2N, \mathbb{R})$. Based on the discussion in the previous examples, to ensure that the above expression is convergent in the context of bosons, we must impose certain constraints on the Lie algebra space that the matrix $i\widetilde{M}_j(t_k)$ can explore. Specifically, it must be restricted to the positive convex cone within $i \cdot so(2N, \mathbb{R})$, meaning that $iA_{M,j}(t_k) > 0$.

Additionally, it is necessary to ensure that the off-diagonal blocks $iB_{M,j}(t_k)$ and $iC_{M,j}(t_k)$ remain sufficiently small compared to the diagonal block $iA_{M,j}(t_k)$, in order to preserve the matrix's position within the positive convex cone in $i \cdot so(2N, \mathbb{R})$.

Let us now formalize these conditions with an explicit mathematical description. Before proceeding, we introduce a slight change in notation: henceforth, we will omit the time index t_k and the lattice site index j to avoid excessive indexing.

The matrix $i\widetilde{M} = \begin{pmatrix} iA_M & iB_M \\ -iB_M^\dagger & -iA_M^T \end{pmatrix}$ is in $i \cdot so(2N, \mathbb{R})$, and can be diagonalized using a matrix g that satisfies the condition $(g^{-1})^\dagger = g = \Sigma_1(g^{-1})^T \Sigma_1$. This transformation can be expressed as follows:

$$i\widetilde{M} = M_H = \begin{pmatrix} iA_M & iB_M \\ -iB_M^\dagger & -iA_M^T \end{pmatrix} = g \begin{pmatrix} \lambda & 0 \\ 0 & -\lambda \end{pmatrix} g^{-1} = gDg^{-1}, \quad (257)$$

where $\lambda = \text{diag}(\lambda_1, \dots, \lambda_N)$. To ensure that M_H resides in the positive convex cone of $i \cdot so(2N, \mathbb{R})$, and that the expression in (256) is well-defined, the following condition must be satisfied:

$$\lambda_r > 0, \quad r = 1, \dots, N. \quad (258)$$

Given the aforementioned constraint, and drawing inspiration from the discussion on the

chi-squared distribution, we propose the following probability measure for the computation of the average \mathbb{E}_M :

$$(\text{const.}) \text{Det}^\chi(M_H) \exp\left(-\frac{1}{2\sigma^2} \text{Tr} M_H^2\right) d\mu(M_H) \Big|_{\lambda>0}. \quad (259)$$

The key observation here is that instead of using $\text{Tr} M_H$ in the exponential, we are using $\text{Tr} M_H^2$. This change is necessary because, as previously noted, $\text{Tr} M_H = 0$. To ensure the probability measure has a decaying factor that allows for proper normalization, one obvious choice is to substitute $\text{Tr} M_H$ with $\text{Tr} M_H^2$.

The expression for $\text{Tr} M_H^2$ is given by:

$$\text{Tr} M_H^2 = \sum_{r=1}^N 2(B_M^\dagger B_M - A_M^2)^{rr}. \quad (260)$$

Another important point to note is that the measure in equation (259) is constrained by the condition specified in (258). For the measure $d\mu(M_H)$, we use the fact that the Lie algebra can be regarded as a vector space, allowing us to use the Lebesgue measure [77, 74, 78] to define $d\mu(D)$:

$$d\mu(D) = \prod_{r=1}^N d\lambda_r. \quad (261)$$

By using the expression for $d\mu(D)$ along with the expression for M_H as provided in (257), the Lebesgue measure [77, 74, 78] with respect to the variables M_H reads:

$$d\mu(M_H) = dg \prod_{r=1}^N d\lambda_r \prod_{r<r'} (\lambda_r^2 - \lambda_{r'}^2)^2, \quad (262)$$

where dg represents the Haar measure on $SO(2N, \mathbb{R})$. We can now proceed to define the expression in equation (256) as follows:

$$\begin{aligned} & \mathbb{E}_M \left(e^{-\Delta t \sum_{r,r'=1}^N \sum_{\eta,\eta'=p,h} \sum_{\kappa} \hat{\Psi}_{\kappa;\eta,r}(M_H)_{\eta\eta'}^{rr'} \hat{\Psi}_{\eta',r';\kappa}} \right) \\ &= (\text{const.}) \int_{SO(2N,\mathbb{R})} dg \int_{\lambda>0} \prod_{r=1}^N d\lambda_r \prod_{r<r'} (\lambda_r^2 - \lambda_{r'}^2)^2 \text{Det}^\chi(M_H) \exp\left(-\frac{1}{2\sigma^2} \text{Tr} M_H^2\right) \\ & \quad e^{-\Delta t \sum_{r,r'=1}^N \sum_{\eta,\eta'=p,h} \sum_{\kappa} \hat{\Psi}_{\kappa;\eta,r}(M_H)_{\eta\eta'}^{rr'} \hat{\Psi}_{\eta',r';\kappa}}. \end{aligned} \quad (263)$$

The argument of the exponential $\sum_{r,r'=1}^N \sum_{\eta,\eta'=p,h} \sum_{\kappa} \hat{\Psi}_{\kappa;\eta,r}(M_H)_{\eta\eta'}^{rr'} \hat{\Psi}_{\eta',r';\kappa}$ can be

reformulated as follows:

$$\begin{aligned} \sum_{r,r'=1}^N \sum_{\eta,\eta'=p,h} \sum_{\kappa} \widehat{\Psi}_{\kappa;\eta,r} (M_H)_{\eta\eta'}^{rr'} \widehat{\Psi}_{\eta',r';\kappa} &= \sum_{r,r'=1}^N \sum_{\eta,\eta'=p,h} \sum_{\kappa} (M_H)_{\eta\eta'}^{rr'} \widehat{\Psi}_{\eta',r';\kappa} \widehat{\Psi}_{\kappa;\eta,r} = \text{Tr} (M_H P) \\ &= \text{Tr} (g D g^{-1} P), \end{aligned} \quad (264)$$

where $\widehat{\Psi}_{\kappa;\eta,r}$ is defined by taking $\widehat{\Psi}_{\kappa;\eta,r}$ and multiplying all the fermionic operators within it by -1 . In the last equality, we have used equation (257). The matrix P has elements defined by:

$$P_{\eta'\eta,r'r} = \sum_{\kappa} \widehat{\Psi}_{\eta',r';\kappa} \widehat{\Psi}_{\kappa;\eta,r}. \quad (265)$$

It can be shown that P belongs to $so(2N, \mathbb{C})$ Lie algebra.

By substituting the expression (264) into equation (263), and applying the identities $\text{Det}^\chi (M_H) = \text{Det}^\chi (g D g^{-1}) = \text{Det}^\chi (D)$ and $\text{Tr} M_H^2 = \text{Tr} D^2$, we can reformulate equation (263) as follows:

$$\begin{aligned} \mathbb{E}_M \left(e^{-\Delta t \sum_{r,r'=1}^N \sum_{\eta,\eta'=p,h} \sum_{\kappa} \widehat{\Psi}_{\kappa;\eta,r} (M_H)_{\eta\eta'}^{rr'} \widehat{\Psi}_{\eta',r';\kappa}} \right) \\ = (\text{const.}) \int_{\lambda>0} \prod_{r=1}^N d\lambda_r \prod_{r<r'} (\lambda_r^2 - \lambda_{r'}^2)^2 \text{Det}^\chi (D) \exp \left(-\frac{1}{2\sigma^2} \text{Tr} D^2 \right) \int_{SO(2N, \mathbb{R})} dg e^{-\Delta t \text{Tr} (g D g^{-1} P)}. \end{aligned} \quad (266)$$

The integral over g can be evaluated using the Itzykson-Zuber integral⁴⁰ for $SO(2N, \mathbb{R})$ [80, 81, 78, 79]. This integral is expressed as follows:

$$\int_{SO(2N)} dg e^{-\Delta t \text{Tr} (g D g^{-1} P)} = (\text{const.}) \sum_{\hat{\pi} \in W[SO(2N, \mathbb{R})]} \frac{(-1)^{|\hat{\pi}|} e^{-\Delta t \text{Tr} (g D g^{-1} \hat{\pi}(P))}}{V(D)V(P)}, \quad (267)$$

where $W[SO(2N, \mathbb{R})]$ represents the Weyl group⁴¹. The action of $\hat{\pi}$ on P is defined as: $\hat{\pi}P := \pi P \pi^{-1}$, with $\pi \in SO(2N, \mathbb{R})$. The notation $|\hat{\pi}| = 0, 1$ denotes the parity of $\hat{\pi}$. $V(D)$ and $V(P)$ denote the generalized Vandermonde determinants of D and P , respectively.⁴² For a diagonal matrix D , the Vandermonde determinant simplifies to $V(D) = \prod_{r<r'} (\lambda_r^2 - \lambda_{r'}^2)$.

The right-hand side of equation (267) can be represented as a function of P , denoted by $f(P_{\eta'\eta,r'r}) = f(\sum_{\kappa} \widehat{\Psi}_{\eta',r';\kappa} \widehat{\Psi}_{\kappa;\eta,r})$. Based on this, we assert two key points:

⁴⁰An interpretation of the Itzykson-Zuber integral is as follows [79]: the right-hand side of integral (267) may be regarded as the stationary-phase approximation for the left-hand side, with stationary points represented by the elements $\hat{\pi} \in W[SO(2N, \mathbb{R})]$.

⁴¹Let G denote a connected compact semisimple Lie group. Let \mathcal{T} be a maximal torus in $\text{Lie}(G)$. The normalizer of \mathcal{T} is defined as: $N_G(\mathcal{T}) = \{g \in G | g t g^{-1} \in \mathcal{T}, \forall t \in \mathcal{T}\}$. The centralizer of \mathcal{T} is defined as: $Z_G(\mathcal{T}) = \{g \in G | g t g^{-1} = t, \forall t \in \mathcal{T}\}$. The Weyl group $W[G]$ [82] of G is defined as the quotient of the normalizer of the Cartan subalgebra by its centralizer: $W[G] = N_G(\mathcal{T})/Z_G(\mathcal{T})$.

⁴²It is noteworthy that the Vandermonde determinant is invariant under conjugation by elements of the Lie group; specifically, $V(P) = V(g P g^{-1})$, for $g \in SO(2N, \mathbb{R})$.

1. On general grounds⁴³, one anticipates the existence of a function F of quadratic invariants $\sum_{r,\eta} \bar{\Psi}_{\kappa;\eta,r} \Psi_{\eta,r;\kappa'}$ such that

$$f\left(\sum_{\kappa} \Psi_{\eta',r';\kappa} \bar{\Psi}_{\kappa;\eta,r}\right) = F\left(\sum_{r,\eta} \bar{\Psi}_{\kappa;\eta,r} \Psi_{\eta,r;\kappa'}\right). \quad (268)$$

2. Furthermore, note that in equation (268), the bosonic and fermionic operators have been replaced with complex bosonic and fermionic variables (i.e., $\hat{\Psi}_{\kappa;\eta,r} \hat{\Psi}_{\eta,r;\kappa'} \rightarrow \bar{\Psi}_{\kappa;\eta,r} \Psi_{\eta,r;\kappa'}$). We assume that in the large N -limit, these operators can be approximated by complex bosonic and fermionic variables, with corrections of the order of $\frac{1}{N}$, stemming from the (anti-)commutation relations, which are neglected in the first approximation.

The immediate question arises: what is the precise form of the function F ? Although we do not possess an exact answer, we argue that determining the precise form of F is not crucial. The ultimate objective is to capture the universal physics of entanglement phase transitions in class D systems. According to the principle of universality, the result should not depend heavily on the microscopic details of the model. Therefore, we propose choosing a function F of the quadratic invariants $\sum_{r,\eta} \bar{\Psi}_{\kappa;\eta,r} \Psi_{\eta,r;\kappa'}$ that provides a sufficiently accurate description of the problem, without requiring its exact form. However, care must be taken to ensure that the function is well-defined and free from convergence issues. Under these conditions, it should be possible to employ the superbosonization technique, as F is a function of quadratic invariants, and reformulate the theory using the new variables introduced by this formula.

At this point, we acknowledge that further progress has not been made, and we leave this for future investigation. What we have accomplished is a suggestion for reformulating the theory, providing a different starting point for analyzing the system. The way forward would involve selecting an appropriate form for the function F and using it to explore the phase diagram of the system in relation to entanglement phase transitions. Below, we summarize the main results of this chapter.

8.4 Summary

In this chapter, we investigated monitored free fermion systems belonging to symmetry class D by utilizing the supersymmetry technique. The second Rényi entropy served as the focus for illustrating our method, which we expressed in terms of bosonic and fermionic operators. We then focused on the measurement-only model case ($J = 0$)⁴⁴, and introduced a new approach for averaging over the measurement outcomes. By “new”, we refer to employing a

⁴³We draw upon a result from classical invariant theory [28], which is also mentioned in the discussion of the superbosonization formula in Section 6.2, and assume that the function f is invariant under $O(2N, \mathbb{C})$, which implies the existence of F .

⁴⁴To extend this analysis to the case where $J \neq 0$, we suggest following the approach outlined in this chapter. For averaging over the random variables J , we propose using a Gaussian distribution, as it does not encounter convergence problems. The reason is that this part of the Hamiltonian contributes to unitary evolution, unlike the measurement part, which affects “non-unitary” evolution and requires more caution. We specifically examined the measurement-only model to illustrate our ideas, but the core discussion remains valid when $J \neq 0$.

probability distribution different from the conventional Gaussian one commonly used in the literature, motivated by the need to avoid divergence issues when working with bosons.

Finally, by utilizing the concepts of universality and scaling, we proposed a reformulation of the theory, which offers an alternative method for analyzing the system and examining its phase diagram. We plan to address the further development of this approach in future research.

9 Conclusion from the Second Project

This chapter concludes the second project of this thesis, providing a summary of the key findings and suggesting potential avenues for future research. The focus of this project has been on strongly disordered systems within symmetry class D, as defined by the Altland-Zirnbauer classification [3] for non-interacting fermions. This exploration was inspired by prior work in [4, 5, 6], which proposed a novel spontaneous symmetry breaking phenomenon in disordered systems of symmetry class A. Our goal was to investigate whether similar phenomena could also be observed in class D systems.

The primary analytical tool employed in this study was the superbosonization formula, introduced in [1, 2], which has not been extensively explored in the literature. This approach was chosen as an alternative to the more conventional Hubbard-Stratonovich transformation, which is typically applied to weakly disordered systems. Given the strongly disordered nature of the systems we studied, superbosonization proved more suitable for our analysis.

We began by formulating the supersymmetric field theory for general strongly disordered class D systems without focusing on a specific model. This allowed us to explore the solution space in the limit of strong disorder, or more precisely, as the disorder strength approaches infinity. In this regime, we observed that the dominant contributions to the field integral arise from the nilpotent orbit, where the invariant metric degenerates. This result aligns with previous findings in symmetry class A systems, which served as the foundation for the proposed novel spontaneous symmetry breaking phenomenon in those systems [4, 5, 6]. However, to conclusively observe such symmetry breaking in class D, further investigation using a specific model is needed to examine the associated phases.

Subsequently, we focused on a particular system to continue investigating the potential for a novel spontaneous symmetry breaking phenomenon in class D. Specifically, we studied monitored free fermions within this symmetry class that exhibit measurement-induced entanglement phase transitions. Our approach differed from traditional methods like the replica trick by utilizing supersymmetry. Finally, we proposed a reformulation of the theory through the introduction of new variables based on the original model's variables, offering a fresh perspective for analyzing the system. Future work will involve applying this reformulated theory to study the phase diagram in greater depth, with the goal of offering new insights into the “critical phase” discussed in the literature.

In summary, this thesis has introduced an alternative approach based on superbosonization for examining disordered systems within symmetry class D. Although the progress made toward uncovering a potential novel spontaneous symmetry breaking phenomenon has been modest, the groundwork has been laid, and we believe this approach holds promise for further exploration. While much remains to be understood, the methods discussed here offer a fresh perspective that could prove valuable not only in this context but also in tackling other challenging problems. For instance, the two-dimensional random bond Ising model, which has primarily been explored under weak disorder [83, 84], could gain from these new

perspectives, especially with the growing interest [85] in studying disorder beyond just the weak regime. We remain hopeful that the ideas presented in this thesis will inspire deeper investigation and provide a foundation for advancing our understanding of strongly disordered class D systems.

REFERENCES

References

- [1] P. Littelmann, H.J. Sommers, and M.R. Zirnbauer. “Superbosonization of Invariant Random Matrix Ensembles.” In: *Commun. Math. Phys.* 283, 343–395 (2008). URL: <https://doi.org/10.1007/s00220-008-0535-0>.
- [2] J. E. Bunder et al. “Superbosonization Formula and its Application to Random Matrix Theory”. In: *J Stat Phys* 129, 809–832 (2007). URL: <https://doi.org/10.1007/s10955-007-9405-y>.
- [3] Alexander Altland and Martin R. Zirnbauer. “Nonstandard symmetry classes in mesoscopic normal-superconducting hybrid structures”. In: *Phys. Rev. B* 55 (2 Jan. 1997), pp. 1142–1161. DOI: 10.1103/PhysRevB.55.1142. URL: <https://link.aps.org/doi/10.1103/PhysRevB.55.1142>.
- [4] Martin R. Zirnbauer. “The integer quantum Hall plateau transition is a current algebra after all”. In: *Nuclear Physics B* 941 (2019), pp. 458–506. ISSN: 0550-3213. DOI: 10.1016/j.nuclphysb.2019.02.017. URL: <https://www.sciencedirect.com/science/article/pii/S0550321319300458>.
- [5] J. Arenz and M. R. Zirnbauer. *Wegner model on a tree graph: $U(1)$ symmetry breaking and a non-standard phase of disordered electronic matter*. 2023. arXiv: 2305.00243 [cond-mat.dis-nn]. URL: <https://arxiv.org/abs/2305.00243>.
- [6] Martin R. Zirnbauer. *Wegner model in high dimension: $U(1)$ symmetry breaking and a non-standard phase of disordered electronic matter, I. One-replica theory*. 2023. arXiv: 2309.17323 [cond-mat.dis-nn]. URL: <https://arxiv.org/abs/2309.17323>.
- [7] P. W. Anderson. “More Is Different”. In: *Science* 177.4047 (1972), pp. 393–396. DOI: 10.1126/science.177.4047.393. eprint: <https://www.science.org/doi/pdf/10.1126/science.177.4047.393>. URL: <https://www.science.org/doi/abs/10.1126/science.177.4047.393>.
- [8] J. Bardeen, L. N. Cooper, and J. R. Schrieffer. “Theory of Superconductivity”. In: *Phys. Rev.* 108 (5 Dec. 1957), pp. 1175–1204. DOI: 10.1103/PhysRev.108.1175. URL: <https://link.aps.org/doi/10.1103/PhysRev.108.1175>.
- [9] Eduardo Fradkin. *Field Theories of Condensed Matter Physics*. 2nd ed. Cambridge University Press, 2013.
- [10] A.O. Gogolin, A.A. Nersesyan, and A.M. Tsvelik. *Bosonization and Strongly Correlated Systems*. Cambridge University Press, 2004. ISBN: 9780521617192. URL: <https://books.google.de/books?id=BZDfFIpCoaAC>.
- [11] H. Bethe. “Zur Theorie der Metalle.” In: *Z. Physik* 71, 205–226 (1931). URL: <https://doi.org/10.1007/BF01341708>.
- [12] Murray T. Batchelor. “The Bethe ansatz after 75 years”. In: *Physics Today* 60.1 (Jan. 2007), pp. 36–40. ISSN: 0031-9228. DOI: 10.1063/1.2709557. eprint: https://pubs.aip.org/physicstoday/article-pdf/60/1/36/16652607/36_1_online.pdf. URL: <https://doi.org/10.1063/1.2709557>.

- [13] P. Jordan and E. Wigner. “Über das Paulische Äquivalenzverbot”. In: *Z. Physik* 47 (1928), pp. 631–651. DOI: [10.1007/BF01331938](https://doi.org/10.1007/BF01331938).
- [14] M. Stone. *Bosonization*. Bosonization. World Scientific, 1994. ISBN: 9789810218478. URL: <https://books.google.de/books?id=PFx-tWFiEBcC>.
- [15] Sin-itiro Tomonaga. “Remarks on Bloch’s Method of Sound Waves applied to Many-Fermion Problems”. In: *Progress of Theoretical Physics* 5, 4 (1950), pp. 544–569. DOI: <https://doi.org/10.1143/ptp/5.4.544>.
- [16] JM Luttinger. “An exactly soluable model of a many-fermion system”. In: *J Math Phys* 4, 9 (1963). DOI: <https://doi.org/10.1063/1.1704046>.
- [17] DC Mattis and EH Lieb. “Exact Solution of a Many-Fermion System and Its Associated Boson Field”. In: *J Math Phys* 6, 2 (1965), pp. 544–569. DOI: <https://doi.org/10.1063/1.1704281>.
- [18] Sidney Coleman. “Quantum sine-Gordon equation as the massive Thirring model”. In: *Phys. Rev. D* 11 (8 Apr. 1975), pp. 2088–2097. DOI: [10.1103/PhysRevD.11.2088](https://doi.org/10.1103/PhysRevD.11.2088). URL: <https://link.aps.org/doi/10.1103/PhysRevD.11.2088>.
- [19] S. Mandelstam. “Soliton operators for the quantized sine-Gordon equation”. In: *Phys. Rev. D* 11 (10 May 1975), pp. 3026–3030. DOI: [10.1103/PhysRevD.11.3026](https://doi.org/10.1103/PhysRevD.11.3026). URL: <https://link.aps.org/doi/10.1103/PhysRevD.11.3026>.
- [20] Daniel C Mattis. “New wave-operator identity applied to the study of persistent currents in 1D”. In: *Journal of Mathematical Physics* 15.5 (1974), pp. 609–612.
- [21] A. Luther and I. Peschel. “Single-particle states, Kohn anomaly, and pairing fluctuations in one dimension”. In: *Phys. Rev. B* 9 (7 Apr. 1974), pp. 2911–2919. DOI: [10.1103/PhysRevB.9.2911](https://doi.org/10.1103/PhysRevB.9.2911). URL: <https://link.aps.org/doi/10.1103/PhysRevB.9.2911>.
- [22] F D M Haldane. “‘Luttinger liquid theory’ of one-dimensional quantum fluids. I. Properties of the Luttinger model and their extension to the general 1D interacting spinless Fermi gas”. In: *J. Phys. C: Solid State Phys.* 14, 2585 (1981). DOI: [10.1088/0022-3719/14/19/010](https://doi.org/10.1088/0022-3719/14/19/010).
- [23] E. Witten. “Non-abelian bosonization in two dimensions”. In: *Commun. Math. Phys.* 92 (1984), pp. 455–472. DOI: [10.1007/BF01215276](https://doi.org/10.1007/BF01215276).
- [24] A. Polyakov and P.B. Wiegmann. “Theory of nonabelian goldstone bosons in two dimensions”. In: *Physics Letters B* 131.1 (1983), pp. 121–126. ISSN: 0370-2693. DOI: [10.1016/0370-2693\(83\)91104-8](https://doi.org/10.1016/0370-2693(83)91104-8). URL: <https://www.sciencedirect.com/science/article/pii/0370269383911048>.
- [25] V.G. Knizhnik and A.B. Zamolodchikov. “Current algebra and Wess-Zumino model in two dimensions”. In: *Nuclear Physics B* 247.1 (1984), pp. 83–103. ISSN: 0550-3213. DOI: [10.1016/0550-3213\(84\)90374-2](https://doi.org/10.1016/0550-3213(84)90374-2). URL: <https://www.sciencedirect.com/science/article/pii/0550321384903742>.

- [26] I. Affleck. “Critical Behavior of Two-Dimensional Systems with Continuous Symmetries”. In: *Phys. Rev. Lett.* 55, 1355 (1985). DOI: 10.1103/PhysRevLett.55.1355. URL: <https://link.aps.org/doi/10.1103/PhysRevLett.55.1355>.
- [27] Yen-Ta Huang and Dung-Hai Lee. “Non-abelian bosonization in two and three spatial dimensions and applications”. In: *Nuclear Physics B* 972, 0550-3213 (2021), p. 115565. DOI: <https://doi.org/10.1016/j.nuclphysb.2021.115565>. URL: <https://www.sciencedirect.com/science/article/pii/S0550321321002625>.
- [28] R. Howe. “Remarks on classical invariant theory”. In: *TAMS* 313, 539–570 (1989).
- [29] Alexander Altland and Ben D. Simons. *Condensed Matter Field Theory*. 2nd ed. Cambridge University Press, 2010.
- [30] Alex Kamenev. *Field Theory of Non-Equilibrium Systems*. Cambridge University Press, 2011.
- [31] J. Rammer. *Quantum Field Theory of Non-equilibrium States*. Cambridge University Press, 2007.
- [32] Yoni BenTov. *Schwinger-Keldysh path integral for the quantum harmonic oscillator*. 2021. arXiv: 2102.05029 [hep-th]. URL: <https://arxiv.org/abs/2102.05029>.
- [33] B. Collins and P. Śniady. “Integration with Respect to the Haar Measure on Unitary, Orthogonal and Symplectic Group”. In: *Commun. Math. Phys.* 264 (2006), pp. 773–795. DOI: 10.1007/s00220-006-1554-3.
- [34] Subir Sachdev. “The Landscape of the Hubbard Model”. In: *String Theory and Its Applications*. WORLD SCIENTIFIC, Nov. 2011, pp. 559–620. DOI: 10.1142/9789814350525_0009. URL: http://dx.doi.org/10.1142/9789814350525_0009.
- [35] Fabian H. L. Essler et al. *The One-Dimensional Hubbard Model*. Cambridge University Press, 2005.
- [36] P. Di Francesco, P. Mathieu, and D. Sénéchal. *Conformal Field Theory*. Graduate texts in contemporary physics. Island Press, 1996. ISBN: 9781461222576. URL: <https://books.google.de/books?id=mcMbswEACAAJ>.
- [37] Paul Ginsparg. *Applied Conformal Field Theory*. 1988. arXiv: hep-th/9108028 [hep-th]. URL: <https://arxiv.org/abs/hep-th/9108028>.
- [38] *elements of nonequilibrium statistical mechanics*. Ane Books. ISBN: 9789380156255. URL: <https://books.google.de/books?id=TTxONJRNgFQC>.
- [39] J. Zinn-Justin and Oxford University Press. *From Random Walks to Random Matrices*. Oxford graduate texts. Oxford University Press, 2019. ISBN: 9780191829840. URL: <https://books.google.de/books?id=v0E7yQEACAAJ>.
- [40] I. Karatzas and S. Shreve. *Brownian Motion and Stochastic Calculus*. Graduate Texts in Mathematics (113) (Book 113). Springer New York, 1991. ISBN: 9780387976556. URL: https://books.google.de/books?id=ATNy_Zg3PSSC.

- [41] Leo P. Kadanoff. “The application of renormalization group techniques to quarks and strings”. In: *Rev. Mod. Phys.* 49 (2 Apr. 1977), pp. 267–296. DOI: 10.1103/RevModPhys.49.267. URL: <https://link.aps.org/doi/10.1103/RevModPhys.49.267>.
- [42] M. R. Zirnbauer. “Quantum Field Theory II”. In: *Lecture Notes* (2020/21). URL: https://www.thp.uni-koeln.de/zirn/011_Website_Martin_Zirnbauer/3_Teaching/MZ_lecture_notes.html.
- [43] F.D.M. Haldane. “Continuum dynamics of the 1-D Heisenberg antiferromagnet: Identification with the O(3) nonlinear sigma model”. In: *Physics Letters A* 93.9 (1983), pp. 464–468. ISSN: 0375-9601. DOI: 10.1016/0375-9601(83)90631-X. URL: <https://www.sciencedirect.com/science/article/pii/037596018390631X>.
- [44] F. D. M. Haldane. “Nonlinear Field Theory of Large-Spin Heisenberg Antiferromagnets: Semiclassically Quantized Solitons of the One-Dimensional Easy-Axis Néel State”. In: *Phys. Rev. Lett.* 50 (15 Apr. 1983), pp. 1153–1156. DOI: 10.1103/PhysRevLett.50.1153. URL: <https://link.aps.org/doi/10.1103/PhysRevLett.50.1153>.
- [45] FDM Haldane. ““ Θ physics” and quantum spin chains”. PhD thesis. American Institute of Physics, 1985.
- [46] Ian Affleck. “The quantum Hall effects, σ -models at $\Theta = \pi$ and quantum spin chains”. In: *Nuclear Physics B* 257 (1985), pp. 397–406. ISSN: 0550-3213. DOI: 10.1016/0550-3213(85)90353-0. URL: <https://www.sciencedirect.com/science/article/pii/0550321385903530>.
- [47] A Perelomov. “*Generalized Coherent States and their Applications*”. Berlin: Springer-Verlag, 1986.
- [48] Kevin E. Cahill and Roy J. Glauber. “Density operators for fermions”. In: *Phys. Rev. A* 59 (2 Feb. 1999), pp. 1538–1555. DOI: 10.1103/PhysRevA.59.1538. URL: <https://link.aps.org/doi/10.1103/PhysRevA.59.1538>.
- [49] “Glauber P-representations for fermions”. In: *Physica Scripta* 98.4 (Mar. 2023), p. 044006. DOI: 10.1088/1402-4896/acc432. URL: <https://dx.doi.org/10.1088/1402-4896/acc432>.
- [50] Patrick A. Lee, Naoto Nagaosa, and Xiao-Gang Wen. “Doping a Mott insulator: Physics of high-temperature superconductivity”. In: *Rev. Mod. Phys.* 78 (1 Jan. 2006), pp. 17–85. DOI: 10.1103/RevModPhys.78.17. URL: <https://link.aps.org/doi/10.1103/RevModPhys.78.17>.
- [51] Zheng Zhu, D. N. Sheng, and Ashvin Vishwanath. “Doped Mott insulators in the triangular-lattice Hubbard model”. In: *Phys. Rev. B* 105 (20 May 2022), p. 205110. DOI: 10.1103/PhysRevB.105.205110. URL: <https://link.aps.org/doi/10.1103/PhysRevB.105.205110>.
- [52] Ferdinand Evers and Alexander D. Mirlin. “Anderson transitions”. In: *Rev. Mod. Phys.* 80 (4 Oct. 2008), pp. 1355–1417. DOI: 10.1103/RevModPhys.80.1355. URL: <https://link.aps.org/doi/10.1103/RevModPhys.80.1355>.

- [53] Ilya Gruzberg. “Supersymmetry method in the study of disordered systems”. In: (Jan. 1998).
- [54] P. W. Anderson. “Absence of Diffusion in Certain Random Lattices”. In: *Phys. Rev.* 109 (5 Mar. 1958), pp. 1492–1505. DOI: 10.1103/PhysRev.109.1492. URL: <https://link.aps.org/doi/10.1103/PhysRev.109.1492>.
- [55] E. Abrahams et al. “Scaling Theory of Localization: Absence of Quantum Diffusion in Two Dimensions”. In: *Phys. Rev. Lett.* 42 (10 Mar. 1979), pp. 673–676. DOI: 10.1103/PhysRevLett.42.673. URL: <https://link.aps.org/doi/10.1103/PhysRevLett.42.673>.
- [56] F. Wegner. “The mobility edge problem: Continuous symmetry and a conjecture”. In: *Z. Physik B* 35, 207-210 (1979). DOI: 10.1007/BF01319839. URL: <https://doi.org/10.1007/BF01319839>.
- [57] K.B. Efetov. “Supersymmetry and theory of disordered metals”. In: *Advances in Physics* 32.1 (1983), pp. 53–127. DOI: 10.1080/00018738300101531. eprint: <https://doi.org/10.1080/00018738300101531>. URL: <https://doi.org/10.1080/00018738300101531>.
- [58] Alexander D. Mirlin. “Distribution of local density of states in disordered metallic samples: Logarithmically normal asymptotics”. In: *Phys. Rev. B* 53 (3 Jan. 1996), pp. 1186–1192. DOI: 10.1103/PhysRevB.53.1186. URL: <https://link.aps.org/doi/10.1103/PhysRevB.53.1186>.
- [59] Nigel Goldenfeld and Roger Haydock. “Phase diagram for Anderson disorder: Beyond single-parameter scaling”. In: *Phys. Rev. B* 73 (4 Jan. 2006), p. 045118. DOI: 10.1103/PhysRevB.73.045118. URL: <https://link.aps.org/doi/10.1103/PhysRevB.73.045118>.
- [60] Hans-Jürgen Sommers. *Superbosonization*. 2007. arXiv: 0710.5375 [cond-mat.stat-mech]. URL: <https://arxiv.org/abs/0710.5375>.
- [61] A. Mildenberger et al. “Density of quasiparticle states for a two-dimensional disordered system: Metallic, insulating, and critical behavior in the class-D thermal quantum Hall effect”. In: *Phys. Rev. B* 75 (24 June 2007), p. 245321. DOI: 10.1103/PhysRevB.75.245321. URL: <https://link.aps.org/doi/10.1103/PhysRevB.75.245321>.
- [62] Martin R. Zirnbauer. “Riemannian symmetric superspaces and their origin in random-matrix theory”. In: *Journal of Mathematical Physics* 37.10 (Oct. 1996), pp. 4986–5018. ISSN: 0022-2488. DOI: 10.1063/1.531675. eprint: https://pubs.aip.org/aip/jmp/article-pdf/37/10/4986/19056249/4986_1_online.pdf. URL: <https://doi.org/10.1063/1.531675>.
- [63] Chao-Ming Jian et al. “Criticality and entanglement in nonunitary quantum circuits and tensor networks of noninteracting fermions”. In: *Phys. Rev. B* 106 (13 Oct. 2022), p. 134206. DOI: 10.1103/PhysRevB.106.134206. URL: <https://link.aps.org/doi/10.1103/PhysRevB.106.134206>.

- [64] Chao-Ming Jian et al. “Measurement-induced entanglement transitions in quantum circuits of non-interacting fermions: Born-rule versus forced measurements”. In: *arXiv: 2302.09094 [cond-mat.stat-mech]* (2023). URL: <https://arxiv.org/abs/2302.09094>.
- [65] M. Buchhold et al. “Effective Theory for the Measurement-Induced Phase Transition of Dirac Fermions”. In: *Phys. Rev. X* 11 (4 Oct. 2021), p. 041004. DOI: 10.1103/PhysRevX.11.041004. URL: <https://link.aps.org/doi/10.1103/PhysRevX.11.041004>.
- [66] O. Alberton, M. Buchhold, and S. Diehl. “Entanglement Transition in a Monitored Free-Fermion Chain: From Extended Criticality to Area Law”. In: *Phys. Rev. Lett.* 126 (17 Apr. 2021), p. 170602. DOI: 10.1103/PhysRevLett.126.170602. URL: <https://link.aps.org/doi/10.1103/PhysRevLett.126.170602>.
- [67] Adam Nahum and Brian Skinner. “Entanglement and dynamics of diffusion-annihilation processes with Majorana defects”. In: *Phys. Rev. Res.* 2 (2 June 2020), p. 023288. DOI: 10.1103/PhysRevResearch.2.023288. URL: <https://link.aps.org/doi/10.1103/PhysRevResearch.2.023288>.
- [68] Xhek Turkeshi et al. “Measurement-induced entanglement transitions in the quantum Ising chain: From infinite to zero clicks”. In: *Phys. Rev. B* 103 (22 June 2021), p. 224210. DOI: 10.1103/PhysRevB.103.224210. URL: <https://link.aps.org/doi/10.1103/PhysRevB.103.224210>.
- [69] Igor Poboiko et al. “Theory of Free Fermions under Random Projective Measurements”. In: *Phys. Rev. X* 13 (4 Dec. 2023), p. 041046. DOI: 10.1103/PhysRevX.13.041046. URL: <https://link.aps.org/doi/10.1103/PhysRevX.13.041046>.
- [70] Michele Fava et al. “Nonlinear Sigma Models for Monitored Dynamics of Free Fermions”. In: *Phys. Rev. X* 13 (4 Dec. 2023), p. 041045. DOI: 10.1103/PhysRevX.13.041045. URL: <https://link.aps.org/doi/10.1103/PhysRevX.13.041045>.
- [71] K. Chahine and M. Buchhold. “Entanglement phases, localization, and multifractality of monitored free fermions in two dimensions”. In: *Phys. Rev. B* 110 (5 Aug. 2024), p. 054313. DOI: 10.1103/PhysRevB.110.054313. URL: <https://link.aps.org/doi/10.1103/PhysRevB.110.054313>.
- [72] Xiangyu Cao, Antoine Tilloy, and Andrea De Luca. “Entanglement in a fermion chain under continuous monitoring”. In: *SciPost Phys.* 7 (2019), p. 024. DOI: 10.21468/SciPostPhys.7.2.024. URL: <https://scipost.org/10.21468/SciPostPhys.7.2.024>.
- [73] Martin R. Zirnbauer. *Another critique of the replica trick*. 1999. arXiv: cond-mat/9903338 [cond-mat.mes-hall]. URL: <https://arxiv.org/abs/cond-mat/9903338>.
- [74] W. Fulton and J. Harris. *Representation theory, Series “Graduate Texts in Mathematics”*. Vol. 129. Springer, 1991.

- [75] C. Sünderhauf, L. Piroli, and XL. et al. Qi. “Quantum chaos in the Brownian SYK model with large finite N : OTOCs and tripartite information”. In: *J. High Energ. Phys.* 38 (2019). URL: [https://doi.org/10.1007/JHEP11\(2019\)038](https://doi.org/10.1007/JHEP11(2019)038).
- [76] Morris H. DeGroot and Mark J. Schervish. *Probability and Statistics*. 4th. Pearson, 2012.
- [77] M.L. Mehta. *Random Matrices*. Academic Pr., 1991.
- [78] A. Prats Ferrer, B. Eynard, and P. et al. Di Francesco. “Correlation Functions of Harish-Chandra Integrals over the Orthogonal and the Symplectic Groups”. In: *J Stat Phys* 129, 885–935 (2007). URL: <https://doi.org/10.1007/s10955-007-9350-9>.
- [79] Martin R Zirnbauer. “Supersymmetry for systems with unitary disorder: circular ensembles”. In: *Journal of Physics A: Mathematical and General* 29.22 (Nov. 1996), p. 7113. DOI: 10.1088/0305-4470/29/22/013. URL: <https://dx.doi.org/10.1088/0305-4470/29/22/013>.
- [80] Harish-Chandra. “Differential Operators on a Semisimple Lie Algebra”. In: *American Journal of Mathematics* 79.1 (1957), pp. 87–120. ISSN: 00029327, 10806377. URL: <http://www.jstor.org/stable/2372387> (visited on 09/28/2024).
- [81] C. Itzykson and J.-B. Zuber. “The planar approximation. II”. In: *Commun. Math. Phys.* 21 411–421 (1980).
- [82] Brian C. Hall. *Lie Groups, Lie Algebras, and Representations: An Elementary Introduction, Graduate Texts in Mathematics*. Vol. 222. Springer, 2015.
- [83] Sora Cho and Matthew P. A. Fisher. “Criticality in the two-dimensional random-bond Ising model”. In: *Phys. Rev. B* 55 (2 Jan. 1997), pp. 1025–1031. DOI: 10.1103/PhysRevB.55.1025. URL: <https://link.aps.org/doi/10.1103/PhysRevB.55.1025>.
- [84] Ilya A. Gruzberg, N. Read, and Andreas W. W. Ludwig. “Random-bond Ising model in two dimensions: The Nishimori line and supersymmetry”. In: *Phys. Rev. B* 63 (10 Feb. 2001), p. 104422. DOI: 10.1103/PhysRevB.63.104422. URL: <https://link.aps.org/doi/10.1103/PhysRevB.63.104422>.
- [85] Guo-Yi Zhu et al. “Nishimori’s Cat: Stable Long-Range Entanglement from Finite-Depth Unitaries and Weak Measurements”. In: *Phys. Rev. Lett.* 131 (20 Nov. 2023), p. 200201. DOI: 10.1103/PhysRevLett.131.200201. URL: <https://link.aps.org/doi/10.1103/PhysRevLett.131.200201>.